STAR

(Contract Number: Fission-2010-3.5.1-269672)

DELIVERABLE (D-N°5.3)

Radiation Quality: studying sub-cellular modes of action using biomarkers and "omics" tools

Author(s): **Deborah Oughton, Christelle Adam-Guillermin, Frédéric Alonzo, Turid Hertel-Aas, Nele Horemans, Alicja Jaworska, Catherine Lecomte-Pradines, Jan L. Lyche, Sandrine Pereira, Hans Christian Teien, Nathalie Vanhoudt**

Editor: **Deborah Oughton, Almudena Real, Laureline Février, Frédéric Alonzo**

Reporting period: 01/08/12 – 31/01/14

Date of issue of this report: 29/11/2013

Start date of project: 01/02/2011   Duration: 54 Months

[STAR]

DISTRIBUTION LIST

Name	Number of copies	Comments
André Jouve, STAR EC Project Officer	1	Electronically
Thomas Hinton, STAR Co-ordinator (WP-1), IRSN	1	Electronically (pdf file)
Laureline Février, IRSN	1	Electronically (pdf file)
STAR Management Team members: WP-2; T. Ikaheimonen, STUK WP-3; M. Dowdall, NRPA WP-4; H. Vandenhove, SCK•CEN WP-5; F. Alonzo, IRSN WP-6; D. Oughton, UMB WP-7; B. Howard, NERC	1 per member	Electronically (pdf file)
STAR Steering Committee G. Kirchner, BfS A. Real, CIEMAT J-C. Gariel, IRSN T. Ikaheimonen, STUK H. Vandenhove, SCK•CEN C. Bradshaw, SU A. Liland, NRPA B. Howard, NERC B. Salbu, UMB	1 per member	Electronically (pdf file)
STAR Wiki site		Electronically (pdf file)
STAR's External Advisory Board	1 per member	Electronically (pdf file)
ALLIANCE members	1 per member	Electronically (pdf file)

(D-N°: 5.3) – Radiation Quality: studying sub-cellular modes of action using biomarkers and "omics" tools

Dissemination level: PU

Date of issue of this report: **29/11/2013**

Executive Summary

This report addresses some of the issues associated with the impact of radiation quality on biological effects in non-human organisms. It is a summary of work in progress to (ultimately) test the overarching hypotheses that RBEs and radiation weighting factors for ecologically relevant endpoints will be different to those for human cancer risks. More specifically, we posit that differences will be grounded in the metabolic behaviour of radionuclides (and thus which organ or tissue receives the highest dose) and the variation in sensitivity to radiation quality that might be seen for different cells and different biological endpoints. Thus a common approach for experiments is to focus on MoA, and studies include a range of biomarkers for the tested organisms. The deliverable reports a series of different experiments related to RBE and questions of radiation quality. These cover studies on Arabidopsis, zebrafish (cell cultures and whole fish), nematodes and daphnia. A decision was made in STAR to focus on comparison of Am-241 with external gamma irradiation. However, one study reported here (daphnia) compares gamma with uranium, and one study (zebrafish cells) uses an external Am-241 alpha irradiator. The nematode and whole body zebrafish RBE studies are still ongoing, hence the deliverable only reports results of pilot studies to support experimental design. The results from these studies will be made available later.

The deliverable starts with a review of the state-of-the-art in RBE and radiation quality, including the ways in which biomarker and "omic" approaches can help in understanding MoA. Section 3 addresses experimental design issues and section 4 presents the results of ongoing studies. Overall conclusions and future work is given in section 5.

Assessment of the effects of ionising radiation in biological organisms needs to address the variability in biological effect with radiation quality, specifically, the different levels of linear energy transfer (LET) associated with different types of radiation. While gamma and beta emitters are classed as low LET emitters, alpha emitters have high LET and are linked with a relatively higher adverse biological effect due to a more concentrated deposition of energy (and ionisation) in tissues. This phenomenon is classified by the Relative Biological Effectiveness (RBE) of different types of radiation, which is defined as the ratio of the absorbed dose of reference radiation (X-rays or Co-60) to the absorbed dose of the compared radiation that is required to attain the same biological effect.

In radioecology, the main issue is whether the radiation weighting factors derived for human cancer are appropriate to use for the ecological endpoints of relevance for protection of wildlife, such as reproduction. This is relevant for both alpha emitters versus gamma irradiation, but also for tritium, since the ERICA Assessment tool proposes a radiation weighting factor of 3 for low energy beta emitters, which goes against recommendations for human cancer risk. A further complication when deriving RBEs for both human and non-human biota is the inhomogeneous distribution of short-range (alpha and low energy beta) internally-deposited radionuclides (microdosimetry).

[STAR]   3/94
(D-N°: 5.3) – Radiation Quality: studying sub-cellular modes of action using biomarkers and "omics" tools
Dissemination level: PU
Date of issue of this report: **29/11/2013**

The results from the few studies allowing a direct comparison between gamma and alpha exposure (Arabidopsis, zebrafish cells and daphnia), are in line with the existing paradigm, namely that the effects of alpha irradiation are greater than gamma. However there are exceptions, such as a higher rate of DNA double strand breaks in fish cell cultures exposed to gamma as compared to alpha. Furthermore the variety across experiments and endpoints demonstrates quite clearly that the relative differences in biological response between alpha and gamma emitters is dependent on the endpoint or biomarker analysed, the time after irradiation, and the tissue or organ in which the measurement is taken. Differences in distribution of alpha and gamma exposure within the organism need to be addressed, and more work will be needed to link molecular levels changes with those at tissue and organism levels. Future work will be directed to focused and hypothesis driven comparisons, and on expanding the preliminary data on biomarker and future omics analysis.

Table of Content

(D-N°: 5.3) – Radiation Quality: studying sub-cellular modes of action using biomarkers and "omics" tools

Dissemination level: PU

Date of issue of this report: **29/11/2013**

1. Introduction

1.1 Background

Assessment of the effects of ionising radiation in biological organisms needs to address the variability in biological effectiveness with radiation quality, specifically, the different levels of linear energy transfer (LET) associated with different types of radiation. While gamma and beta emitters are classed as low LET emitters, alpha emitters have high LET and are linked with a relatively higher adverse biological effect due to a more concentrated deposition of energy (and ionisation) in tissues. The Relative Biological Effectiveness (RBE) of different types of radiation, is defined as the ratio of the absorbed dose of reference radiation (X-rays or Co-60) to the absorbed dose of the compared radiation that is required to attain the same biological effect.

RBE values are the basis for development of radiation weighting factors with respect to assessment of cancer risks in human radiation protection (i.e. as part of the derivation of Sv from Gy). It is important to note that RBE is an objective, experimentally obtained number to compare the damaging effect of radiation having different LET (e.g. α, β) with the reference radiation for a particular endpoint under specific conditions. RBEs depend on many factors such as the type of radiation (LET) and how it is delivered, the dose and dose rate, the cell, tissue type or life stage being irradiated, the endpoint and individual radiosensitivity (Chambers et al., 2006; ERICA 2006; Highley et al.2011). The radiation weighting factor (W_R) is a subjective, generic value that is derived from RBE experimental data for the purpose of assessing radiation risk. In human radiation biology, weighting factors refer specifically to cancer risk, and underlie the mathematical conversion from Gy to Sv. The W_R for cancer risks from gamma and beta particles is 1, and for alpha particles, 20.

In radioecology, the main issue is whether the radiation weighting factors derived for human cancer are appropriate to use for the ecological endpoints of relevance for protection of wildlife, such as reproduction. This is relevant for both alpha emitters versus gamma irradiation, but also for tritium beta particles, which are an important environmental source. The ERICA Assessment tool proposes a radiation weighting factor of 3 for low energy beta emitters, which is not in line with recommendations for human cancer risk, which have a weighting factor of 1. A further complication when deriving RBEs for both human and non-human biota is the inhomogeneous distribution of short-range (alpha and low energy beta) internally-deposited radionuclides (microdosimetry).

The dependence of RBE on the effects or endpoint measured means that it is possible to observe a range of "RBEs" in the same experiment, in the same organism, depending on what is exactly being measured. Although this causes complexity in interpreting results, these differences offer important

insight into the different modes of action (MoA) that might arise between different types of radiation exposure.

For this reason, the experiments presented in this report represent an attempt to address some of the above issues, by consolidating results from a range of different experiments on a variety of species. As such they are not classic "RBE" experiments in the strict definition of being able to compare to a fixed gamma source, but rather a set of pilot studies that explore some of the challenges in these types of experiments.

1.2 Overview of the Deliverable

This report addresses some of the issues associated with the impact of radiation quality on biological effects in non-human organisms. It is a summary of work in progress to (ultimately) test the overarching hypotheses that RBEs and radiation weighting factors for ecologically relevant endpoints will be different to those for human cancer risks. More specifically, we posit that differences will be grounded in the metabolic behaviour of radionuclides (and thus which organ or tissue receives the highest dose) and the variation in sensitivity to radiation quality that might be seen for different cells and different biological endpoints. Thus a common approach for experiments is to focus on the mode of action (MoA), and studies include a range of biomarkers for the tested organisms. The deliverable reports a series of different experiments related to RBE and questions of radiation quality. These cover studies on Arabidopsis, zebrafish (cell cultures and whole fish), nematodes and daphnia. A decision was made in STAR to focus on comparison of Am-241 with external gamma irradiation (see STAR D5.1). However, one study reported here (daphnia) compares gamma with uranium, and one study (zebrafish cells) uses an external Am-241 alpha irradiator. The nematode and whole body zebrafish RBE studies are still ongoing, hence the deliverable only reports results of pilot studies to support experimental design. The results from these studies will be made available later.

The deliverable starts with a review of the state-of-the-art in RBE and radiation quality, including the ways in which biomarker and "omic" approaches can help in understanding MoA. Section 3 addresses experimental design issues and section 4 presents the results of ongoing studies. Overall conclusions and future work is given in section 5.

2. Radiation Quality Review

2.1 State of the Art in RBE

The Relative Biological Effectiveness (RBE) of a particular radiation type is the ratio of absorbed dose of reference radiation R (often taken to be ^{60}Co gamma rays or high voltage (180-300 kV) X-rays) to the absorbed dose of the particular examined radiation, Y, that is required to attain the same biological effect, e.g. for reference radiation of 250 kVp X-rays:

$$RBE = \frac{\text{Dose of 250-kVp x-rays required to produce effect X}}{\text{Dose of test radiation required to produce effect X}}$$

The term is generally used in relation to experimental work in radiation biology and related fields. RBE is the basis for and is related to quality and risk factors used in human radiation protection for cancer and hereditable disease's, and medical applications of radiation (especially in clinical treatment planning in radiotherapy), but it is not identical with these. As opposite to quality and risk factors the explicit definition of biological effect at particular level and the nature of biological endpoint are needed to define RBE (ICRU 33, 1980)

RBE is dependent on the quality of radiation, which is commonly defined by Linear Energy Transfer (LET). LET is a measure of average energy deposition along the path of the radiation track, but ignores the large fluctuation in energy deposition along the track. The LET of α particle can have different discreet values along the track. For low levels of high LET radiation, this can be a limitation in estimating the magnitude of molecular events causing changes in the measurement of the biological endpoint, and this characterization of the particular biological effect (Alper 1998).

The RBE also depends on several factors such as the biological system studied, the absorbed dose, the irradiation parameters (e.g. dose rate, discrete energy deposition etc.) and the environmental conditions (e.g. the well documented dependence on the level of oxygenation).

As RBE depends on several factors, the experimental approach to determine the value of RBE is not an easy task. Model approaches for RBE derivation within clinical treatment planning have been developed for human ion beam therapy. The two models presently used in clinical treatment planning are the (local effect model (LEM) and microdosimetric kinetic model (MKM) (Friedrich et al 2013 and references herein). In space research, there are other approaches for using RBE in risk assessment (Cucinotta et al.2013)

2.1.1 RBE and quality of reference and examined radiation

It is essential that any given value of RBE is accompanied by the information of what specific reference radiation has been used. There is a significant difference between the LET of ^{60}Co and ^{137}Cs photons which have a LET of below 1 keV/μm and that of high energy X-rays (for example

200 keV) which have a LET of about 3.5 keV/μm (Kellerer 2002). However, at least for the endpoint of cell survival, RBEs over this span of keV tend to be rather constant (see Annex). Many radiobiological studies have shown that at low doses, the biological effectiveness of orthovoltage X rays can be 2-3 times higher, than the biological effectiveness of higher-energy photons (e.g., 60Co gamma rays) (NCRP, 1990; ICRP, 2003).

For high LET radiation, and especially at low levels of exposure, several biophysical factors need to be considered. These include the inhomogeneity of the deposited radionuclides in the given tissue or organ, and dependence on the micrososimetric and nanodosimetric features of given radiation track structure (i.e. pattern of discreet energy deposition and cluster ionisations) (Goodhead 2006) in the cell, tissues and/or organisms. In comparison to reference gamma or X-rays, one can expect only very few radiation tracts in the tissue exposed to low levels of high LET radiation and the majority of cells will not experience radiation exposure. This low density of tracks will occur even if we assume a homogenous distribution of α emitting radionuclides in the tissue or organism.

2.1.2 RBE dependence on dose, and dose rate

The majority of data (experimental and epidemiological) that have been used to determine RBEs has been obtained at considerably larger doses than those of interest for radiation protection or environmental risk assessment. RBE is dependent on dose and with decreasing dose and dose rate, the effectiveness per unit dose for low-LET radiations generally decreases more rapidly than for high- LET radiation. (ICRP 58, 1990). As it is believed that deterministic effects have a threshold dose at which they can be observed, it can be assumed that there is an upper limit for the value for RBE for deterministic low level effects. This is denoted as RBE_m. (ICRP 92, 2003). For low doses and for low dose rates for stochastic effects ICRP publication 92 proposes to use the ideal upper value of RBE that is denoted RBE_M.

ICRP 58 also states that it is essential to distinguish between different types of RBEs, and proposed, after Kocher, to use the term "Radiation effectiveness factor (REF)" that describes cancer risk and the probability of its causation by radiation for exposures that cause risks of magnitude comparable to the background risk. To develop such a term and quantity for radiation protection for non- human biota could be a desired approach (Kocher and Trabalka, 2000). Suggested terms for non-humans include the Dose equivalent for fauna and flora (DEFF), Ecodosimetry weighting factor (e_R), (Radiation) weighted absorbed dose (rate), among others.

2.1.3 RBE and type of effects

Ideally RBE can be only derived by comparing the same specific effects. In experimental work, it is often only possible to compare the same endpoints. One has to consider that the change of the endpoint measured in an experiment might be a manifestation of changes in different effects. However the designation of what is an endpoint and what is an effect vary between authors

publishing RBE data (and indeed many other dose-response studies). In environmental radiation protection (e.g., ICRP, European projects as FASSET and ERICA) the relevant effects for deriving quality factors are grouped under four umbrella effects categories: mortality, morbidity, reproduction success and chromosomal damage and mutations. There is also a difference between RBEs for stochastic and deterministic effects. For high LET radiation, RBEs for stochastic effects tend to be higher than RBEs for deterministic effects.

In research aiming to find quality factors of different radiations for non-human biota, deterministic effects are considered to be more relevant that the stochastic ones, although it is not always easy to differentiate between the stochastic and deterministic effects impact (Higley et al., 2012). Another consideration is that RBE for the potentially comparable effects can vary significantly between species. For example, substantially higher RBEs for fission neutrons were found for plant generic endpoints as compared with insects or mammals (Sinclair 1985 and references herein). Other issues for developing RBE- like factors for environmental risk assessment include the question of whether it is better to use results from the experiments measuring parameters of cell culture survival in vitro, or results from DNA damage and repair studies.

The new developments in understanding of non-target radiation biological effects that cannot be related directly to the RBE/ LET relationship add an additional level of complexity to the derivation of RBE-like values. The RBE is related to LET of radiation and the LET concept is based on target theory. Non targeted effects of radiation show no clear absorbed dose dependence and might be not universally occurring for all types of radiations (i.e. neutron and probably proton radiation do not induce bystander effects). So it will be an additional complication if one should take into consideration contribution of non–target effects for deriving RBE like values for environmental low level exposures.

When deriving weighting factors for environmental exposures to humans it is necessary to take into consideration that different quality radiations are delivered in the different ways. Low LET irradiation will be delivered in many cases both from external irradiation and from internally deposited radionuclides, while for higher LET radiations like alpha, the internally deposited radionuclides will have the greatest contribution to dose. For internal exposure, problems with inhomogeneity of dose distribution (or more precisely energy deposition and ionisations in the target of interest), and mixed fields may need to be considered (Howell et al., 1994).

For risk assessment, the quality factors used in radiation protection are not applicable and LET or microdosimetric parameters must be invoked in combination with radiobiological experiment results (ICRP 92, 2003).

In the last decade or so it was recognised that it is a need to derive risk estimates for the protection of the non- human species and the environment as a whole and several groups review the radiobiological literature looking for RBE data for high LET α and β radiations that can be used for deriving quality factors for environmental risk assessment (FASSET 2003 Deliverable 2, ERICA Deliverable (X), SENES 2005, Chambers et all (2006) and reference herein, Higley et al. 2012). A very important source for these investigations was the FREDERICA Radiation Effects Database that was developed as a part of ERICA project (Copplestone et al., 2008). Authors reviewing this literature have noticed that in the large amount of the literature on RBEs there is only small fraction of the papers that can be suitable for deriving quality factors for environmental exposure risk assessments, and even less if one searches for papers that are suitable for population–relevant endpoints.

The available values of RBE that are in the literature were not only derived for high doses and different modes of exposure, but also for different purposes. Experimental design of numerous effect studies very often makes it difficult to use this data for deriving RBEs. An additional caveat is that in many published effect studies the information on dosimetry is insufficient or inadequate (or even sometimes there is an indication that dosimetry was not performed properly). Moreover, dose uncertainties at low doses and especially for internal emitters are considerable. They pose a challenge for assessing the risk (Saloma et al., 2013)

2.2 Biomarkers and Omics approaches

Compared to many other environmental stressors, the underlying mechanisms and modes of action (MoA) of ionising radiation toxicity are rather well defined, but the majority of work has been driven by a focus on human effects, and especially cancer. Testing for ecological effects involves the use of various biological models and endpoints relevant to important biological functions (survival, reproduction, etc…) (European Commission, 2003). Little attention is given to identifying the MoA of pollutants. However, substantial benefits can be realized by basing testing and subsequent risk management decisions on known or probable MoA: for example, a priori knowledge of MoA can lead to identification of mechanism-based (and hence, stressor-specific) molecular indicators that can potentially be linked to environmental concentrations. Furthermore, knowledge of MoA can serve as a basis for extrapolation of biological effects across species, biological levels of organization and chemical/physical groups of pollutants (Ankley et al., 2009).

Developments in molecular biology have the potential to improve the mechanistic understanding of the effects of stressors and underlying processes (NRC, 2007; Ankley et al., 2009). Improved understanding of the underlying MoA of toxicity for different types of pollutants can aid in the development of methods for assessing exposure and effects, thereby reducing uncertainties related to extrapolation across species, endpoints and chemical groups with similar function or structure (Ankley et al., 2009). On this basis a tiered testing framework is proposed, using short-term toxicity assays to identify pollutant toxicity before processing with longer-term tests better suited to quantifying adverse effects (e.g. USEPA, 1998; NRC, 2007) for a better rationalization of risk assessment costs. The efficiency of these programs could be enhanced by the use of emerging technologies in the field of 'omics' and computational biological models, allowing to take into account ecologically relevant and mechanism-specific endpoints.
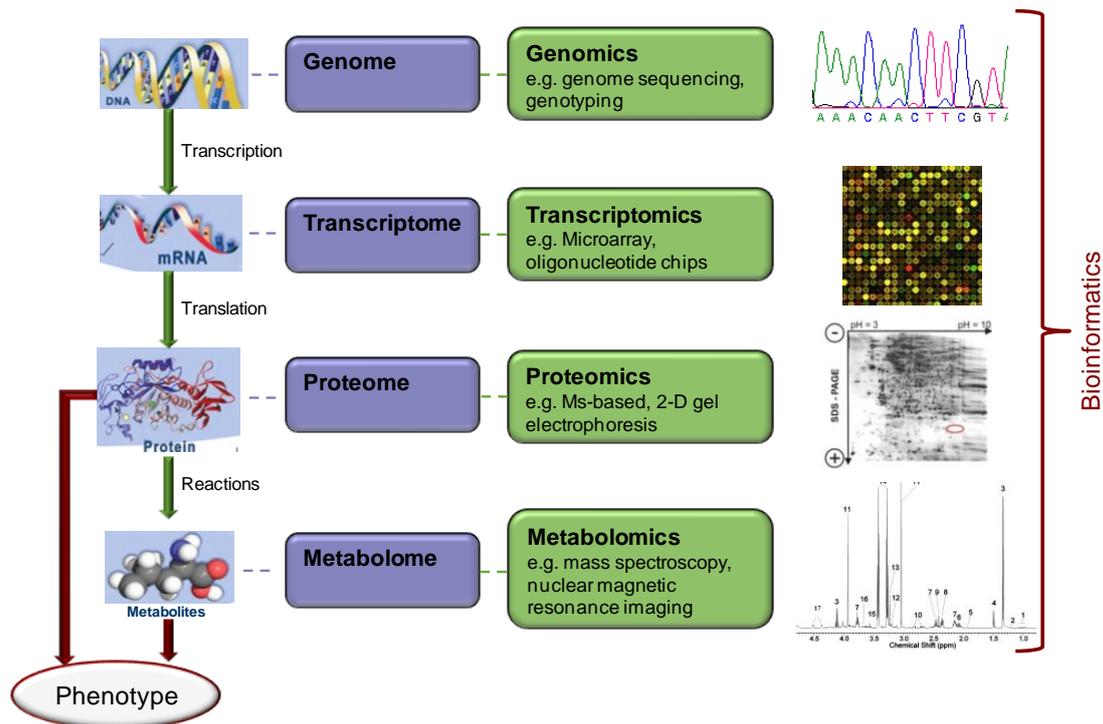
Figure 1: Overview of Toxicogenomics (Slide courtesy of Turid Hertel-Aas)

In Deliverable 5.1, a review was made of the different types of biomarkers that might be applicable to radiation toxicity studies, including biomarkers of exposure, effects and radiosensitivity. This included a review of possible "omics" approaches, including transcriptomics, proteomics, and metabolomics, (Boverhof and Gollapudi, 2011). The table of biomarkers (Table 1) is reproduced below, and will be referred to in the different experiments carried out during this deliverable. While not as deeply focused on omics as the approach proposed by Ankley et al. (2009), the generic idea of taking a holistic approach, by combining a variety of biomarkers and endpoints, is relevant to the study of radiation quality, and especially in understanding differences in MoA of different radiation qualities.

Table 1: Overview of biomarkers of both exposure and sensitivity that can be utilized within human and ecological toxicology to identify the response to ionising radiation (Taken from STAR D5.1. References to the techniques can be found therein).

Biomarker	Method/assay	Tested endpoint	Correlation with dose or radiation sensitivity	Species tested	Used in these radiation quality studies
DNA damage and repair mechanisms					
Antibody against Gamma-H2AX	fluorescence imaging, Western blot, 2-D gel electrophoresis, flow cytometry ELISA High-throuput	DNA damage (Double strand breaks)	Sensitive to and correlating with degree of damage	Human but gamma-H2AX phosphorylation site has been shown to be highly conserved throughout eucaryotes	Arabidopsis Zebrafish cells (ZF4) and in vivo
Cytogenic biomarker	Chromosomal abberations	Genotoxicity	Validated correlation with long-term morbidity endpoints like risk to induce cancer	Human blood	
Mitochondrial DNA mutation frequency	Sequence analysis	DNA mutation	Not sensitive enough for environmental relevant concentrations	Compost worm (Eisenia fetida)	
Oxidation of DNA	7,8-Dihydro-8-oxo-guanine (8-OHgua) (HPLC-analysis, GC-MS, modified Comet-assay)	DNA damage and repair	Not clear whether good biomarker (Collins 1996) due to high background	Numerous Including Compost worm (*Eisenia fetida)*	Arabidopsis
Oxidation of DNA	8-OHgua detection with antibodies) (HPLC-analysis, GC-MS) Comet-assay	DNA damage and repair	Linear relationship with gamma-irradiation dose and sensitive (Bruskov et al. 1999)		Arabidopsis

Repair capacity of blood cells	Comet assay	DNA damage and repair	Correlate with chronic exposure	Numerous Including blood cells of chronic (Chernobyl) exposed people	Zebrafish
Cytogenic endpoints		DNA repair		human	
Methylation status of DNA specifically of	Bisulphite sequencing, RT-PCR Methylation specific-PCR Western blotting	Reduced transcription through gene silencing of protein involved in DNA-repair	Relation between radiosensitivity and methylation status of ERCC1 (excision repair cross complementing protein 1) promotor	Human gliomas	Arabidopsis Zebrafish cells (ZF4)
DNA alterations	RAPD-qPCR	DNA damage	Non linear relationship with depleted U concentration (Lerebours et al., 2013; Plaire et al., 2013) Zebrafish (Danio rerio)	Zebrafish (Danio rerio) Waterflea (*Daphnia magnia*)	Daphnia magnia
Antioxidants and antioxidant enzymes	Spectrophotometric assays of enzyme activities (POD, SOD, catalase) Carotenoids levels	Oxidative stress	No correlation between oxidative stress tolerance and gamma radiation resistance	bacteria	Arabidopsis
Fe/Mn ratio	Atomeric Absorption Spectrometry	Protection of proteins and DNA for oxidative damage	Inverse correlation between [Mn]/[Fe] ratio and level of protein oxidation (Confalonieri and Sommer 2011) No direct correlation with radiation resistance (Shashidhar, Kumar et al. 2011)	Bacteria: *Deinococcus, Thermophyllus*	
Heat Shock Proteins	Antibody detection: Western blot	Stress induced proteins			

(D-N°: 5.3) – Radiation Quality: studying sub-cellular modes of action using biomarkers and "omics" tools

Radiation proteomics	Orbitrap MS-MS	Changed protein abundance	Time and dose dependent	Rat mouse and human cells	Zebrafish cells (ZF4)
Transcriptomic changes	Microarray etc,..	Changed gene expression	Acute exposure was comparable to other abiotic stressors whereas chronic exposure revealed a complete distinct gene expression profile (KOV07) Down regulation of growth/rhythm responses and up-regulation of defence/stress regulation in post irradiation reproduction state (KIM07)	*Arabidopsis* vegetative (Kovalchuk et al., 2007), *Arabidopsis* during flowering (Kim et al., 2007)	Arabidopsis Zebrafish
Radiation metabolomics	GS-MS QTOFMS	Changed metabolite abundance Some could be linked to food deprivation and starvation (Johnson et al., 2011)	Dose and time dependent, cross-species (Johnson et al., 2011)	Rat, cell and mouse	

Due to limitations in cost and manpower, and because many of the experiments are still at a pilot stage, it has not been possible to apply biomarkers across all species for this deliverable, but the data produced in the report acts as a first step to designing experiments that might provide the basis for further investigations of possible modes of action using other techniques. In accordance with a tiered-approach, it was decided prior to this deliverable that the selection and application of "omics" approaches would be done after the first experiments, and samples have been taken for analysis at a later date.

3. Experimental Design and Challenges

3.1 Choice of Alpha Emitter

For the experiments in question, it was agreed that all studies would use the same alpha emitter, to approach some level of consistency. The choice of alpha emitter was made according to a set of criteria which included (STAR D5.1):

- Concentration factor of the selected species from the exposure medium;
- Accumulation in target cell/organ/tissue(s) that are related to the studied endpoint (*e.g.,* digestive system for assimilation endpoints ; gonads for reproductive endpoints; cell DNA for genotoxicity…), or homogeneously distributed;
- A manageable exposure route: either direct route and/or trophic route
- Radiation protection, safety and waste constraints;
- Suitable and cost effective methods of analysis.
- The toxicity is due mainly to alpha radiation and not other emissions from the radionuclide and/or its daughters, or chemical toxicity.

On the basis of these, americium (Am-241) was chosen as the alpha emitter. More detailed reasons for the selection can be found in Deliverable 5.1, but they include a good thermodynamic database on speciation of americium(III), as well as broad knowledge on environmental concentrations. Trace levels of Am-241 are found worldwide in aquatic ecosystems (10^{-6} to 10^{-5} Bq/L) as a consequence of former atmospheric nuclear weapon testing and accidental releases, with regional higher levels of 10^{-5} to 10^{-2} Bq/L in freshwaters (Matsunaga et al., 1998; Choppin, 2006), and higher levels seen at accidental sites (Agapkina et al., 1995; Pourcelot et al., 2003). It is also a radionuclide that increases in activity over time following accidental or deliberate releases, due to the ingrowth from Pu-241.

3.2 Dose Calculations

The determination of the internal alpha irradiation of organisms (Table 2) needs to address both the bioaccumulation of Am-241 and then the subsequent calculation of internal alpha dose rates. While doses to the whole organism can be calculated rather straightforwardly (using the ERICA tool and relevant organism sizes), more detailed dosimetry to tissues and organs will need more sophisticated calculations, particularly for small organs or animals. Dose conversion coefficients (DCC), expressed in mGy/h / Bq/kg, are derived from the alpha particles (5.5 MeV) and beta(−) particles (from 4.6 keV to 1.0 MeV) emitted by Am-241. These propagate over distances from 2 to 400 µm in the exposure medium and in the contaminated tissues. For organisms and tissues greater than c.a. 1 mm, the DCC are relatively constant, and the greatest contribution to the dose (>90%) comes from the internal alpha irradiation in tissues, and the doses are well-correlated with the activity concentrations. For small aquatic organisms or *C. elegans*, a low bioaccumulation can result

in a greater fraction for external dose from the test media. These are discussed in more detail below under the individual experiments.

Dosimetry from gamma irradiation (Table 2) is more straightforward, but also needs to address the change in radiation field that occur during irradiation, particularly when shielding is used (as in the zebrafish gamma exposures). This can mean a significant change in the energy spectra, making it impossible to compare to classic RBE definitions (see Annex). But on the other hand, for whole organism exposures in environmental media, the energy spectra to the tissues will also be moderated from that measured in air. What is most important is that the doses are characterised to the best possible degree, and the difficulties addressed in discussions.

3.3 Overview of experiments reported

Table 2. Synopsis of organisms and exposures regimes studies

Organism	Gamma irradiation	Alpha Irradiation
Arabidopsis	Cs-137 20- 350 mGy/h	Am-241 in growth media (Am_2CO_3) 1 µGy/h – 35 mGy/h
Zebrafish (In vitro cell cultures)	Cs-137 3 – 23 mGy/h	Am-241 irradiatior 100 – 500 mGy (acute 0.3 Gy/min)
Zebrafish (In vivo whole fish)	Co-60 1 µGy/h – 10 mGy/h	Am-241 in feed 1 µGy/h (~ 12 µGy/h in target tissues)
Nematodes	Cs-137 40 µGy/h – 27 mGy/h	Pilot test only
Daphnia	Cs-137 8 µGy/h – 32 mGy/h	Am-241 in water 300 µGy/h – 23 mGy/h

3.4 Dose exposure regimes

A more challenging problem when comparing gamma external and alpha internal doses is that, while the gamma irradiation can be switched on and off, the dose from alpha increases as the organism reaches equilibrium with its food, and does not cease when the feeding or exposure stops. This is not such a problem when the effects or endpoints are measured, or biomarkers are sampled at the end of the irradiation, since it is possible to calculate the total dose from alpha based on metabolic data. But comparing endpoints during depletion period can be problematic and these types of measurement are often important for genetic and DNA-repair markers.

3.5 General guidance

In the following experiments we have always reported the alpha doses as unweighted and made it very clear when weighted doses are being described. Data is given on whole organism and tissues (when available) to ensure that comparisons of effects for different radiation quality can be calculated for a variety of endpoints and different tissues (to show the type of variation that can be achieved even from one experiment). Since dose calculations are based on fresh weight, activities re provided as fresh weight (and/or dry/fresh weight conversions). For the smaller test species (or organs) data is given on both internal and external and alpha/beta contributions.

4. Results from Radiation Quality Experiments

4.1 Arabidopsis

The objective of the experiments on Arabidopsis was to compare the effects in plants induced by two different radiation types, namely external gamma radiation or the alpha emitting Am-241. Different dose rates of gamma radiation and different concentrations of Am-241 were used to evaluate and compare dose-effect relationships. In total three different types of experiments were performed: (i) 14 day old *Arabidopsis* plants exposed for 7 days to different gamma dose rates (ii) 7 day old *Arabidopsis* plants exposed for 14 days to different gamma dose rates and (iii) 14 day old *Arabidopsis* plants exposed for 7 days to different concentrations of Am-241. Furthermore different endpoints, chosen at different levels of biological complexity from the individual down to the molecular level, were analysed to test for a sensitive and possible radiation specific biomarker. As described above we proposed different possible biomarkers to be tested. An overview of the endpoints used for the different experiments on *Arabidopsis* is given in Table 3.

Table 3. Overview of different endpoints measured in the three different Arabidopsis experiments performed.

	Endpoint	14-day old plants 7-day gamma treatment	7-day old plants 14-day gamma treatment	14-day old plants 4 or 7-day exposure to Am-241
General stress	Biomass (roots-shoots)	Fresh weight	Fresh weight	Fresh weight, dry weight, leaf area index
	Performance of photosynthesis based on chlorophyll fluorescence (Fv/Fm,)	X		X
	Photosynthetic pigments (chla, chlb, carotenoiden)	X		X
Oxidative stress	Antioxidants levels and redox status	ASC+DHA (GSH+GSSG)	ASC+DHA GSH+GSSG	ASC+DHA GSH+GSSG
	Activity of antioxidative enzymes (G…	SOD, APX, GPOD, SPOD, CAT	SOD, APX, GPOD, SPOD, CAT	
	RT-qPCR of genes encoding for antioxidative enzymes		RBOHB,C,E,G,H,I, LOX1-6, CAT1, 2, APX1, 2, GR1, CSD1, FSD1,2…	RBOHA, C, E, LOX1, CSD1, 2, 3, FSD1, 2, 3, CAT1, 2, 3 GR1
DNA damage and repair	Oxidation of DNA (8-oxyguanine)			X
	RT-qPCR of DNA damage and repair genes		KRP2, MND1, PARP1,2	KU80, LIG4, RAD51, DMC1, PARP1, 2, LPP1, POLG1, CKS1, GAR1

ASC: ascorbate, DHA: dehydroascorbate, GSH: reduced glutathione, GSSG: oxidised glutathione, SOD superoxide dismutase, APX: Ascorbate peroxidase, GPOD: guaiacol peroxidase, SPOD: syringaldizine peroxidase, CAT: catalase, RBOH: Respiratory burst oxidase homologue, LOX: lipoxugenase, CAT: catalase, GR: glutathione reductase, CSD Cu-Zn superoxide dismutase, FSD Fe superoxide dismutase, KRP Kip related protein, MND1: meiotic nuclear division1 homolog, PARP: poly(ADP-ribose) polymerase, KU80: KU80 homolog, LIG4: ligase 4, RAD51: RAD51 homolog 1, DMC1: disruption of meiotic conctrol1, LPP1: lipid phosphate phosphatase, POLG1: polymeras gamma 1, CKS1: cyclin dependent kinase subunit, GAR: GAI AN revertant

4.1.1 Experimental Set Up

Arabidopsis plants were grown from seeds on a hydroponic, nutrient medium as previously described (Saenen et al., 2013, Vanhoudt et al., 2008). As recent findings in Arabidopsis show that the effect of external γ-radiation depends on plant age (Kurimoto et al. 2010), suggesting that younger plants are more radiosensitive, a pilot study was first performed to test for age dependent-sensitivity in the Arabidopsis seedlings. Plants of 7, 10 and 14 days old were exposed for 4 and 7 days to an external gamma source (137Cs) at 110 mGy/h. Based on the results of this pilot study (data not shown) it was chosen to work with 14-day old plants and expose them to 7 day treatment. To expose plants to gamma radiation, the plants were transferred to the radiation unit of SCK•CEN

fourteen days after sowing where they were irradiated for 7 days with gamma radiation from a ^{137}Cs source. Control plants were placed next to the radiation unit. In a second experiment plants were moved to the radiation unit already after 7 days and were subsequently irradiated for 14 days instead of 7 days. The dose rates and total dose obtained in the two different experiments is depicted in Table 4

Table 4. Overview of dose rates and total dose used - the gamma irradiation experiments

14-day old plants exposed for 7 days		7-day old plants exposed for 14 days	
Dose rate (mGy/h)	Total dose (Gy)	Dose rate (mGy/h)	Total dose (Gy)
23.3	3.9	21.5	7.1
40.4	6.7	36.3	12.0
89.2	14.8	79.2	26.2
353	59	321	106

For exposure to Am-241, 14-day old seedlings were exposed for 4 or 7 days to 0, 50, 500, 5000 and 50000 Bq/L Am-241 (added as Am_2CO_3). The pH of the liquid medium was adjusted to that of the 0 Bq/L treatment prior to exposure of the plants.

After irradiation or exposure to Am-241 fresh weight was determined. Leaves and roots were harvested separately as approximately 100 mg samples, snap frozen in liquid nitrogen and stored at -80°C for further analyses of different biomarkers. Samples for transfer measurements of Am-241 were dry-ashed in a muffle furnace at 550 °C for 24 hours, and subsequently digested in 0.1 M HCl. Subsequently samples were brought to 20 mL with dH_2O after adjusting to pH 3 with 12 M HCl, and the Am-241 activity subsequently measured by LEGe gamma spectrometry (Canberra).

Chlorophyll fluorescence

Immediately after harvest, 4 rosettes were randomly selected for each exposure condition and the control plants. From each rosette, the 4th leaf was identified, removed and stored in the dark on wet paper in a closed petri dish. The selected leaves were dark-adapted for at least 15 minutes. Using PAM Fluorometry (Dual PAM-1000, Waltz, Germany), the induction curve (IC) for photosystem II (P680) was measured (Schreiber, 2004). From these data, values for photosynthetic capacity (F_v/F_m), photosynthetic efficiency (φPSII), non-photochemical quenching (NPQ) and non-regulated energy dissipation (NO) were calculated. Subsequently, to give information about the electron transport rate (ETR), a rapid light curve (RLC) was measured with the determination of the parameters α, E_k and ETR_{max} (Ralph and Gademann, 2005).

Pigment concentrations

Pigments were extracted from leaves (weighted half rosette) by incubation in 1 mL dimethylformamide (DMF) for 24 hours at 4°C under dark conditions. Pigments were measured spectrophotometrically at 664, 647 and 480 nm. Chlorophyll a, chlorophyll b and carotenoid concentrations were calculated according to Wellburn (1994). Pigment concentrations were determined for 6 biological replicates per treatment.

Enzyme capacities and antioxidant determination

Frozen root or leaf tissue (approximately 100 mg) was homogenized in ice cold 0.1 M Tris-HCl buffer (pH 7.8) containing 1 mM EDTA, 1 mM dithiotreitol and 4% insoluble polyvinylpyrrolidone (2 mL buffer for 100 mg root or leaf fresh weight) using a mortar and pestle. The homogenate was squeezed through a nylon mesh and centrifuged at $20000 \times g$ for 10 min at 4°C. The enzyme capacities were measured spectrophotometrically in the supernatant at 25°C. Capacities of guaiacol peroxidase (GPX) and syringaldazine peroxidase (SPX) were measured at 436 nm and 530 nm according to Bergmeyer et al. (1974) and Imberty et al. (1984) respectively. Ascorbate peroxidase (APX) capacity was measured at 298 nm following the method of Gerbling et al. (1984). Superoxide dismutase (SOD) capacity analysis was based on the inhibition of cytochrome c at 550 nm according to McCord and Fridovich (1969). Capacity analysis of catalase (CAT) was performed as described by Bergmeyer et al. (1974). Enzyme capacities were determined for 6 biological replicates per treatment.

Ascorbate and glutathione levels were determined in the leaves and roots of *Arabidopsis thaliana* seedlings. The concentrations were determined using a spectrophotometric assay as described by (Queval & Noctor, 2007), which enables measurement of both oxidised and reduced forms for both components of the ascorbate-glutathione cycle. Minor modifications to the procedure were described in (Saenen et al., 2013).

Base modification (8-OHdG formation)

Frozen root tissue (75-100 mg), harvested from plants irradiated for 7 days, was mechanically shredded (-80 °C; 2.5 min. at 30 Hz) with beads (MM400, Retsch), and the DNA extracted from the samples using DNeasy Plant Mini Kit (Qiagen) following the manufacturer's instructions. DNA concentrations were measured spectrophotometrically (Nanodrop 2000, Isogen Life Sciences).

The DNA samples were then digested as described in Debiane et al. (2009). 38 µL of DNA extract was incubated for 2 minutes at 100 °C, and subsequently digested with Nuclease P1 (2µL 5U/µL; Sigma) in the presence of 3 µL 250 mM potassium acetate buffer (pH 5.4) and 3 µL 10 mM zinc sulphate. Digestion was performed at 37°C overnight, after the digests were treated for 2 hours at 37°C with 2 µL alkaline phosphatase (0.3 U/µL; Sigma) in the presence of 6 µL 0.5 M Tris-HCl buffer (pH 8.3). Base modification (8-OHdG) was determined by competitive ELISA (New 8-OHdG Check kit, Japan Institute of Aging) according to the manufacturer's instructions. The assay is based on spectrophotometric detection at 415 nm.

Gene expression analysis

For gene expression analysis Frozen root and shoot tissue (50-100 mg) was homogenized in a tissue shredder (MM400, Retsch; -80 °C; 2.5 min. at 30 Hz) and the RNA extracted. RNA from shoot tissue was extracted using Ambion RNaqueous Kit (Invitrogen), and root RNA with RNeasy Plant Mini Kit (Qiagen, Venlo, Netherlands). Genomic DNA was removed from the samples with TURBO DNA-free™ Kit (Invitrogen) according to the manufacturer's instructions. RNA was then transformed to cDNA with the High-Capacity cDNA Reverse Transcription Kit (Applied Biosystems), using equal amounts of starting material (1 µg). Quantitative realtime-PCR was performed using SYBR Green fluorescence on a 7500 Fast Real-Time PCR system (Applied Biosystems) in a 10µL volume, containing 2.5 µL cDNA sample, 5 µL of Fast SYBR Green Master Mix (Applied Biosystems), 0.3 µL forward primer, 0.3 µL reverse primer and 1.9 µL RNase-free water. Gene expression data were normalized to housekeeping genes using GeNorm software as previously described (Saenen et al., 2013).

Statistics

Statistical analyses were performed using one way ANOVA and Tukey multiple comparison testing with the freeware software package R. To evaluate the assumption of normality, a Shapiro-Wilk test was used.

4.1.2 Results

Plants of 14 days old were exposed for 7 days to different dose rates of gamma radiation as depicted in Table 4. Although this treatment resulted in a total dose of nearly 60Gy for the highest dose rate, this resulted in total dose up to no significant changes on individual endpoints that could be used to build a dose-response curve (see results) were found. We therefore performed a second series of experiments in which we enhanced the total dose received by the plants by exposing 7-day old plants for 14 days. Results of both experiments are shown here separately.

4.1.2.1 Exposure of 14-day old plants for 7-days to external gamma radiation at different dose rates
(These results have recently been accepted for publication Journal of Environmental radioactivity (Vanhoudt et al. DOI: 10.1016/j.jenvrad.2013.11.011).

In general moderate or no effects were observed in different endpoints measured. As such, exposure of *A. thaliana* seedlings to different gamma radiation doses resulted in fluctuations of root and leaf fresh weights but no dose-dependent growth inhibition was observed (Figure 2)

Gamma radiation caused a transient increase of the quantum yield of PSII (φPSII)

As light energy absorbed by chlorophyll molecules can competitively be used (1) to drive photosynthesis, (2) to be dissipated as heat or (3) to be emitted as chlorophyll fluorescence, by using chlorophyll fluorescence measurements information about the two other competing processes can be obtained (Maxwell and Johnson, 2000). Based on these measurements, the photosynthetic parameter F_v/F_m, which is a measure of the potential efficiency of photosystem II (PSII), can be calculated. A significant increase is observed for the highest radiation dose (data not shown. As under optimal conditions this value is expected to be around 0.83 (Maxwell and Johnson, 2000), we can conclude that the light harvesting capacity of PSII remains intact within the applied range of radiation dose rates and doses and certainly at the highest dose. Gamma radiation causes a transient increase of the quantum yield of PSII (φPSII) (Figure 3A). Already after exposure to 3.9 Gy, plant leaves showed a significant increase in the efficiency of PSII photochemistry. A maximum was reached at 6.7 Gy and values returned to the control after exposure to 58.8 Gy (Figure 3A)
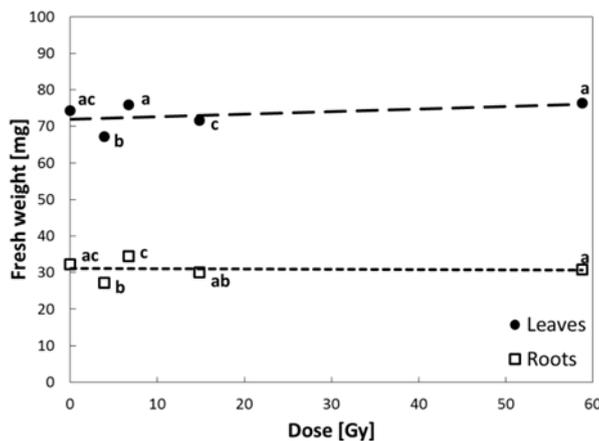
Figure 2. Fresh weight [mg] of roots and leaves of Arabidopsis seedlings exposed to 3.9 Gy, 6.7 Gy, 14.8 Gy and 58.8 Gy of gamma radiation. Data represent the mean ± SE of at least 140 biological replicates. Different letters indicate significant differences between the treatments (p<0.05).
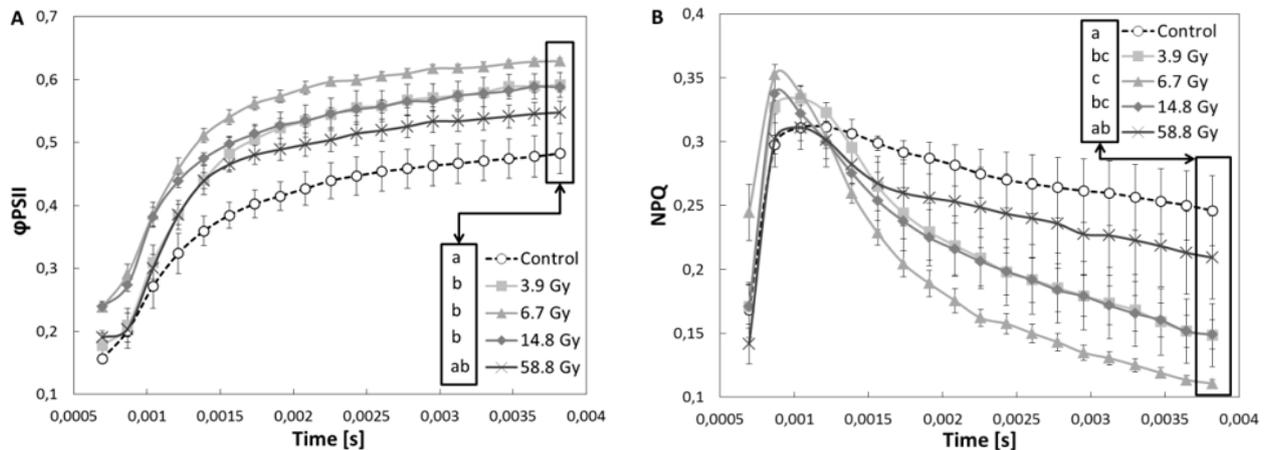
Figure 3: Quantum efficiency of PSII (φPSII) (A) and non-photochemical quenching (NPQ) (B) in Arabidopsis leaves exposed to different gamma radiation doses. Data represent the mean ± SE of 4 biological replicates. Statistical analyses were performed on the last data point of each curve. Different letters indicate significant differences between the treatments (p<0.05).

As these measurements were only performed at the end of the exposure treatment, it is conceivable that plants exposed to higher doses (58.8 Gy) also increased their PSII efficiency but already at an earlier stage. The increases of φPSII were accompanied by corresponding decreases in non-photochemical quenching (NPQ) (Figure 3B) but no alterations in non-regulated energy dissipation were observed (NO) (data not shown). Our results indicate that plants irradiated with 3.9 Gy to 14.8 Gy can hold their light harvesting capacity and start to optimize their photosynthetic process by increasing the efficiency of PSII and decreasing the heat dissipation.

No differences were observed in chlorophyll a and b concentrations or on total carotenoid concentrations following exposure to one week gamma radiation. As carotenoids can deactivate triplet chlorophyll and singlet oxygen they have an important protective role of PSII, but are also both the most radio-sensitive and fastest recovering pigments in plants (Kim et al., 2005).

Roots are more radio-sensitive than leaves

As plant cells contain a considerable amount of water, this will be an important radiation target resulting in the production of reactive oxygen species (ROS) which will cause important cellular damage. Superoxide dismutase (SOD) represents the first line of ROS-defense as it catalyzes the disproportionation of superoxide into hydrogen peroxide (McCord and Fridovich, 1969). Catalase (CAT) and peroxidases (PX) function as important hydrogen peroxide scavengers. To get an overview of the effects of gamma radiation on these ROS-scavenging enzymes, capacities of SOD, CAT, ascorbate peroxidase (APX), guaiacol peroxidase (GPX) and syringaldazine peroxidase (SPX) were determined in roots (Figure 4 A) and leaves (Figure 4B. In general it can be stated from Figure 4 that on the level of enzyme capacities the roots seem more radio-sensitive than leaves as enzyme capacities are mostly affected in the roots.
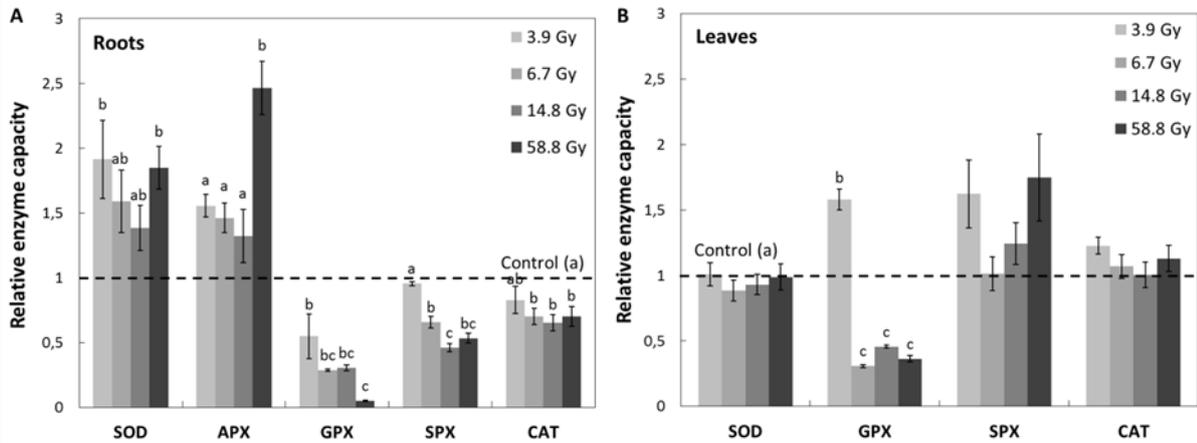
Figure 4: Capacities of reactive oxygen species (ROS)-scavenging enzymes in Arabidopsis roots (A) and leaves (B) exposed to different gamma radiation doses and expressed relative to the control (dashed line). Data represent the mean ± SE of 6 biological replicates. Different letters indicate significant differences between the treatments (p<0.05).

In the roots, SOD generally increased its capacity after irradiation, but only significantly for the lowest and highest radiation doses (Figure 4A). Capacities of CAT, SPX and GPX significantly decreased for almost all radiation conditions. GPX capacity decreased extremely after exposure to the highest radiation dose but in contrast APX capacity significantly increased at that radiation dose (Figure 4A). Leaves on the other hand seem less radiosensitive as most enzymatic capacities remain unaffected. However GPX was, in accordance with the roots, also highly affected in the leaves (Figure 4B). But while in the roots the GPX capacity already started to decrease after exposure to the lowest radiation dose, plant leaves are still able to increase the GPX capacity at this dose but at higher doses a significant decrease in GPX capacity also occurs in the leaves.

In conclusion, the experiments showed that when *Arabidopsis* seedlings are exposed to different gamma radiation doses at which no deleterious effects on growth and development are visible, the plants can already start optimizing their photosynthetic process in a transient way. On a subcellular level, plant roots seem more radiation-sensitive than leaves, which could be explained by a higher occurrence of water radiolysis in the roots and/or the protection of leaf cells against photo-oxidative damage. Overall, plants appear capable of defending and/or adapting themselves at the lower radiation doses while these mechanisms mostly disappeared at the higher radiation doses.

4.1.2.2. Two week gamma exposure of 7-day old seedlings *(part of the results are obtained within the post-doctoral fellowship of Rajesh Tewari)*

The biomass of plants exposed to different gamma dose rates for 14 days was in general significantly smaller than the control (Figure 5). However, as the control was kept in a room

(D-N°: 5.3) – Radiation Quality: studying sub-cellular modes of action using biomarkers and "omics" tools
Dissemination level: PU
Date of issue of this report: **29/11/2013**

adjacent to the exposure room it cannot be completed excluded that this difference is due to small differences in growth circumstances rather than exposure to gamma radiation. Comparing the different dose rates it seems that gamma radiation had a small growth promoting effect until a dose rate of 79.2 mGy h^{-1}, whereafter growth again slowed down in both roots and shoots.
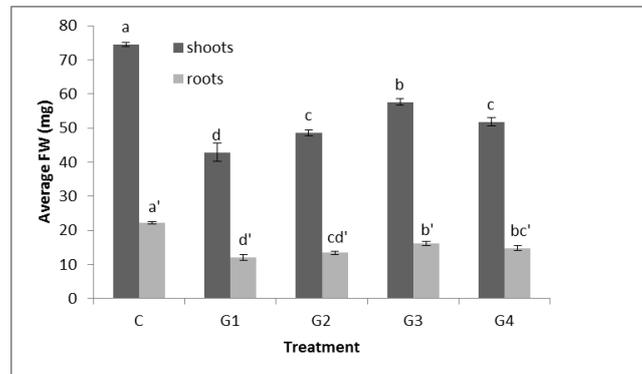

Figure 5: Fresh weight [mg] of roots and leaves of Arabidopsis seedlings exposed to 21.45 (G1) 36.25(G2), 79.15 (G3) 320.5 (G4) mGy h^{-1} of gamma radiation for 14 days. Data represent the mean ± SE of at least 100 biological replicates. Different letters indicate significant differences between the treatments (p<0.05).

14-day exposure to gamma radiation results in a dose-dependent antioxidative response.

The activity of different antioxidative enzymes was analysed in the plants exposed to 14days to different levels of gamma radiation (Figure 6A and 6B). Most enzymes showed a similar activity pattern in roots and shoots. In general enzyme activity did not show a significant difference compared to control (CAT, SOD) or was decreasing (SPX, APX) with increasing dose-rates. Only GPX activity was strongly induced at the lowest dose rate in leaves compared to control. Also in roots GPX was induced compared to control. However, GR showed a striking different response in roots compared to shoots. Whereas in shoots a dose dependent decrease in GR activity is observed, the activity of this enzyme is clearly induced in the roots. This pattern coincided with the redox state of GSH that was increasing *i.e.* more reduced in the roots whereas it was not significantly different in the shoots (data not shown). In addition the overall GSH+GSSG levels in shoots were decreasing with increasing dose rate in contrast to that in the roots. Therefore it is conceivable that the need for GR activity in the shoots is less at higher dose rates and still GSH redox status is maintained.
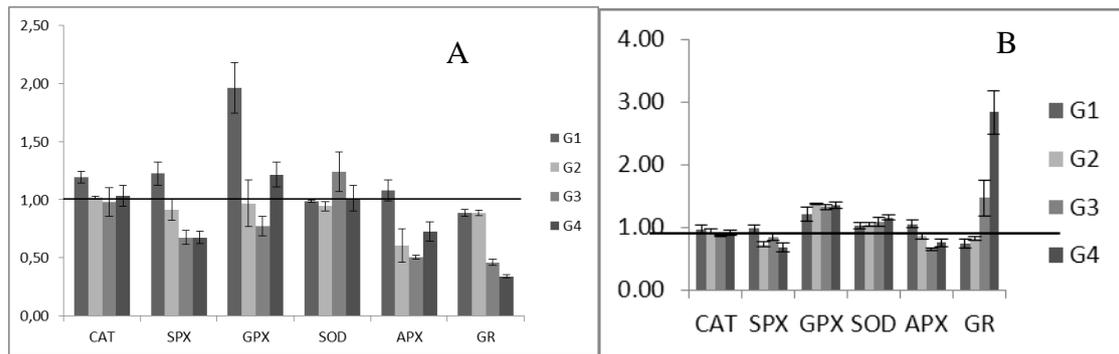
Figure 6: Capacities of reactive oxygen species (ROS)-scavenging enzymes in Arabidopsis leaves (A) and roots (B) exposed to 21.45 (G1) 36.25(G2), 79.15 (G3) 320.5 (G4) mGy h^{-1} of gamma radiation for 14 days and expressed relative to the control (line). Data represent the mean ± SE of 6 biological replicates.

The levels of ASC in the plant roots increase with increasing dose rate indicating plants are actively responding to the gamma-induced oxidative stress. This is, however, accompanied with a transient increase of DHA but certainly at higher dose rates it is clear that the roots exposed for 14 days to the highest gamma dose rates are able to keep a high redox status of the major antioxidants. Results on enzyme activity are mostly supported by similar increases or decreases in transcript levels of the different antioxidative enzymes (data not shown). Only the expression of GR was high in both roots and shoots despite the dose dependent decrease in GR activity levels in the shoots. Similar to the results obtained after 7 days we saw an increasing trend in APX activity with increasing dose rate in both roots and shoots (data not shown).

Correlation of gene-expression with gamma dose in roots

In search of a potential biomarker for gamma radiation-induced oxidative stress or DNA damage in plants we further analysed the transcription levels of genes involved in the active induction of ROS in plants, and in DNA damage and repair (see Figure 7 for expression of a limited number of antioxidative genes, other genes as depicted in Table 3 not shown). Unfortunately expression in leaves of control plants of all tested genes was very high compared to radiation-exposed ones independent of the dose rates applied. Therefore it is at this point hard to compare expression levels in leaves. In roots, however, clear radiation-dependent patterns could be observed (Figure 7). As such expression of several respiratory burst homologue genes increased in a dose-dependent manner in the roots. In addition also lipoxygenases were induced. Together the induction of RBOHs and LOX-genes indicate the induction of free radicals either through the formation of superoxide or the peroxidation of membrane lipids with the concomitant production of peroxy radicals as well as singlet oxygen. This formation of ROS is in addition to the hydrolysis of water known to be induced by gamma radiation. Hence exposure of plant roots to gamma radiation induces a substantive and long lasting oxidative burst in plants or at least in the roots. In addition RBOHs as well as LOX have been implicated in signal transduction pathways and the regulation of the oxidative stress responses in plants. As such their induction also indicates that plants are actively

defending themselves against the radiation induced stress. For a number of genes, including LOX, gene expression showed a transient increase with increasing dose-rates. This transient response is in contrast to the changes observed in most oxidative stress enzymes.
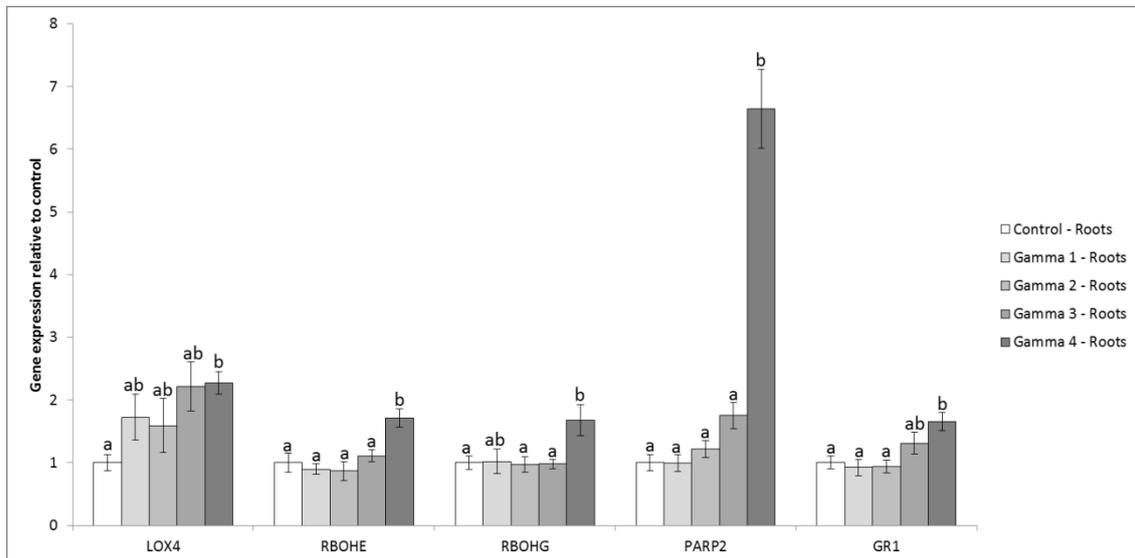

Figure 7: Relative gene expression levels of a limited number of genes involved in oxidative stress and DNA damage and repair in of Arabidopsis roots exposed to 21.45 (G1) 36.25(G2), 79.15 (G3) 320.5 (G4) Gy h-1 of gamma radiation for 14 days and expressed relative to the control (control is set at 1). Data represent the mean ± SE of 4 biological replicates.

Only a limited number of genes involved in DNA damage and repair were tested for gene expression. Selection was based on literature as well as on the results of Am-241-exposed *Arabidopsis* plants (see later sections). The most prominent change after exposure for 14 days to gamma radiation was found in Poly- (ADP-ribose])polymerase 2 (PARP2) expression (Figure 7) PARP2 is a protein involved in DNA repair after single strand breaks and in protein deacetylation. In addition it has been attributed roles in the maintenance of genomic integrity, control of cell cycle and in oxidative signal transduction. It is increased after exposure to a number of stressors and also, as indicated later, after exposure to Am-241.

In conclusion, in contrast to plants only exposed for one week to similar dose rates, after 14 days exposure, despite the observed decrease in growth, plants have re-established major oxidative stress defence mechanisms also at higher dose rates.

4.1.2.3. Four and seven day exposure of 14-day old seedlings to Am-241 *(the data obtained here are part of the PhD work of Geert Biermans)*

Plants were exposed for 4 or 7 days to different concentrations of Am-241. The measured activity concentrations of the Am-241 in solution corresponded relatively well with the desired nominal concentrations (Table 5). The amounts of Am-241 measured before and after stirring of the medium were identical (data not shown), indicating that most of the Am-241 was in solution. The transfer factors (based on dry weight) for Am-241 in the roots were significantly higher at 4 days for the 36700 Bq L^{-1} treatment compared to other treatments (Table 6). A similar observation could be made for the concentration ratio (based on fresh weight) (Table 7). Both were roughly 2-fold higher. However, at 7 days this difference has disappeared for both parameters due to a significant 2-fold decrease in transfer factor in the highest Am-241 treatment. For the other treatments, concentration ratios and transfer factors for the roots remained identical between harvest points.

Table 5: Nominal and soluble activity concentrations for each Am-241 treatment. Values presented are mean ± SE of 4 replicates.

Activity Concentration [Bq L^{-1}]	
Nominal	In solution (after stirring)
0	0.01 ± 0.01
50	60 ± 5
500	360 ± 30
5 000	2970 ± 140
50 000	36700 ± 1100

Table 6: *Transfer factors for Arabidopsis thaliana seedlings exposed for 4 and 7 days to Am-241. Results present mean ± S.E. of at least 3 biological replicates. Analysis was done separately for each tissue type. Differences in lower case letters indicate significant differences in dose rate between treatments on the same harvest day (p<0.05). Differences in upper case letters indicate significant differences in dose rate between harvest points for a specific treatment (p<0.05).*

		^{241}Am Transfer Factor [Bq kg^{-1} DW / Bq L^{-1}]	
		ROOTS	SHOOTS
4 DAYS	60 Bq L^{-1}	[ac] 3350 ± 160 [A]	-
	360 Bq L^{-1}	[a] 3000 ± 500 [A]	[a] 46.4 ± 1.9 [A]
	2970 Bq L^{-1}	[bc] 5530 ± 250 [A]	[b] 290 ± 27 [A]
	36700 Bq L^{-1}	[b] 6100 ± 1100 [A]	[b] 337 ± 25 [A]
7 DAYS	60 Bq L^{-1}	[a] 3950 ± 220 [A]	-
	360 Bq L^{-1}	[a] 3700 ± 300 [A]	[a] 32 ± 4 [A]
	2970 Bq L^{-1}	[b] 4500 ± 500 [A]	[b] 138 ± 17 [B]
	36700 Bq L^{-1}	[a] 3410 ± 29 [B]	[b] 199 ± 18 [B]

Table 7: *Concentration Ratios for Arabidopsis thaliana seedlings exposed for 4 and 7 days to Am-241. Results present mean ± S.E. of at least 3 biological replicates. Analysis was done separately for each tissue type. Differences in lower case letters indicate significant differences in dose rate between treatments on the same harvest day (p<0.05). Differences in upper case letters indicate significant differences in dose rate between harvest points for a specific treatment (p<0.05).*

		^{241}Am Concentration Ratio [Bq kg^{-1} FW / Bq L^{-1}]		
		ROOTS	SHOOTS	TOTAL PLANT
4 DAYS	60 Bq L^{-1}	[ab] 151 ± 21 [A]	-	[a] 60 ± 3 [A]
	360 Bq L^{-1}	[b] 126 ± 27 [A]	[a] 5 ± 0.2 [A]	[a] 55 ± 9 [A]
	2970 Bq L^{-1}	[ac] 250 ± 40 [A]	[b] 30.7 ± 2.2 [A]	[b] 119 ± 8 [A]
	36700 Bq L^{-1}	[cd] 300 ± 40 [A]	[b] 38 ± 3 [A]	[b] 116 ± 15 [A]
7 DAYS	60 Bq L^{-1}	[ab] 152 ± 12 [A]	-	[ab] 67,4 ± 2,6 [A]
	360 Bq L^{-1}	[b] 120 ± 9 [A]	[a] 3.6 ± 0.6 [A]	[ab] 62,1 ± 2,9 [A]
	2970 Bq L^{-1}	[ac] 201 ± 25 [A]	[b] 15.3 ± 1.6 [B]	[a] 92 ± 7 [A]
	36700 Bq L^{-1}	[b] 92 ± 8 [B]	[b] 22.6 ± 1.9 [B]	[bc] 56 ± 3 [B]

Internal and external root dose rates and internal shoot dose rates at each harvest point, and the corresponding absorbed doses over the exposure period, were determined by the plant dosimetry method described in (Biermans et al., 2013), which uses separate dosimetry models for *Arabidopsis* root and shoot, and is based on the measured activity concentrations in the organs. Shoot dose conversion coefficient (DCC) values for each harvest point were determined by taking into account the leaf area measurements. Doses were calculated under assumption of linear increase in tissue activity concentration during the exposure. The estimated dose rates are depicted in Table 8. Dose rates in the roots at 4 days increased correlated well with the nominal environmental activity concentration of Am-241. Between 4 and 7 days, the dose rates remained constant, except in the 36700 Bq L^{-1} treatment, where it was reduced from 35 mGy h^{-1} with a factor 3 to 10.8 mGy h^{-1} due to a decline in medium-to-root transfer (Table 8). It has to be noted that in the roots, the external contribution to the dose rate is considered to be zero, due to the short range of α-particles. Total absorbed doses in the roots amounted to 1.7 and 3.3 Gy respectively at 4 and 7 days at the highest Am-241 activity concentration.

Biomarker assays and growth response in Arabidopsis plants exposed for 4 or 7 days to different Am-241 concentrations.

After estimating the external and internal dose absorbed in the plants the possible effect on plant growth, photosynthesis and different possible oxidative stress and DNA damage and repair parameters was estimated. At level of the individual plants both growth responses, measured as biomass and photosynthetic performance was evaluated. The biomass of the shoots measured was not affected by the Am-241-treatment. Results show that root fresh weight and dry weight were affected in a dose-dependent way by exposure to Am-241 at 4 and 7 days. Root dry weight was decreased by 48% at 7 days in the highest treatment.

*Table 8. Dose rates (A) and Total absorbed doses (B) for Arabidopsis thaliana seedlings exposed for 4 and 7 days to Am-241. Results present mean ± S.E. of at least 3 biological replicates. Analysis was done separately for each tissue type. Significant differences in dose rate between harvest days are shown as * p<0.05; **p<0.01; ***p<0.001*

A

		Am-241 Dose rates [µGy/h]	
		ROOTS	SHOOTS
4 DAYS	*0 Bq L⁻¹*	<0.5	<0.6
	60 Bq L⁻¹	29 ± 4	<1.0
	360 Bq L⁻¹	140 ± 30	5.66 ± 0.23
	2970 Bq L⁻¹	2400 ± 400	291 ± 21
	36700 Bq L⁻¹	35000 ± 5000	4500 ± 400
7 DAYS	*0 Bq L⁻¹*	<0.6	<1.0
	60 Bq L⁻¹	29.6 ± 2.3	<0.5
	360 Bq L⁻¹	135 ± 10	4.1 ± 0.7
	2970 Bq L⁻¹	1910 ± 240	145 ± 15
	36700 Bq L⁻¹	10800 ± 900***	2650 ± 22

B

		Am-241 Dose [mGy]	
		ROOTS	SHOOTS
4 DAYS	*0 Bq L⁻¹*	<0.005	<0.12
	60 Bq L⁻¹	1.41 ± 0.19	<0.05
	360 Bq L⁻¹	6.9 ± 1.4	0.271 ± 0.011
	2970 Bq L⁻¹	113 ± 18	14 ± 1
	36700 Bq L⁻¹	1670 ± 240	214 ± 19
7 DAYS	*0 Bq L⁻¹*	0.03 ± 0.019	<0.24
	60 Bq L⁻¹	3.5 ± 0.3	<0.1
	360 Bq L⁻¹	16.9 ± 2	0.62 ± 0.03
	2970 Bq L⁻¹	267 ± 28	29.7 ± 1.7
	36700 Bq L⁻¹	3300 ± 300	470 ± 30

No biological significant effects were observed in the maximum efficiency of photosynthesis, measured as Fv/Fm, in any of the treatments (data not shown). By following chlorophyll fluorescence we were able to further dissect the photosynthetic process as described above for plants exposed for 7-days to gamma radiation. After 4 days of exposure to Am-241, none of the estimated parameters (the photosynthetic yield, the yield in photochemical quenching or in the non-photochemical quenching) showed dose-dependent changes. In contrast after 7 days there were clear effects on energy use within the photosynthetic process. Up to 145 µGy h^{-1} delivered over a period of 7 days, there was a significant declining trend in regulated non-photochemical quenching (data not shown). This reduction in buffering by regulated heat dissipation was accompanied by a corresponding increase in photosynthetic yield (data not shown). At the highest dose rate (2650 µGy h^{-1}) however, the quantum yield of photosynthesis was reduced by 4% compared to the control treatment. This was a result of significantly increased non-regulated non-photochemical quenching (data not shown) rather than controlled heat dissipation, indicating a loss of photo-protective capacity. An increase in non-regulated non-photochemical quenching is taken as a sign of irreparable damage to the photosynthetic apparatus. No real big changes in the concentrations of different photosynthesis relevant pigments (chlorophyll a, chlorophyll b and carotenoids) were found (data not shown).

Base modification by oxidative damage in the roots was measured spectrophotometrically by ELISA as the concentration of 8-OHdG in the genomic DNA. No significant changes in levels of modified base were found at either harvest point (data not shown).

We measured the expression in *Arabidopsis* seedlings of different genes involved in DNA damage and repair and the cell cycle after exposure to α-radiation from ^{241}Am for 4 and 7 days. For DNA damage and repair related genes transcript levels are shown in Table 9 (roots) and Table 10 (shoots). Transcription data of (anti)oxidative genes are not shown.

In the roots (Table 9), genes involved in the homologous recombination pathway (*RAD51 / DMC1*) were up-regulated at 4 days starting at 140 µGy h^{-1}, but showed no difference to the control treatment at 7 days. For the non-homologous end-joining pathway (NHEJ), only DNA ligase IV (*LIG4*) was differentially expressed after 7 days at 1910 µGy h^{-1}. Repair of organelle DNA was also up-regulated starting at 140 µGy h^{-1} at 4 days, as measured by the transcript levels of Polymerase Gamma 1 (*POLG1*), but not after 7 days.

Transcript levels of PARP2 (Poly- (ADP-ribose])polymerase 2), a protein involved in the signalling response to single-stranded breaks (SSB) in DNA, were significantly increased compared to control at both time points. At 4 days, transcripts were elevated at 140 and 2400 µGy h^{-1}, whereas those at 1910 µGy h^{-1} and 10800 µGy h^{-1} were increased at 7 days of ^{241}Am exposure. *PARP1*, however, did not show dose-rate dependent expression. Among the genes involved in the cell cycle, only GAR1 was differentially expressed, with strong up-regulation at 140 µGy h^{-1} at 4 days, and above 1910 µGy h^{-1} after 7 days. *CKS1*, which is involved in cell cycle timing, showed an increasing trend in expression levels at both time points.

No changes in gene expression were found in the shoots, except for *PARP2*, which was up-regulated starting at 4.1 µGy h^{-1} at 7 days of exposure (Table 10).

For plants exposed for only for 4-days to different levels of Am-241 transcription showed up-regulation of enzymes involved in the ascorbate-glutathione cycle (*APX1/GR1*), *PARP2* signalling and DSB DNA repair pathways (*LIG4*/*RAD51*) starting at 140 µGy h^{-1} . Steady-state oxidative DNA damage did not increase throughout exposure, indicating that DNA repair was able to keep up with the rate of single-strand radiation damage. Up to 2,400 µGy h^{-1}, we found up-regulation of superoxide (O$_2$$^{\bullet-}$) CuZnSOD scavengers (*CSD1/3*) and hydrogen scavenging catalases (*CAT2/3*), while in the highest treatment (35,000 µGy h^{-1}) there was an increase in lipoxygenase (*LOX1*) and ROS-producing NADPH oxidase (*RBOHA*) transcripts, which suggests the involvement of jasmonate signalling and oxidative burst. After 7-days exposure most molecular and physiological effects in the roots were found at the two highest dose rates, with a very strong up-regulation of genes involved in cell cycle arrest (*CKS1/GAR1*). In the highest treatment, the transcripts of NADPH oxidase RBOHC and LOX1 were respectively increased and suppressed, indicating that jasmonate signalling is transient and that several NADPH oxidases are involved in the response.

Table 9: Gene expression of genes involved in DNA repair and the cell cycle in the roots of Arabidopsis thaliana after exposure to 241Am for 4 and 7 days. Data are presented relative to 0 Bq L-1. Dark grey shading indicate significant up-regulation (p<0.05) compared to the control at that time point. Light grey shading indicates significant down-regulation (p<0.05). Values are mean ± SE of at least 3 biological replicates.

		0 Bq L^{-1}	50 Bq L^{-1}	500 Bq L^{-1}	5 000 Bq L^{-1}	50 000 Bq L^{-1}
	4 d	0 $\mu Gy\ h^{-1}$	29 $\mu Gy\ h^{-1}$	140 $\mu Gy\ h^{-1}$	2400 $\mu Gy\ h^{-1}$	35000 $\mu Gy\ h^{-1}$
	7 d	0 $\mu Gy\ h^{-1}$	30 $\mu Gy\ h^{-1}$	135 $\mu Gy\ h^{-1}$	1910 $\mu Gy\ h^{-1}$	10800 $\mu Gy\ h^{-1}$
KU80	4 d	1.00 ± 0.06	1.05 ± 0.05	1.16 ± 0.22	0.97 ± 0.06	0.81 ± 0.13
	7 d	1.04 ± 0.20	0.49 ± 0.03	0.43 ± 0.03	1.15 ± 0.24	1.14 ± 0.27
LIG4	4 d	1.00 ± 0.11	1.91 ± 0.72	4.02 ± 0.76	2.70 ± 0.64	2.13 ± 0.92
	7 d	1.64 ± 0.36	0.92 ± 0.22	1.22 ± 0.35	4.95 ± 1.34	3.62 ± 0.89
RAD51	4 d	1.00 ± 0.33	0.78 ± 0.42	3.96 ± 1.19	3.10 ± 0.90	4.10 ± 1.19
	7 d	2.63 ± 0.91	2.51 ± 0.80	3.86 ± 0.94	3.17 ± 1.26	1.77 ± 1.05
DMC1	4 d	1.00 ± 0.34	1.60 ± 0.60	2.15 ± 0.60	7.05 ± 2.53	3.70 ± 1.34
	7 d	1.96 ± 0.82	1.94 ± 0.63	1.83 ± 0.63	0.84 ± 0.28	1.26 ± 0.81
PARP1	4 d	1.00 ± 0.91	1.04 ± 1.08	3.10 ± 2.19	2.82 ± 1.81	2.52 ± 1.97
	7 d	1.62 ± 1.08	0.50 ± 0.34	0.42 ± 0.29	1.23 ± 0.95	0.86 ± 0.63
PARP2	4 d	1.00 ± 0.37	0.45 ± 0.18	2.83 ± 0.83	2.57 ± 0.70	1.25 ± 0.39
	7 d	0.52 ± 0.14	0.89 ± 0.33	0.85 ± 0.25	2.72 ± 0.86	2.43 ± 0.90
LPP1	4 d	1.00 ± 0.20	0.29 ± 0.05	2.81 ± 1.40	1.96 ± 0.64	1.79 ± 0.59
	7 d	5.23 ± 1.28	4.34 ± 0.91	14.9 ± 4.80	11.9 ± 5.70	9.04 ± 2.20
POLG1	4 d	1.00 ± 0.13	1.18 ± 0.32	4.79 ± 1.20	3.99 ± 0.74	3.46 ± 0.67
	7 d	1.77 ± 0.29	1.31 ± 0.28	1.24 ± 0.26	1.93 ± 0.43	1.65 ± 0.38
CKS1	4 d	1.00 ± 1.25	0.52 ± 0.53	7.39 ± 6.86	3.96 ± 3.62	3.48 ± 3.14
	7 d	1.32 ± 1.24	2.00 ± 1.90	1.32 ± 1.18	8.74 ± 8.18	6.39 ± 5.66
GAR1	4 d	1.00 ± 1.39	0.05 ± 0.06	7.54 ± 7.74	4.03 ± 4.03	9.25 ± 9.25
	7 d	9.82 ± 10.3	3.81 ± 3.99	3.69 ± 3.67	25.4 ± 25.8	16.8 ± 16.9

Table 10: Gene expression of genes involved in DNA repair and the cell cycle in the shoots of Arabidopsis thaliana after exposure to 241Am for 4 and 7 days. Data are presented relative to 0 Bq L-1. Dark grey shading indicate significant up-regulation (p<0.05) compared to the control at that time point. Light grey shading indicates significant down-regulation (p<0.05). Values are mean ± SE of at least 3 biological replicates.

		0 Bq L^{-1}	50 Bq L^{-1}	500 Bq L^{-1}	5 000 Bq L^{-1}	50 000 Bq L^{-1}
	4 d	0 µGy h^{-1}	<1.0 µGy h^{-1}	5.7 µGy h^{-1}	291 µGy h^{-1}	4500 µGy h^{-1}
	7 d	0 µGy h^{-1}	<0.5 µGy h^{-1}	4.1 µGy h^{-1}	145 µGy h^{-1}	2650 µGy h^{-1}
KU80	4 d	1.00 ± 0.23	0.75 ± 0.16	0.69 ± 0.22	1.26 ± 0.21	0.58 ± 0.14
	7 d	0.91 ± 0.20	1.21 ± 0.23	1.42 ± 0.28	1.89 ± 0.44	2.38 ± 0.66
LIG4	4 d	1.00 ± 0.31	1.14 ± 0.41	0.74 ± 0.19	0.80 ± 0.19	1.40 ± 0.61
	7 d	0.68 ± 0.15	0.65 ± 0.18	0.67 ± 0.16	0.55 ± 0.16	0.77 ± 0.21
RAD51	4 d	1.00 ± 0.31	1.36 ± 0.45	0.75 ± 0.22	0.86 ± 0.21	0.93 ± 0.45
	7 d	0.69 ± 0.16	0.65 ± 0.18	0.67 ± 0.16	0.57 ± 0.14	0.95 ± 0.26
DMC1	4 d	1.00 ± 0.31	1.14 ± 0.41	0.74 ± 0.19	0.80 ± 0.19	1.40 ± 0.61
	7 d	0.68 ± 0.15	0.65 ± 0.18	0.67 ± 0.16	0.72 ± 0.22	0.9 ± 0.23
PARP1	4 d	1.00 ± 0.06	0.54 ± 0.16	0.62 ± 0.2	1.23 ± 0.27	0.45 ± 0.05
	7 d	0.95 ± 0.18	1.47 ± 0.15	1.60 ± 0.28	1.41 ± 0.20	1.69 ± 0.25
PARP2	4 d	1.00 ± 0.26	0.79 ± 0.26	0.35 ± 0.08	0.77 ± 0.22	1.46 ± 0.83
	7 d	0.39 ± 0.09	1.05 ± 0.21	1.13 ± 0.26	1.13 ± 0.24	1.47 ± 0.38
LPP1	4 d	1.00 ± 0.31	1.36 ± 0.45	0.74 ± 0.19	0.80 ± 0.19	1.40 ± 0.61
	7 d	0.68 ± 0.15	0.65 ± 0.18	0.67 ± 0.16	0.75 ± 0.27	0.9 ± 0.23
POLG1	4 d	1.00 ± 0.31	1.14 ± 0.41	0.74 ± 0.19	0.80 ± 0.21	1.40 ± 0.61
	7 d	0.69 ± 0.16	0.65 ± 0.18	0.67 ± 0.16	0.72 ± 0.22	0.90 ± 0.23
CKS1	4 d	1.00 ± 0.53	5.65 ± 2.14	1.21 ± 0.74	2.88 ± 1.10	1.05 ± 0.47
	7 d	1.47 ± 0.57	2.07 ± 1.09	3.68 ± 1.39	2.76 ± 1.41	3.05 ± 1.43
GAR1	4 d	1.00 ± 0.42	0.08 ± 0.03	0.25 ± 0.19	0.18 ± 0.06	0.91 ± 0.62
	7 d	0.19 ± 0.06	0.59 ± 0.29	0.21 ± 0.07	0.18 ± 0.09	0.69 ± 0.47

Finally, we analysed the state of the ascorbate-glutathione scavenging pathway in roots and shoots after 7 days by spectrophotometrically measuring the concentration levels of the reduced and oxidised forms of ascorbate and glutathione (Figures 8 and 9). These levels also allowed for a calculation of the reduction state of each redox couple. In the shoots, total Ascorbate levels remained constant at all dose rates, while the redox couple shifted progressively towards the oxidised form, with significantly reduced AsA levels and increased DHA levels at 2650 µGy h^{-1}).

At this dose rate, the reduction state had decreased to 63%. Together with the decrease in photosynthetic performance at this dose rate it is clear that plants are under heavy oxidative stress.
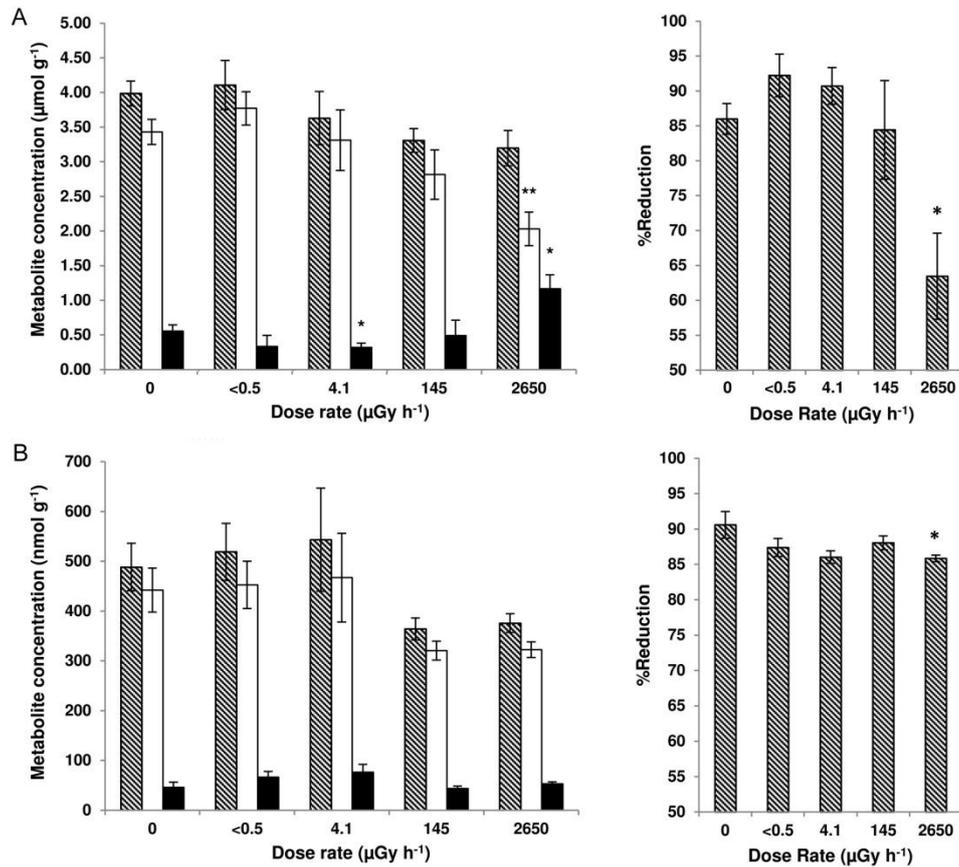

*Figure 8: Antioxidative metabolite concentrations in Arabidopsis shoots exposed to 241Am for 7 days. **A.** Concentrations of total ascorbate (AsA + DHA; grey bars), reduced ascorbate (white bars), dehyroascorbate (DHA; black bars) and the reduction status (right graph). B. Concentrations of total glutathione (GSH + GSSG; grey bars), GSH (white bars) , GSSG (black bars) and the degree of reduction (right graph). Significance levels for each metabolite compared to control are * p<0.05, ** p<0.01 *** p<0.001. Values are mean and SE of at least 3 biological replicates.*
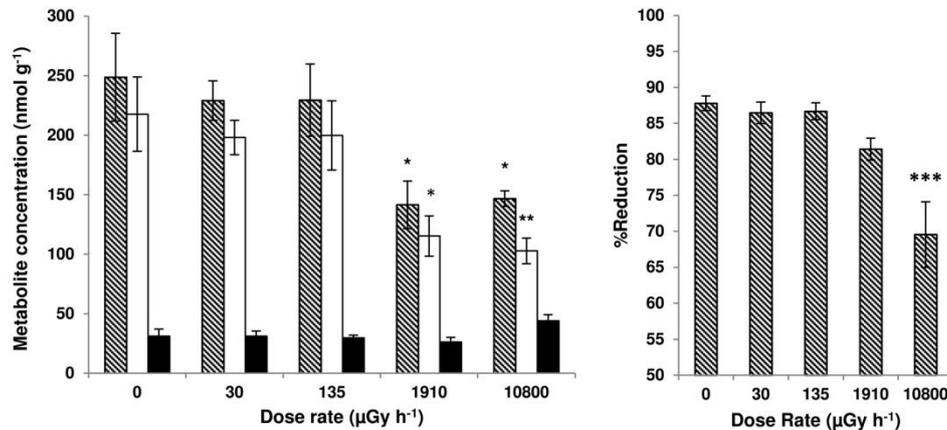
*Figure 9: Concentrations of total glutathione (GSH + GSSG; grey bars), GSH (white bars) , GSSG (black bars) and the degree of reduction (right graph) in Arabidopsis roots exposed to 241Am for 7 days. Significance levels for each metabolite compared to control are * p<0.05, ** p<0.01 *** p<0.001. Values are mean and SE of at least 3 biological replicates.*

Glutathione levels remained constant at all dose rates (Figure 8) for total glutathione, the oxidised form GSSG and the reduced form GSH. However, as for ascorbate, the reduction state of the GSH/GSSG couple was significantly decreased by 5% at 2650 µGy h^{-1}.

4.1.3 Conclusions and perspectives

Experiments were set up to compare the effects induced in plants exposed to external gamma with those induced by alpha radiation added as Am-241. It was the intention to establish first dose response curves for individual endpoints like growth or photosynthesis. As Am-241 is an element that predominately accumulates in the roots with little transfer to the shoots, alpha exposure was not homogenous over the total plant. As such roots were much more exposed then shoots with a maximum dose rate in the roots of 10.8 mGy h^{-1} and a total dose of 3.3Gy to gamma. Due to safety regulations Am-241 could, within our experimental set up, not be administered in higher concentrations. Hence, we were unable to reach higher dose rates. However, we can say that there is a small overlap between the highest dose rate for gamma radiation can the lowest dose delivered to the plants in the 7-day gamma exposure experiment.

We were unable to obtain full dose response curves for growth (estimated as biomass) under the current experimental set up. As such it is confirmed here that *Arabidopsis* is rather radiation resistant. Small decreases in growth were only observed at the highest total dose of gamma (106 Gy at 320 mGy h^{-1} (14 day exposure)) and at the highest alpha dose rates. Although these data are very limited and exposure situations were not completely comparable (alpha more restricted to the roots

whereas gamma evenly distributed over the whole plants) these data do confirm that exposure to alpha radiation is more deleterious than a comparable gamma dose. The data are however too preliminary to enable RBE calculation in plants, however they form a good basis for future experiments aiming in this direction.

Different possible biomarkers were tested at cellular, biochemical and molecular level. Clearly both gamma and alpha radiation induce a strong oxidative challenge in the plants as visualised by changes in antioxidants, antioxidative enzyme activities and gene expression. The enhancement in photosynthesis efficiency is a clear gamma radiation induced effect that was not present in the alpha-exposed plants at least in the current experimental set up. It cannot be concluded from this study that alpha radiation might not have the same effect on photosynthesis as gamma as the total dose of alpha radiation in the photosynthetic active shoots is much lower than that of gamma radiation.

In general gene expression of genes involved in antioxidative response and in DNA repair seemed to be more prominently present in alpha exposed compared to gamma exposed plants. As for the growth response the changes in gene expression were also observed at much lower dose rates for the alpha-exposed plants. However, it is very difficult to use these data for RBE comparison as exposure conditions were strongly different between the alpha and gamma-exposed plants. For alpha radiation deliverd as Am-241 distribution over tissues and organs or even at a cellular level was not homogeneous and was also not evenly in function of time (depending on the actual uptake of Am-241).

Based on the results the dose-dependent increase in gene expression of PARP2 observed both under gamma and alpha radiation was most striking. At least for alpha radiation changes in PARP2 expression were visible long before changes in biomass were observed. As PARP2 is a protein strongly involved in DNA repair of single strand breaks as well as in oxidative stress signalling in plants it is a possible candidate for a biomarker for alpha and gamma radiation. However also here further research is needed to look at the specificity of this response to radiation compared to other stressors. Also the kinetics of the different possible biomarkers should be further investigated.

4.2 Zebrafish

The zebrafish studies continue the work on exploring the underlying mechanisms for differences in gamma and alpha irradiation. Two sets of studies have been carried out. The first in vitro studies on zebrafish cell cultures with a main focus on MoA investigations, including address the effect of ionizing radiation under various contaminant exposure conditions. The second reports a pilot study on comparing gamma and alpha irradiation in vivo, which involved co-ordinating experiments between IRSN and UMB. Those studies are not yet complete, so only preliminary results are presented here.

Even if DNA damage is the primary event of ionizing radiation effects, a precise knowledge on MoA of gamma versus alpha irradiation is not yet achieved, particularly in the case of non-human species. The main objective of linking cell culture studies with experiments on whole body organisms is to examine the power of "omics" fingerprints for predicting individual life traits consequences of low dose exposure of alpha and gamma emitters. An in vitro approach is proposed to develop cost-effective, predictive tools for radionuclide ecological risk assessment, using information collected from the molecular to the individual responses. The mechanistic information gained from advanced methods in the 'omic-area' will produce early warning and specific biomarkers.

4.2.1 Zebrafish Fibroblasts – Cell Cultures

4.2.1.1. Overview and Objectives

The MoA of gamma and alpha irradiation were studied. The temporal evolution of these responses was assessed, together with their persistence in zebrafish cells. To address potential health risks associated with radiation exposure, the long-term biological consequences of targeted and non-targeted effects in exposed cells and their progeny should be described. The bystander effect was used to describe an effect in which cells that have not been exposed to radiation are affected by irradiated cells though various intracellular signaling mechanisms (Barcellos-Hoff et al, 2001; Azzam et al, 1998; Mothersill and Seymour, 1997). This phenomena occurs when cells which are not directly exposed to radiation, but which receive signals from irradiated cells, respond as though they were irradiated (Mothersill, 2004; Postiglione et al, 2010). Embryogenesis is a particularly radiosensitive stage of the vertebrate life cycle, and zebrafish embryos are ideal for evaluating genotoxic stress as well as radiation-related studies (Yasuda et al, 2006; Jarvis and Knowles, 2003).

In the first study performed at the IRSN laboratory, the radiation-induced bystander effect and the radioadaptive response was investigated in embryonic zebrafish cells (ZF4) exposed to chronic gamma rays. In the second experiment, , the radiation-induced bystander effect in embryonic zebrafish cells (ZF4) exposed to acute alpha rays was done to the aim of comparing acute gamma irradiation effects (previously showed in Pereira et al, 2011) and alpha irradiation effects.

4.2.1.2. Bystander effect and radioadaptation in ZF4 cells exposed to chronic gamma rays *(All results were compiled in an article of Pereira et al, submitted to Plos One)*

According to the literature, ZF4 cells were irradiated with doses of gamma rays ranging from 0.01-0.1 Gy. Under different experimental conditions, the production and repair of DSBs in the embryonic zebrafish ZF4 cell line was assessed. In addition, epigenetics effects via a global methylation analysis and a determination of the factors involved in the bystander effect and

radioadaptative response were examined with the use of OMICS (i.e secretome analysis). All these results were compiled in an article of Pereira et al, submitted to Plos One.

a) Experimental Set Up

One day before irradiation, 1×10^5 cells were seeded in 18 mm diameter slides. Cells were irradiated 4 h at 28°C with a total dose of 12 mGy (dose rate of 70 mGy/d) or 92 mGy (dose rate of 550 mGy/d) of gamma rays that were generated by a ^{137}Cs gamma irradiator. Then inserts with irradiated cells were placed with non-irradiated cells (called bystander cells 1) or the medium from irradiated cells was placed with non-irradiated cells (called bystander cells 2). Cells were co-cultured in these two conditions for 1-24h (Figure 10). Irradiated and non-irradiated cells were then fixed and analyzed for the occurrence of gamma-H2AX foci at the time periods indicated (1h, 2h, 4h and 24 h). To assess the nature of the secreted factor involved in early bystander effect, the irradiated culture medium was either heated at 100 °C during 10 min or ultrafiltered using Amicon ultracentrifugal filter devices with a 3 kDa cut-off (Millipore) operated at 4°C by centrifugation at 4500 g. The resulting samples were then applied on non-irradiated cells during 1h. After the incubation the occurrence of gamma-H2AX was observed in the treated cells.
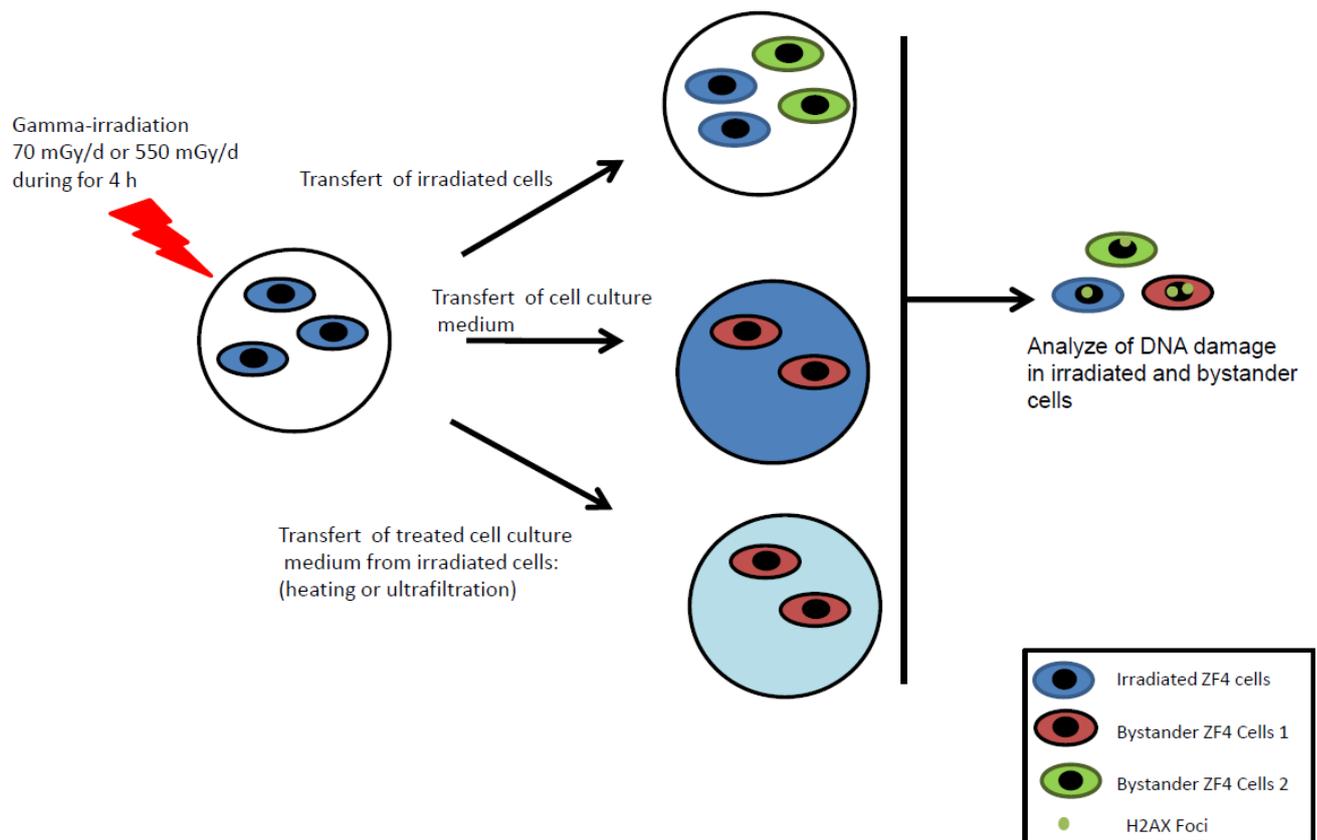

Figure 10: Experimental design for bystander experiments

b) Radioadaptation experiments

One day before irradiation, 1×10^5 cells were seeded in 18 mm diameter slides. Cells were irradiated 4 h at 28°C with a total dose of 12mGy (dose rate of 70 mGy/d) or 92 mGy (dose rate of 550 mGy/d) of gamma rays that were generated by a ^{137}Cs gamma irradiator (see below). Culture medium from irradiated cells were placed with non-irradiated cells and co-cultured for 1h at 28°C and then further irradiated 20h at 28°C with a challenging dose of 58 mGy (dose rate of 70 mGy/d) or 460 mGy (dose rate of 550 mGy/d) (Figure 11). Irradiated and non-irradiated cells were fixed and analyzed for the occurrence of gamma-H2AX foci at the time periods indicated (1h, 2h, 4h and 24 h).
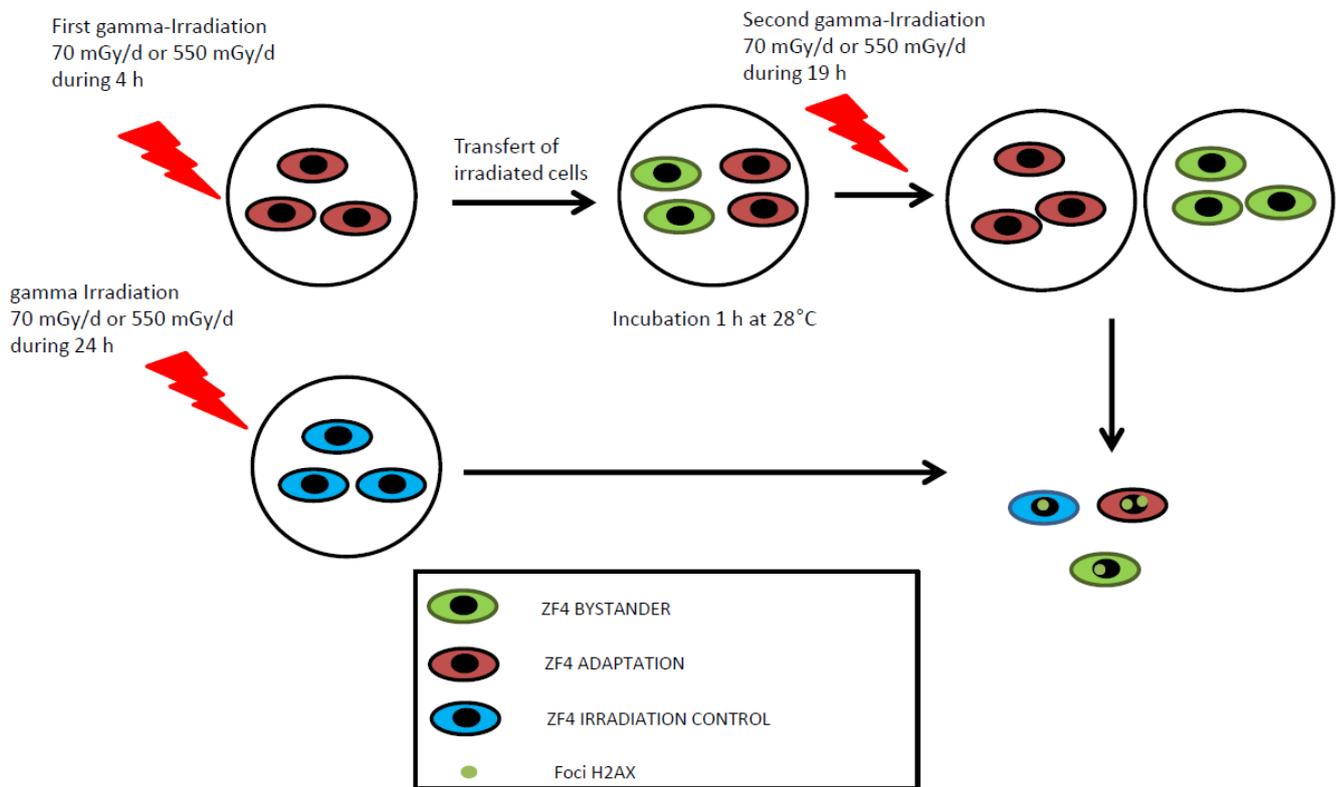

Figure 11: Experimental design for radioadaptation experiments

c) Results

### Induction of gamma-H2AX foci in targeted and bystander cells at very low doses of gamma irradiation

To investigate the bystander effect and the response to DNA damages, ZF4 cells were irradiated during 4 hours at two different dose-rates. Following irradiation, the medium from irradiated cells (bystander cells 1) or the irradiated cells were placed near non- irradiated cells (bystander cells 2)

during 1 hour. We then examined the presence of DNA double strand breaks at 1, 2, 4 and 24 hours post-irradiation via the detection of gamma-H2AX foci in irradiated and bystander cells. Doses rates of 70 mGy/d and 550 mGy/d during 4 hours which represents total doses of 12 mGy or 92 mGy were used respectively (Figures 12A and 12B). For both doses, the number of gamma-H2AX foci was higher in irradiated cells than in bystander cells. An average of 2.7 foci (Figure 12A) or 5.8 gamma-H2AX foci (Figure 12B) could be detected in the nucleus of irradiated cells 1 h after irradiation. For the lower dose (70 mGy/d), bystander cells 1 (culture medium transferred) presented at 1 hour post-irradiation a higher number of H2AX foci than bystander cells 2 (irradiated cells transferred) with an average of 2.2 vs 1.3 foci, respectively (Figure 12A). This implies that a soluble factor contained in the culture medium of irradiated cells is responsible of the appearance of DNA double strand breaks in non-irradiated cells. On the same way for the higher dose, the number of foci in bystander 1 cells (culture medium transferred) is higher than in bystander 2 cells (cells transferred), with an average of 3.6 vs 2.7 foci of gamma-H2AX, respectively (Figure 12B).

A
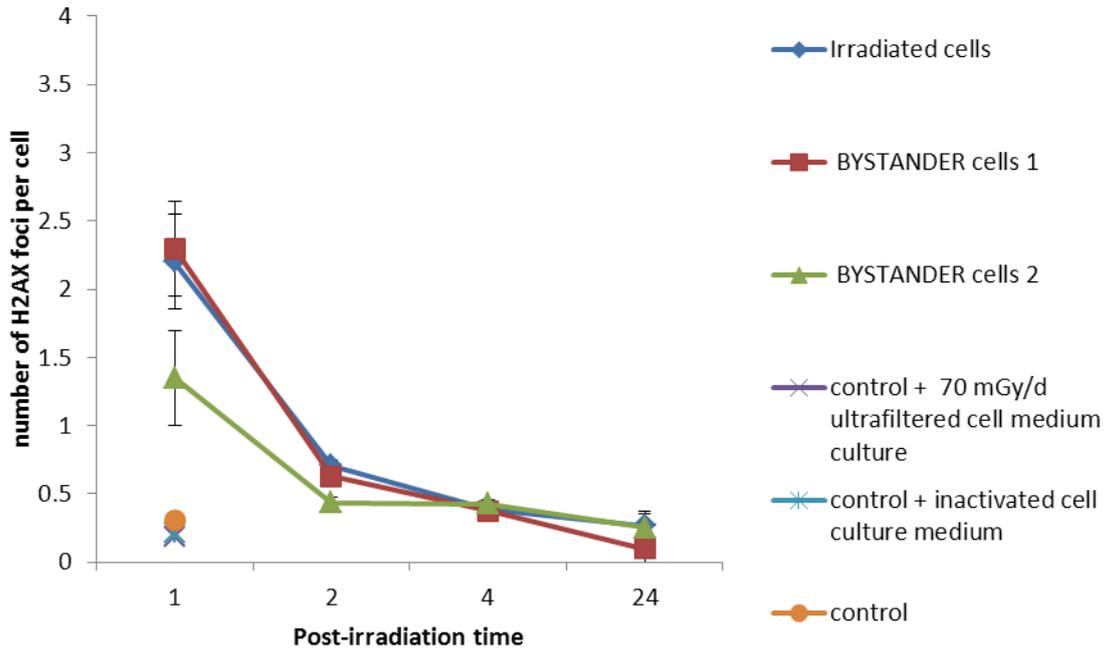
B
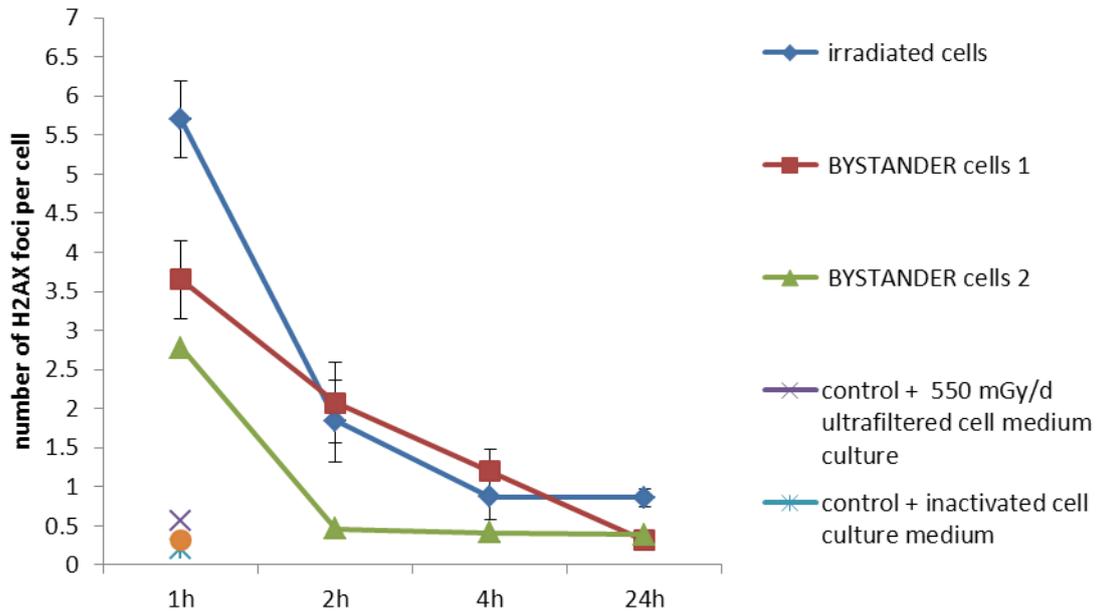

Figure 12: Exposure of ZF4 cells to gamma irradiation induces bystander responses in non-irradiated cells. A. Kinetics of gamma-H2AX foci disappearance on 70 mGy/d gamma-irradiated ZF4 cells, respectively. B. Kinetics of gamma-H2AX foci disappearance on 550 mGy/d gamma-irradiated ZF4 cells, respectively. Each data plot represents the mean+/-SE (n=6) of at least 3 independent experiments.
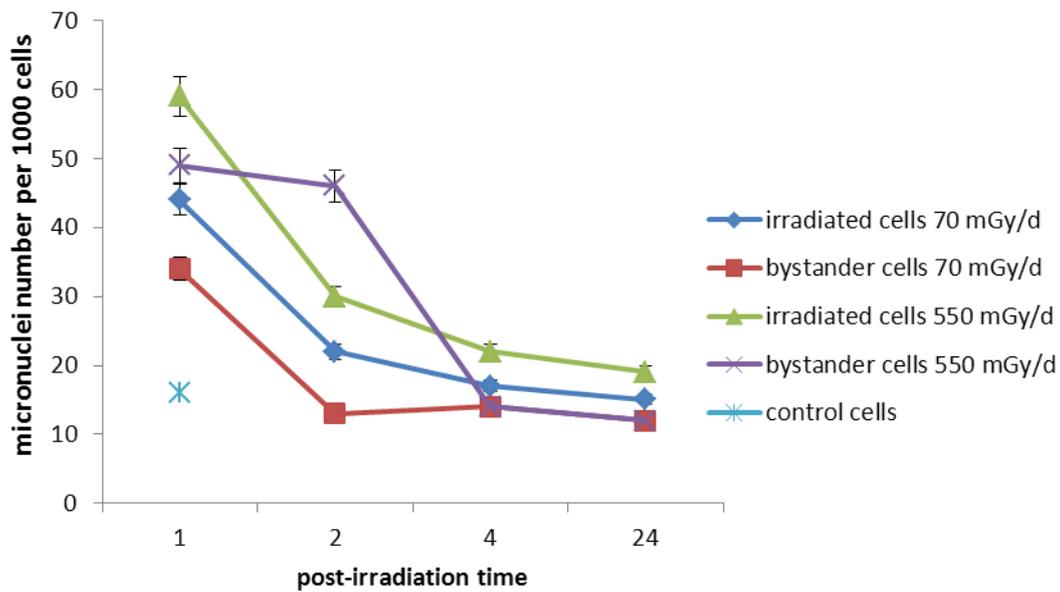
Figure 13: Exposure of ZF4 cells to gamma irradiation induces micronuclei in bystander cells. Micronuclei number was assessed on 1,000 cells stained with DAPI.

A significant part of the biomass of irradiated and bystander cells showed micronuclei supporting the formation of DSB during the gamma rays exposure. Bystander cells 2 (irradiated cells transferred) at 70 mGy/d and 550 mGy/d showed an elevated micronuclei number per cell compared to control cells. Furthermore, bystander cells at 550 mGy/d presented numerous micronuclei compared to irradiated cells at 2h post-irradiation and then a significant decrease was noted (Figure 13).

These results showed that non irradiated cells can, in the contact of the culture medium of irradiated cells, present H2AX foci that could be considered as DNA double strand breaks. It is also important to note that these breaks are repaired at 24 hours (Figures 12A and 12B). This implies that at these low doses the bystander effect observed do not impact the mechanisms of DNA double strand break repair in targeted and bystander cells.

The bystander effect observed here may be due to either a substance present in the sample and modified upon irradiation, a biological molecule such as a protein produced and secreted by the irradiated cells because the same type of results is obtained by transferring the culture medium of irradiated cells on non-irradiated cells.

[STAR]   47/94
(D-N°: 5.3) – Radiation Quality: studying sub-cellular modes of action using biomarkers and "omics" tools
Dissemination level: PU
Date of issue of this report: **29/11/2013**

Gamma irradiation affects global methylation not only in irradiation cells but also in bystander cells

Figure 14 shows the level of methylation of DNA from control, irradiated cells and Bystander responsive cells measured by mass spectrometry. An increase of global methylation of ZF4 cells was observed in irradiated cells and bystander cells compared to control cells. This increase was statistically significant ($p<0.05$) for the higher dose-rate (550 mGy/d) either in irradiated and bystander cells. This was the case till 1 h post-irradiation (Figure 14) suggesting that epigenetic effects are concomitant with the appearance of DNA damages in bystander cells.
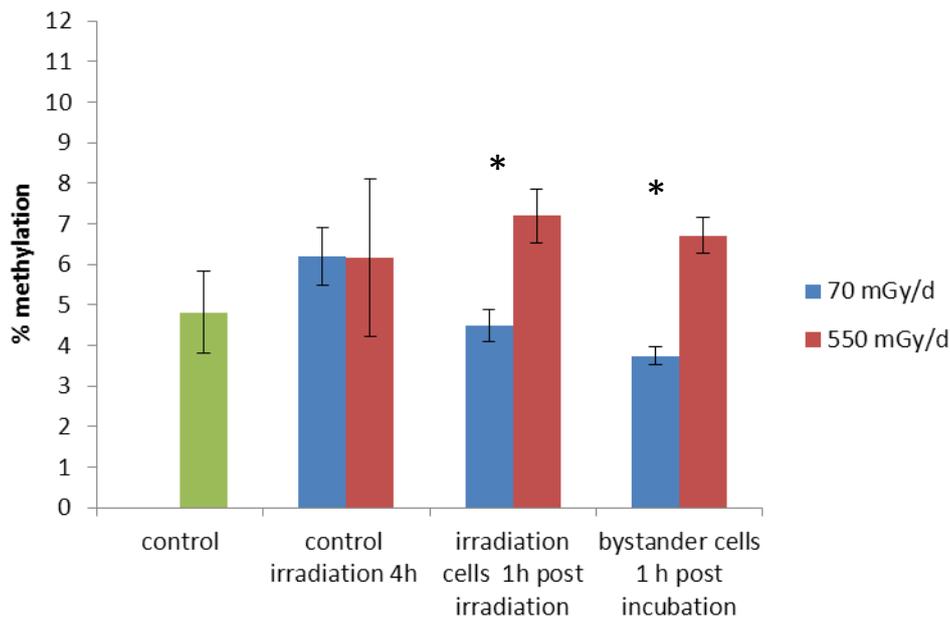

*Figure 14: Gamma irradiation affects global methylation in irradiation and bystander cells. Methylation was measured by HPLC-MS. 3µg of total DNA from irradiated and bystander cells were used. * p-value <0.5.*

Early bystander effect leads to the radioprotection of non-irradiated cells

Some authors recently showed in alpha irradiated and non-irradiated zebrafish embryos, that the stress communicated between un-irradiated zebrafish embryos and irradiated embryos sharing the same medium will help "rescue" the irradiated embryos, and that the strength of the rescue effect depends on the number of rescuing bystander un-irradiated embryos (Choi et al, 2010; Choi et al, 2012). Based on these studies, radioadaptation experiments were done on embryonic ZF4 cells (see Figure 11 for experimental set up). First, ZF4 cells were pre-irradiated during 4 hours at two different dose-rates. Then, these irradiated cells (called adaptation cells) were placed near non-irradiated cells (called bystander cells 2) during 1 hour and this incubation was followed by a

second irradiation of adaptation and bystander cells 2 during 19 hours. The number of H2AX foci was assessed after these 24 hours of exposure.

We observed that adaptation cells which are then irradiated for a second time contained significantly less foci than in 24h gamma-irradiated control cells (approximately 1.2 foci per cell, $p<0.001$) (Figure 15). We showed that bystander cells 2 that have been in contact with adapted cells and which have been then irradiated 19h present less H2AX foci than cells irradiated alone only during 24 hours (6.4 foci vs 13 foci per cell; $p<0.001$) (Figure 13). This radioadaptation effect is significantly more pronounced for the strong doses ($p<0.001$, Student test) (Figure 15).
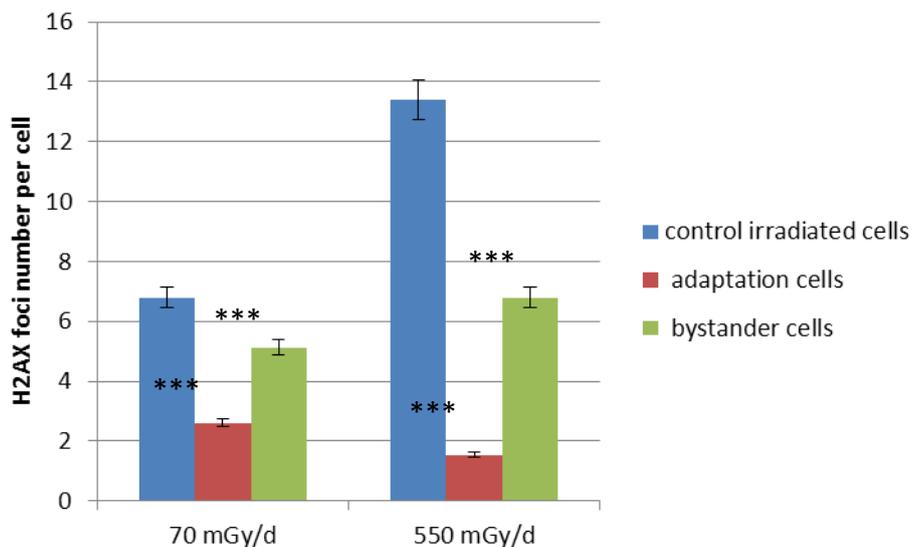
Figure 15: Early bystander effect leads to the radioprotection of non-irradiated cells. Pre-irradiated cells (called adaptation cells) were placed near non- irradiated cells (called bystander cells 2) during 1 hour and this incubation was followed by a second irradiation of adaptation and bystander cells 2 during 19 hours. Assessment of gamma-H2AX foci number was done 24 h post-irradiation on 70 mGy/d and 550 mGy/d gamma-irradiated adaptation, bystander and control ZF4 cells. *** p-value <0.001 (Student Test).

To assess whether the factor responsible of the DNA damages in bystander cells was a protein or a low molecular weight metabolite, we applied on the culture medium of irradiated cells either i) an ultrafiltration with a low molecular weight cut-off (3 kDa), or ii) a denaturation by 10 min heating at 100°C. Then, these treated media were applied to non-irradiated cells (Figure 10). In both cases, no DNA breaks was observed, as the number of H2AX foci in bystander cells 2 was found similar as in control non-irradiated cells (Figures 12A and 12B). This result suggests that the factor responsible of DNA damage in ZF4 cells has a molecular weight higher than 3 kDa and is inactivated by heating. This suggests a possible protein nature of the bystander mediator. With the aim of identifying the factor acting in early bystander effects and responsible of the radioadaptation of ZF4 cells, we studied the secretome of irradiated cells.

[STAR]   49/94
(D-N°: 5.3) – Radiation Quality: studying sub-cellular modes of action using biomarkers and "omics" tools
Dissemination level: PU
Date of issue of this report: **29/11/2013**

Early bystander effect is not due to the secretion of a protein by irradiated cells

We performed an extensive comparative study of the ZF4 secretomes upon irradiation. For this, we collected the conditioned media from two biological replicates from each condition (irradiated cells for four hours or control cells). Proteins present in the conditioned media were concentrated and then resolved by SDS-PAGE, and proteolyzed with trypsin. The resulting peptides were analysed twice by nanoLC–MS/MS (technical replicates). From the MS/MS spectra data set recorded over the 12 nanoLC–MS/MS runs, a total of 22,211 MS/MS spectra corresponding to 71,743 MS/MS query could be assigned (p-value below 0.05). They correspond to 1628 peptide sequences pointing at the presence of 127 proteins. We predicted the cellular localization of these proteins using the Ingenuity Pathway Analysis (IPA) program. 106 proteins that were detected at least twice in the exoproteome of ZF4 control cells (un-irradiated). A relatively low number of proteins present in the control cells exoproteome are predicted to be extracellular (7%), indicating a relatively low level of secretion of ZF4 cells after 4 h incubation while 56% are predicted to be cytoplasmic. That a relatively high number of intracellular proteins are found in ZF4 secretome was expected as this has been systematically observed in all previously published exoproteome studies (Malard et al, 2012). Even if cell viability is very high (higher than 90 %), these intracellular proteins are detected due to the high sensitivity of the mass spectrometer used here. Definitively, the number of secreted proteins observed for ZF4 cells in this condition is low compared to previous studies carried out with human cell lines (Malard et al, 2012). This may be primarily due to the short incubation time, *i.e.* 4 h versus 24 h in most secretome studies. We can thus conclude that, after 4 h of incubation, the number of proteins known to be secreted is moderate.

When merging the exoproteome lists from irradiated and control cells, a total of 127 proteins were identified, among which 10 were predicted as extracellular. No significant difference in their detection was evidenced between the samples on the basis of their normalized spectral counts (fold change of at least 2 and p-value below 0.05). A 2.7 fold increase was observed at 750 mGy for the complement component 7, but this was observed only for one of the two biological replicates. This indicates that a stress consisting of 4 hours of low dose of ionizing radiation does not induce major changes in secretion of a specific protein.

Oxydation of methionine (Figure 16) could be a post-translational modification of proteins induced by ionising radiation. Thus, we analysed whether the level of oxydized methionines was differing among the samples. We directly extract the number of this post-translational modification as seen from the list of peptides detected by tandem mass spectrometry. A slight increase was observed in the irradiated samples compared to the controls: 49 and 57 vs 40 close to the significant (p-value=0.052). In the experimental conditions assayed here, the bystander effect is probably not due to the secretion of specific proteins or the oxidation of these secreted proteins.
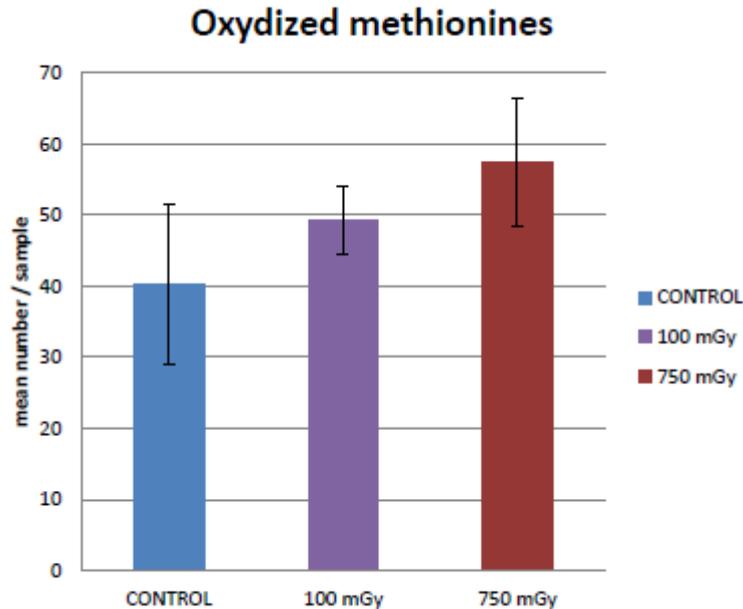
Figure 16. Mean number of oxidized methionines for each gamma external irradiation dose

4.1.1.3. Bystander effect in ZF4 cells exposed to acute alpha rays *(Work was performed at Stockholm University, by E.Staaf, A. Wojcik)*

a) Experimental Set Up

One day before irradiation, 1×10^5 cells were seeded in 18 mm diameter slides. Cells were irradiated at 28°C with a total dose of 100 mGy or 500 mGy of alpha rays that were generated by a [241]Am alpha irradiator. Then inserts with irradiated cells were placed with non-irradiated cells. Cells were co-cultured in these conditions for 1-24h. Irradiated and non-irradiated cells were then fixed and analyzed for the occurrence of gamma-H2AX foci at the time periods indicated (1h, 2h, 4h and 24 h).

b) Results

To investigate the bystander effect and the response to DNA damages, ZF4 cells were irradiated during few minutes at two different dose-rates. Following irradiation, the irradiated cells were placed near non- irradiated cells during 1 hour. We then examined the presence of DNA double strand breaks at 1, 2, 4 and 24 hours post-irradiation via the detection of gamma-H2AX foci in irradiated and bystander cells.

We observed a delay in the appearance of DNA double strand breaks in bystander cells compared to irradiated cells at doses of 100 and 500 mGy (dose rate of 0.27 Gy/min) (Figures 17 and 18)
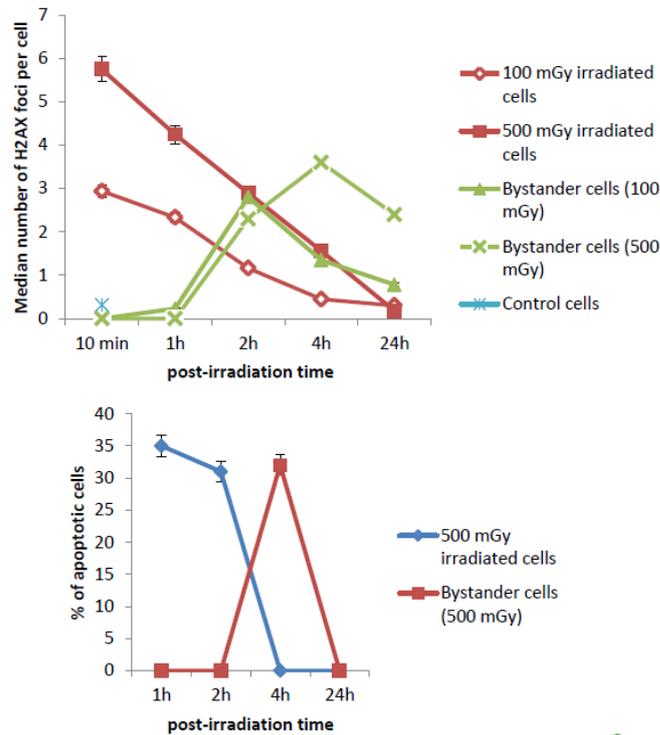
Figure 17: Exposure of ZF4 cells to alpha irradiation induces bystander responses in non-irradiated cells. Top: Kinetics of gamma-H2AX foci disappearance on 100 and 500mGy alpha irradiated ZF4 cells, respectively. B. % of apoptotic cells in 500 mGy irradiated and bystander cells. Each data plot represents the mean+/-SE (n=6) of at least 3 independent experiments.

At the higher dose an increase of the % of apoptotic cells was observed for the higher dose. This increase of apoptotic cells seems to be concomitant with the appearance of DNA double strand breaks in irradiated and bystander cells (Figure 17).
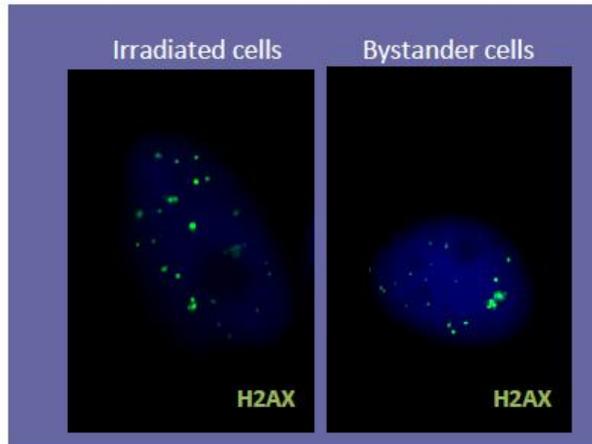
Figure 18: Exposure of ZF4 cells to alpha irradiation induces bystander responses in non-irradiated cells. Top: Immunofluorescence of gamma-H2AX in 100 mGy alpha irradiated and bystander ZF4 cells, respectively.

4.1.1.4. Comparison of acute gamma irradiation effects vs acute alpha irradiation effects in ZF4 cells

For a same range of exposition dose, we showed that gamma irradiated ZF4 cells (in blue, Figure 19) presented more DNA double strand breaks than alpha irradiated cells (in dark, Figure 19) at one hour post-irradiation. Nevertheless, more apoptotic cells were observed with alpha rays exposure (in violet Figure 19) than in gamma irradiated cells (in pink Figure 19) which implies that alpha rays are more deleterious than gamma rays.
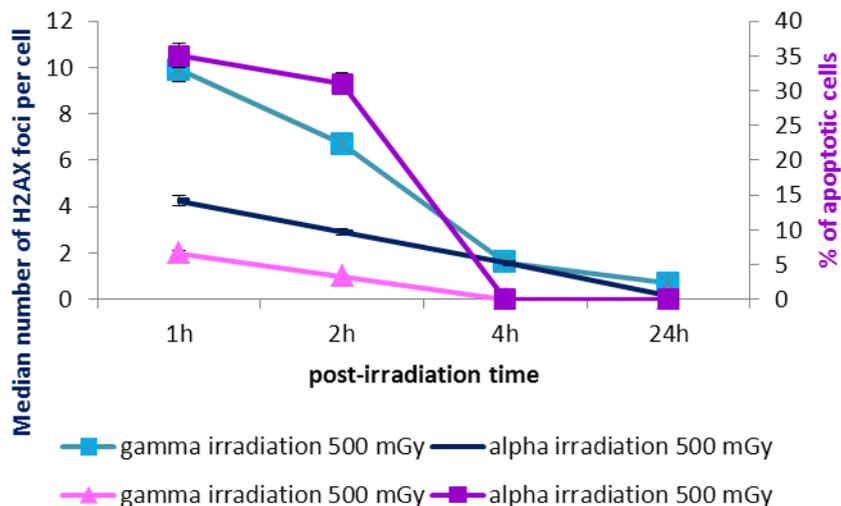

Figure 19: Comparision of DNA damage and apoptose in acute gamma or alpha irradiated ZF4 cells.

4.1.1.5. Conclusions and perspectives

A first set of results were obtained on gamma irradiation effects in various exposure scenarios, including the study of the bystander or radioadaption processes. A bystander effect was observed in non-irradiated cells displaying DNA double strand breaks in a similar way to targeted cells, but without any impact on the mechanisms of DNA double strand break repair in both targeted and bystander cells. The MoA of bystander effect was studied for gamma irradiation using advanced proteomic methods, showing that it may be due to either a substance present in the sample and modified upon irradiation or a biological molecule such as a protein produced and secreted by the irradiated cells.

Concerning gamma and alpha irradiation effect comparison, acute exposure to gamma radiations induced more DNA DSBs than after alpha radiations but the opposite was shown for apoptosis, indicating that cells exposed to alpha radiations were entering into a mitotic death. Using cell cultures allowed several exposure scenarios to be studied in a relatively short time. Moreover, external alpha irradiation could be applied easily which would not have been possible with in vivo studies, hence limiting the difficulties linked to americium kinetic characterization. The results presented here highlight the importance of measuring at the same time several biomarkers at different organization levels (molecular with DNA DSBs repair and cellular with micronuclei) as they may give complementary information.

4.2.2 Zebrafish in vivo (preliminary results)

The IRSN Am-241 results were obtained in the framework of the post-doctoral contract of Iris Barjhoux (09/2013-08/2013)

In addition to the short-term in vitro toxicity assays described in paragraph 4.2.1., longer-term in vivo experiments were performed to compare MoA of alpha and gamma emitters, using Am-241 and external gamma irradiation (Co-60) as model radionuclides. A pilot experiment was conducted in zebrafish to study Am-241 accumulation characteristics in terms of uptake rate and tissue distribution, associated to effect characterization (IRSN), for a control condition and for a single americium dose. The aim of this study was to obtain first results on americium in order to prepare a dose-response experiment. The dose-response experiment will be carried out in parallel to a study of gamma effects in zebrafish at (UMB). Despite the experiments taking place in two different research institutes, the experimental procedures, sampling protocols and analysis methods have been co-ordinated to the greatest degree possible, to allow a first comparison of the effects of alpha and gamma radiation across a number of endpoints. Where possible the two teams also collaborated on biomarker analysis, either by applying the same methods, or for some biomarkers, one team was responsible for analysing material from both experiments.

The approach developed for zebrafish in vivo experiments aimed at comparing alpha and gamma irradiation effects. To do that in a robust way, a pre-requisite is to have a good estimation of americium uptake at the whole body and at the tissue level, since one of the key questions is to link biological responses in a target tissue with dose rates at the same tissue level. Hence, a pilot

experiment was designed to study Am-241 uptake and tissue distribution, in association with the characterization of effects in terms of DNA double strand breaks and gene expression.

The gamma exposure was selected based on the dose range indicated from the pilot study. The range needed to cover the estimated internal doses from Am-241 (both whole body and organ), but extending these into higher doses to allow better coverage of the dose-response range.

4.2.2.1. Experimental Set Up Am-231

Fish maintenance

Adult male zebrafish of AB strain of 3 months-old were obtained from a fish breeding facility (GIS Amagen, France) and were maintained in an aerated tap water at a mean density of 3 fish per liter. Females were excluded to avoid any interference due to reproduction processes. Water was manually renewed by changing 50 % of the total volume each week. The tank was kept in a room with a 12/12 hour light/dark photoperiod and a temperature of 28 ± 1°C. Fish were fed with artificial food (JBL Novo GranoMix Mini) at a feeding rate corresponding to 3 % of fish wet weight, three times a day and supplemented by live neonates of *Daphnia magna* twice a week. Fish were gradually acclimatized to the artificial water used for the experiment (0.155 g/L of Instant Ocean salts, 53mg/L $CaCl_2$; 15mg/L $NaHCO_3$; pH 7.5; ~400µS/cm) for 3 weeks prior to the acclimation phase. At the beginning of the acclimation phase that lasted 2 weeks, fish were randomly distributed in an exposure and a control tank, and were maintained in the same conditions of temperature and day/night cycle as described above.

Dietary exposure to Am-241

Zebrafish were contaminated by the dietary pathway in order to limit Am-241 dispersion for radiological protection reasons and because this pathway mimics in situ exposure conditions. Zebrafish were exposed to dietary Am-241 for 21 days, followed by a recovery phase of 5 days where fish were fed with non-contaminated food in order to study Am depuration and reversibility of the biological responses. During these periods, fish were maintained in the same conditions as during the acclimation phase. Fish density was 2.4 fish per liter of water (60 fish for 25.3 L of water during the exposure phase and 30 fish for 12.7 L of water during the recovery phase). The main physical and chemical parameters of the water were monitored twice a week (pH, temperature, NO_2^-, NO_3^-, NH_3/NH_4^+).

Fish were fed with contaminated food at a feeding rate of 3 %. Control fish were fed non contaminated food. To minimize fish contamination by the water, one-third of the water volume was changed each day and tank bottoms were cleaned daily to remove fish faeces and food remains. At day 6, 21 and 26 (after 5 days of recovery), fish were removed and were killed within seconds by immersion in melting ice. Fish were starved for 24 h in a separate compartment before the sampling in order to avoid an overestimation of Am-241 concentration by taking into account americium remaining in the digestive tract. On each fish, brain, liver, gonads, digestive tract, muscle and rest of

the body were harvested. Americium activity concentrations were measured in brain, liver, gonads, digestive tract, muscle and rest of the body in 3 replicates of a pool of 3 organs for each sampling time, except for liver at T21 and T26 for which analyses were done on one pool of 9 organs. This strategy was applied in order to overcome problems of detection limits. Each replicate was divided into two parts, one for americium and the other for genetic analyses.

Americium contaminated diet

Contaminated diet was made as described in Gonzalez et al. (2005) by mixing artificial fish food (JBL Novo GranoMix Mini) with absolute ethanol containing dissolved americium nitrate ($Am(NO_3)_3$, stock solution in HNO_3 1N, carrier free, CERCA, France). The control diet was made in the same conditions but with americium-free ethanol. Artificial food and ethanol solution were stirred overnight and then ethanol was evaporated under a fume hood for 48 h. The resulting mean food activity was of 9.5 kBq/g dry weight. Food stocks were preserved in a freezer at -20°C.

Americium quantification in water and organisms

Am-241 was measured daily in water using liquid scintillation (detection limit of 0.03 Bq). For americium concentration determination in fish organs, tissues were digested in 3 mL of HNO_3 (15.3 M) over heating at 90°C (180 min) on a sand bath. After complete digestion, samples were then evaporated to incipient dryness (100 °C). The digestion process finishes by addition of 2 mL of H_2O_2 (1 M) and evaporation to incipient dryness (60 min, 100 °C). Before measurement by liquid scintillation, 20 mL of scintillation mixture (Instagel Plus) were added.

Effect parameters

γH2AX The immunofluorescence protocol employed for DNA repair and signaling actors, was described elsewhere (Pereira et al., 2011). It was applied on lymphocytes isolated from spleen. Briefly, anti-pH2AXser139 antibodies (Euromedex) were used at 1:800. Incubations with anti-mouse FITC secondary antibodies were performed at 1:100. Slides were mounted in 4',6' Diamidino-2-Phényl-indole (DAPI)-stained Vectashield (Abcys) and examined with Nikon fluorescence microscope. A total of 200 to 600 nuclei were analyzed per sample and condition. DAPI staining permitted also to indirectly evaluate the ratio of G1 cells (nuclei with homogeneous DAPI staining) and micronuclei. A total of 1000 cells were counted for micronuclei analysis.

RT-PCR Total RNAs were extracted from 40 mg of fresh tissue using the Absolutely RNA RT-PCR Miniprep kit (Stratagene) according to the manufacturer's instructions. The quality of RNAs produced was evaluated by electrophoresis on a 1% agarose-formaldehyde gel. For each exposure condition and each organ, samples were analysed in five replicates. First strand cDNA was synthesized from 5 µg of total RNA using the AffinityScript™ Multiple Temperature cDNA Synthesis Kit (Stratagene) according to the manufacturer's instructions. The cDNA mixture was conserved at -20°C until it was required for use in real-time PCR reactions. The 30 genes used in this study are reported in Table 11. For each gene, the specific primer pairs were determined using the LightCycler probe design software (version 1.0, Roche). The amplification of cDNA was

monitored using the DNA intercaling dye SyberGreen I. Real-time PCR reactions were performed in a LightCycler (Roche) and Mx3005P QPCR System (Stratagene) following the manufacturer's instructions (one cycle at 95°C for 10 min and 50 amplification cycles at 95°C for 5 s, 60°C for 5 s, and 72°C for 20 s for the LightCycler, one cycle at 95°C for 10 min and 50 amplification cycles at 95°C for 1 min, 60°C for 1 min and 72 °C for 1 min for the Mx3005P QPCR System). Each 20 µL reaction contained 2 µL of reverse transcribed product template, 1 µL of master mix including the SyberGreen I fluorescent dye (Roche), and the gene specific primer pair at a final concentration of 300nM for each primer.

The reaction specificity was determined for each reaction from the dissociation curve of the PCR product. This dissociation curve was obtained by following the SyberGreen fluorescence level during a gradual heating of the PCR products from 60 to 95°C. Relative quantification of each gene expression level was normalized according to the actin gene expression.

Table 11. List of the 30 genes chosen to study modes of action of Am-241

Brain	cyp19a	Aromatase
Brain	ache	Acetylcholinesterase
Brain	chat	Choline acetyltransferase
Inflammation	il1b	Interleukin-1
Detoxication	MT2	Metallothionin
DNA repair	bax	bcl2-Associated X protein
DNA repair	gadd45b	Growth arrest and DNA-damage-inducible, beta
Oxidizing stress	gstp1	Glutathione-*S*-transferase
Oxidizing stress	ndufs3	NADH-coenzyme Q reductase
Spermatogenesis	Star	Steroidogenic acute regulatory protein
Spermatogenesis	cyp17a1	cytochrome P450 family17
Spermatogenesis	Ihb	luteinizing hormone
Spermatogenesis	fshb	follicle stimulating hormone beta
Spermatogenesis	fshr	follicle stimulating hormone receptor
Spermatogenesis	Igf3	luteinizing growth factor 3
Spermatogenesis	amh	anti-Mullerian hormone
Spermatogenesis	piwil1	piwi-like 1
DNA Repair/Apoptosis	xpd	Xeroderma pigmentosum group D
DNA Repair/Apoptosis	bax	bcl2-Associated X protein

DNA Repair/Apoptosis	*gadd45b*	Growth arrest and DNA-damage-inducible, beta
DNA Repair/Apoptosis	*rad51*	RAD51 homologue
Hormonal/inflammatory system	*ESR1*	estrogen receptor
Hormonal/inflammatory system	*VEGFa*	Vascular endothelial growth factor a
Hormonal/inflammatory system	*il1b*	Interleukin-1
Hormonal/inflammatory system	*il-10*	Interleukin-10
Hormonal/inflammatory system	*mpx*	myeloid specific peroxidase
Hormonal/inflammatory system	*lysc*	lysosyme C
Stress proteins	*HSF2*	heat shock factor 2
Stress proteins	*HSP60*	heat shock protein 60
Stress proteins	*HSP90a*	heat shock protein 90a

4.2.2.2. Results Am-241

Americium-241 accumulation

The mean activity concentration (± standard deviation) of Am-241 in distributed food was of 9,530 ± 990 Bq/g d.w. Despite the daily renewal of water, Am-241 was also detected in the 0.45 µm filtered water (46.9 ± 12.3 Bq/L) and raw water (53.9 ± 13.2 Bq/L).

Resulting average concentrations at the whole body varied between 1.22 and 1.58 Bq/g d.w. (0.36 to 0.47 Bq/g w.w.) (Figure 20). As a consequence, the Trophic Transfer Factor could be estimated on a dry weight basis, to a value ranging from 0.012 % to 0.018 %. This value is in agreement with the low trophic transfer of Am-241 already observed for aquatic organisms (Véran, 1998). These activity concentrations of Am-241 obtained after 21 days of exposure are one order of magnitude above Am-241 concentrations measured in fish of contaminated lakes in the Chernobyl Exclusion Zone. In rudd and roach of one of the most contaminated lakes in the CEZ, the Glubokoye lake, Am-241 concentrations were measured respectively at 0.05 and 0.022 Bq/g w.w. (Adam-Guillermin, personal data).

[STAR]   58/94
(D-N°: 5.3) – Radiation Quality: studying sub-cellular modes of action using biomarkers and "omics" tools
Dissemination level: PU
Date of issue of this report: **29/11/2013**

Am-241 uptake was fast as the highest concentrations were observed at day 6, though not significantly detectable in liver. A high concentration was observed in the brain at day 6, which indicates that Am-241 is able to reach this organ, either by crossing the blood-brain barrier, or by other pathways (systemic or olfactory pathways). It is possible that in a similar way to uranium, americium could reach the brain via the olfactory pathway (Lerebours et al., 2010 ; Faucher et al., 2012). At day 21, there was a decrease of americium concentration in tissues, that cannot be explained by a biological dilution as no significant growth was observed throughout the experiment. This decrease may come from an active depuration process occurring in fish. Such a mechanism was observed for another actinide (uranium) in the freshwater clam *Corbicula fluminea*, in which the multixenobiotic protein MXR, acting as an efflux pump, was shown to be induced after exposure to uranium. However, with a specific activity of activity Am-241 of 1.27×10^{11} Bq/g, the metal concentrations would be very low.

These bioaccumulation results show that americium is not homogeneously distributed among organs. Target tissues are the digestive tract, gonads, brain and liver, even though for these last three organs, the depuration for these tissues seems to occur very quickly since activity concentrations were below the detection limit for several sampling times (despite the pooling of 9 livers at days 21 and 26). During the depuration, Am-241 seems to be redistributed from the digestive tract into the skeleton (rest of body), where it is stored for a longer period. These results are in agreement with the results of Bustamante et al. (2006) showing a fast depuration of Am-241 in the cuttlefish. Zotina et al. (2011) also found liver, bones and digestive tract to be the target organs in the Crucian carp.

Americium-241 absorbed dose rate

The dose conversion coefficients were calculated for Am-241 and adult zebrafish (Table 12) using the software EDEN v3 (K. Beaugelin IRSN), for external and internal exposure and for weighted or unweighted conditions. The weighted DCC value for internal exposure is very close to the value of 31.65 calculated for zebrafish by Reinardy et al. (2011) using the ERICA tool.
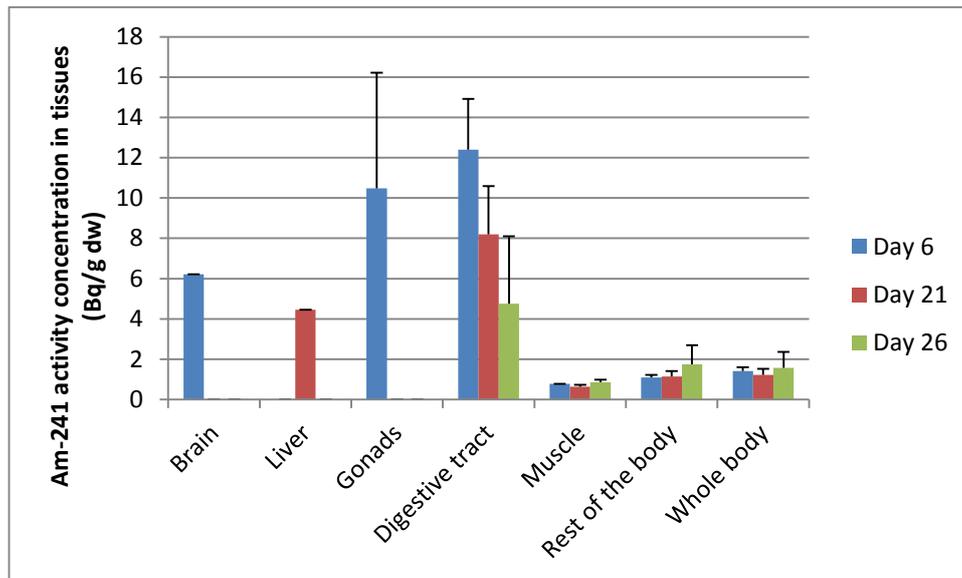
Figure 20. Am-241 accumulation in the 6 organs sampled at day 6, 21 and 26. Whole body activity concentration was estimated by adding the measured activities in the 5 organs and the rest of the body, divided by the total weight. Activity concentrations were measured in brain, liver, gonads, digestive tract, muscle and rest of the body in 3 replicates of a pool of 3 organs for each sampling time, except for liver at T21 and T26 for which analyses were done on one pool of 9 organs. This strategy was applied in order to overcome problems of detection limits. Depuration phase began at day 21.

Table 12. Weighted and unweighed dose conversion coefficients (DCCs) for internal and external dose rate estimations in adult zebrafish (model zebrafish dimensions : length : 3.6 cm, width : 0.4 cm ; height : 0.8 cm)

	Weighted	Unweighted
DCC internal (µGy/h/Bq/g)	31.42	3.16
DCC external (µGy/h/Bq/mL)	0.20	0.03

Using the unweighted DCCs, the dose rates estimated at the whole fish level vary between 1.13 and 1.47 µGy/h, while they vary between 11.27 and 14.60 µGy/h if weighted DCCs are used (Table 13). Hence, considering these weighted DCCs, the dose rates absorbed by the fish during this experiment are slightly above the threshold of 10 µGy/h recommended to protect ecosystems. However, for the comparison of effects with gamma irradiation (in course at UMB), only the unweighted DCCs will be considered. Total dose reach 0.9 mGy in the case of unweighted doses and 9.2 mGy for weighted doses. As a comparison, dose rate estimations in fish from the CEZ range between 0.8 and 2.5 µGy/h, respectively for roach and perch (Adam-Guillermin, personal data).

It must be underlined that these dose rates were calculated using a DCC value estimated for the whole body, whereas the results described above show that americium is not homogeneously distributed between the tissues, with target organs such as liver, digestive tract and bones. Calculations are in course in order to take into account this Am-241 distribution in dose rate calculations to organs, in order to be able to compare results with those from the gamma-exposed zebrafish. Although at a rough estimate, the DCC and internal doses would be expected to be correlated pretty well with activity concentrations. Thus the doses to liver, brain, gonads and digestive tract, would be expected to be between approximately 3 and 12 times that in the whole body.

Table 13. Dose rates (µGy/h) corresponding to Am-241 in whole body of zebrafish throughout the experiment using the unweighted and weighted DCC values and a wet to dry weight ratio of 3.4 (Adam-Guillermin, personal data)

	Dose rate (µGy/h) Unweighted	Total dose (mGy) Unweighted	Dose rate (µGy/h) Weighted	Total dose (mGy) Weighted
Day 6	1.32 ± 0.17	0.19 ± 0.02	13.12 ± 1.66	1.9 ± 0.24
Day 21	1.13 ± 0.29	0.57 ± 0.14	11.27 ± 2.86	5.7 ± 1.4
Day 26	1.47 ± 0.73	0.92 ± 0.46	14.60 ± 7.30	9.2 ± 4.6

Americium-241 induced effects

Gamma H2AX: Double strand breaks were observed in lymphocytes of exposed zebrafish with about 18 % of cells displaying gamma H2AX foci at day 21 (Figure 21). At day 27 (after 6 days of depuration), no significant difference was observed with the control, which indicates that double strand breaks were repaired within the 6 days of depuration. This result shows that significant effects were observed after Am-241 exposure, and were repaired after 6 days of depuration. For chronically exposed fish, these DNA double strand breaks may not be repaired and may have other consequences.
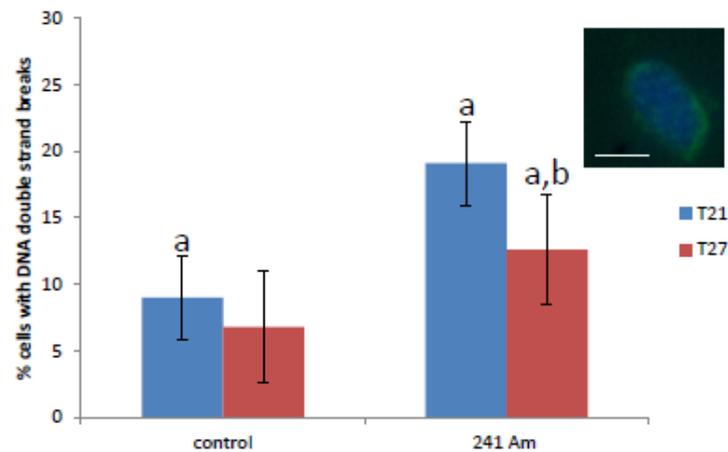
Figure 21. DNA double strand in lymphocytes of Am-241 exposed zebrafish after 21 days of exposure and 6 days of depuration (data : S. Pereira). DNA double strand breaks were assessed by the γH2AX immunofluorescence. Each data point represents the mean +/- standard error of 5 lymphocytes extracts. Different letters =p-values<0.05. Inserts show representative gamma-H2AX signals observed for exposed fish. Epifluorescence microscopy, scale bar= 5 µm.

Conclusion and perspectives

Dose assessment: These results show that the target organs for Am-241 are the digestive tract, the liver, the gonads, the brain and the skeleton, resulting in a heterogeneous distribution of radioactivity and hence, of dose. In order to take this phenomenon into account, dose rates will be refined by a calculation at the organ level. This will allow comparing the whole body dose rates and the organ dose rates, shedding light on the importance of the issue of heterogeneity of dose for alpha emitters.

Effect assessment: Our data show that DNA double strand breaks were observed after 3 weeks of exposure at a dose rate of a few µGy/h, representing a dose rate slightly above environmental dose rate observed in the CEZ. Even if these DNA DSBs were repaired after 6 days of depuration, they may lead to adverse consequences if fish are exposed chronically for a long period. Gene expression analyses are still in course and will give new data on the modes of action of ionizing radiations in terms of changes in gene expression. These genetic data will be compared to the results obtained for gamma externally irradiated zebrafish (UMB) at the same dose rate. In function of these results, another experiment will be launched with higher doses of Am-241 in order to be able to compare effects at several doses of Am-241 and gamma radiations.

4.2.3 External gamma irradiation (Co-60)

4.2.3.1 Experimental set up Co-60

Fish maintenance:

Adult male zebrafish of wild type AB strain of 3 months-old were obtained from the fish stock at the Zebrafish Laboratory at Norwegian School of Veterinary Science (NVH) and were maintained in an aerated tap water (demineralized + Instant Ocean) at a mean density of 10 fish per liter. Females were excluded to avoid any interference due to reproduction processes. Water was manually renewed by changing 90 % of the total volume twice a day. Water physical and chemical parameters (pH, nitrate, nitrite, ammonia, conductivity, carbonate and general hardness) were measured every day. The tank was kept in a room with a 12/12 hour light/dark photoperiod and a temperature of $26 \pm 1°C$. Fish were fed with artificial food (JBL Novo GranoMix Mini) at a feeding rate corresponding to 3 % of fish wet weight, three times a day and supplemented by live neonates of *Daphnia magna* twice a week. Fish were gradually acclimatized to the artificial water used for the experiment (0.155 g/L of Instant Ocean salts, 53mg/L $CaCl_2$; 15mg/L $NaHCO_3$; pH 7.5; ~400µS/cm) for 3 weeks prior to the acclimation phase. At the beginning of the acclimation phase that lasted 2 weeks, fish were randomly distributed in an exposure and a control tank, and were maintained in the same conditions of temperature and day/night cycle as described above.

Study design:

The fish were exposed to 6 doses (Table 14) of gamma irradiation for 26 days.

Samples for analyses were collected at day 6, 21 and 26 after exposure start. The schedule for exposure and sampling are shown in Figure 22. For each time point ten fish/group were sampled for assessing potential genomic damage and histological/morphological lesions and fish/group for assessing gene transcription changes (Figure 23).

Table 14: Number of fish in the study groups

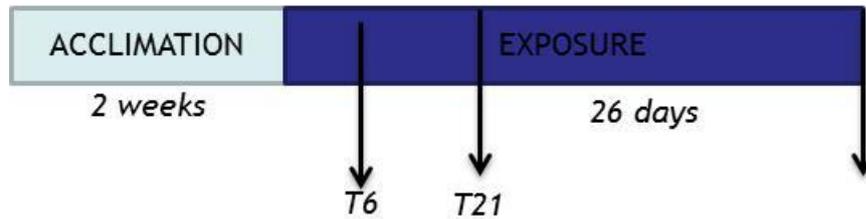| Group	Dose (mGy/hour)	NO (n)
Control	0.000	60
Ex 1	0.001	60
Ex 2	0.010	60
Ex 3	0.100	60
Ex 4	1.000	60
Ex 5	10.000	60

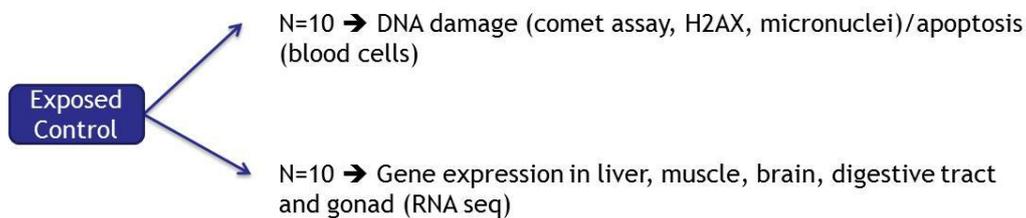*Figure 22: Schedule for exposure and sampling*

Figure 23: Fish sampled each time point

Results: The analyses are still ongoing and the results will be available during December 2014 and January 2015. Field dosimetry and gamma spectra measurements showed a significant shift in the Co-60 energy spectrum (down from a clean Co-60 peak to a broad 100-300 keV spectrum). This will of course have implications for the dose-response assessment, and means that the results cannot be defined a classic RBE study. But it should still be possible to compare the effects of Am-241 internal irradiation with those obtained from an external gamma irradiation at this spectrum.

4.3 Nematodes (preliminary results)

4.3.1 Background and objectives

The aim of this study was to use and to develop a bioenergetics approach based on the DEB theory (Dynamic Energy Budgets) developed by Kooijman (2000) to increase knowledge about links between assimilation disruptions, growth, reproduction, and life span fluctuations in exposed organisms to ionizing radiations.

This study was conducted using the model organism, *Caenorhabditis elegans* (nematode). The *C. elegans* model can be summarised by a short life cycle, a small size and a great ease to handle and cultivate in various devices (Brenner, 1974). These characteristics make it a good animal model to conduct this type of study. In the present study, we acquired accurate data on growth and reproduction of *C. elegans* exposed to chronic gamma radiation to address the following questions:

a- What are the consequences of chronic exposure to gamma radiation on *C. elegans* population?

b- Does chronic exposure to gamma radiation affect life history traits in a dose dependent manner?

c- Can the effects of gamma radiation be analysed by the DEBtox approach?

In an additional pilot study, estimates were made on the ^{241}Am concentrations needed to carry out comparative gamma/alpha experiments.

4.3.2 Experimental protocol for external gamma irradiation

4.3.2.1 Organism husbandry

The wild-type N2 nematode (ie. the most classically used strain) is maintained on the nematode growth medium (NGM) plates seeded with *Escherichia coli* strain OP50 as food resource, at 20 °C (Brenner, 1974; Stiernagle, 2006). Gravid worms are randomly collected from the stock population and placed on a Petri dish at t = 0h. After 2 hours, laid embryos were considered to be age-synchronized.

Eggs were individually placed into petri plate (3.5 cm diameter) containing NGM seeded with OP50 *E. coli* (for each treatment). *E. coli* layer (about 1 cm diameter) was centred in the middle of the plate in order to limit (as much as possible) nematode displacement on the petri dish surface. Worms are cultured at 20°C and 80% RH in the dark.

4.3.2.2 External gamma irradiation

For the purpose of the study we used five different ^{137}Cs sources with activities ranging from 2.1 x 10^6 to 1.6 x 10^9 Bq. Each source was installed in independent incubator and experimental units were placed around the source as shown in Figure 24. During the test, temperature and moisture were continuously measured using data loggers.

a)
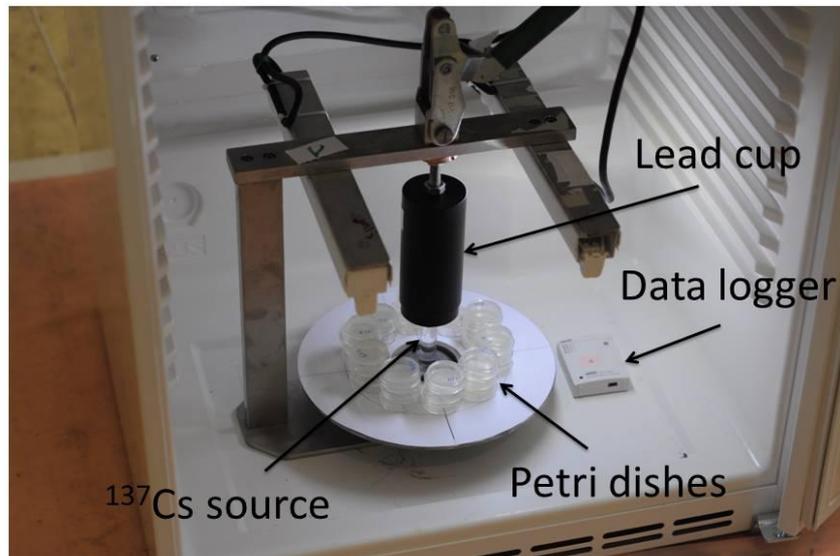
b)
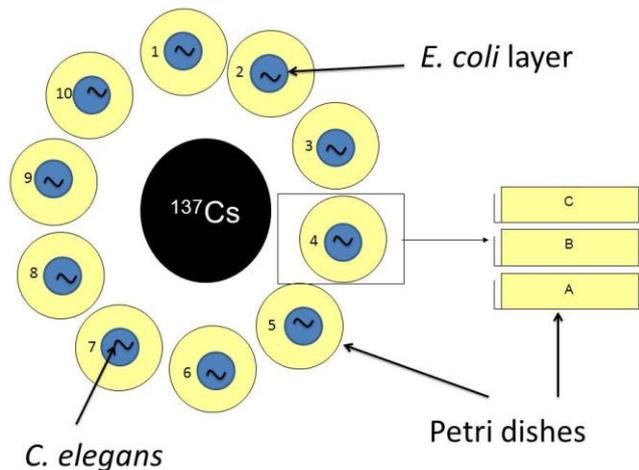
Figure 24: Irradiation facility. Each incubator contained one ^{137}Cs source (a). 10 columns of 3 experimental units (petri plate, one egg per plate) were placed around the source (b).

Dose-rates were calculated (Monte Carlo N-Particle model) using the distance between plates and ^{137}Cs source and the source activities. These predicted dose rates were validated using Thermo Luminescent detector (TLD) before the experimentation. The estimated dose rate presented in Table 15 considers the variability linked to nematode displacement on the *E. coli* layer.

[STAR] 66/94
(D-N°: 5.3) – Radiation Quality: studying sub-cellular modes of action using biomarkers and "omics" tools
Dissemination level: PU
Date of issue of this report: **29/11/2013**

Table 15: Dose rates to C. elegans in function of ^{137}Cs source activity

Source type	Source activity (Bq)	Dose rate ± SD (µGy/h)	Replicates
Solid 1	1.6×10^9	26 750 ± 1 275	27
Solid 2	1.6×10^9	21 279 ± 1 204	30
Liquid 1	1.8×10^8	3 375 ± 417	30
Liquid 2	1.8×10^7	318 ± 38	30
Liquid 3	1.1×10^6	42 ± 4	30

4.3.2.3. Endpoints measurement

4.3.2.3.1 Brood size

To assay brood size we daily transferred worms into new individual plate containing NGM from t = 72h (beginning of lay) till the end of spawn. Hatched progeny was counted twice, the day following each transfer (Swain *et al.*, 2004) allowing the measurement of brood size and hatching rate.

4.3.2.3.2 Growth

Growth was measured (using stereomicroscope with a connected camera) twice a day from hatching to maturity then once a day until maximal size.

4.3.2.3.3 Lifespan

Lifespan was studied by daily counting of dead worms. The death of a nematode was recorded upon failure to respond to repeated touch stimulation of the posterior end.

4.3.2.4 Data treatment and statistical analysis

Prior to the experiment, Power analysis was used to estimate the minimum sample size (replicate number per condition) as a function of the variance of each endpoint already observed on preliminary assay (data not shown) for a given effect level (eg. 5% change in fecundity or growth).

All statistical analyses were done using R version 2.15.3 (R Core Team, 2013).

- *Growth*
  Growth was modelled by fitting a modified Von Bertalanffy model (Jager et al., 2005):

$$s_f(l) = 1 - \left(1 + \frac{l_f^3}{l^3}\right)^{-1} \qquad (1)$$

$$\frac{d}{d_t} l = r_B\left[(l - s_f)f - l\right] \qquad (2)$$

With:

f Scaled ingestion rate (fraction of maximum, 0-1)

l   Scaled body length (fraction of maximum at f=1) (L = l x L_m)

l_f scaled length at which ingestion is half a maximum ($L_f = l_f$ x L_m)

L_m Absolute maximum length (µm)

       r_B Von Bertalanffy growth rate constant (day^{-1})

       s_f Stress level of ingestion, depending on body size (0-1)

The effect of gamma radiation exposure on estimated parameters was assessed using using a mixed-effect ANOVA model and Tukey's all-pair comparison tests.

- *Reproduction*
The effect of gamma radiation exposure on the cumulated number of larvae was analyzed using generalized linear models (dose rate as explanatory variable) with quasi-Poisson error were used to take into account overdispersion of the data.

- *Longevity*
The effect of gamma radiation exposure on survival was analyzed using Cox proportional hazard models.

4.3.3 Results and discussion

4.3.3.1. Growth

As shown in Figure 25, nematode growth was only slightly impacted by gamma exposure in our experimental conditions. Growth rates of the exposed organisms were significantly (p-val < 0.005) lower than control. Nevertheless, no difference on maximum body size was observed between control and tested dose rates. This last result is consistent with previous studies that didn't show any influence of chronic gamma exposure on the growth of invertebrates (Knowles and Greenwood, 1994, Gilbin et al., 2008; Hertel-Aas et al., 2007).

a)
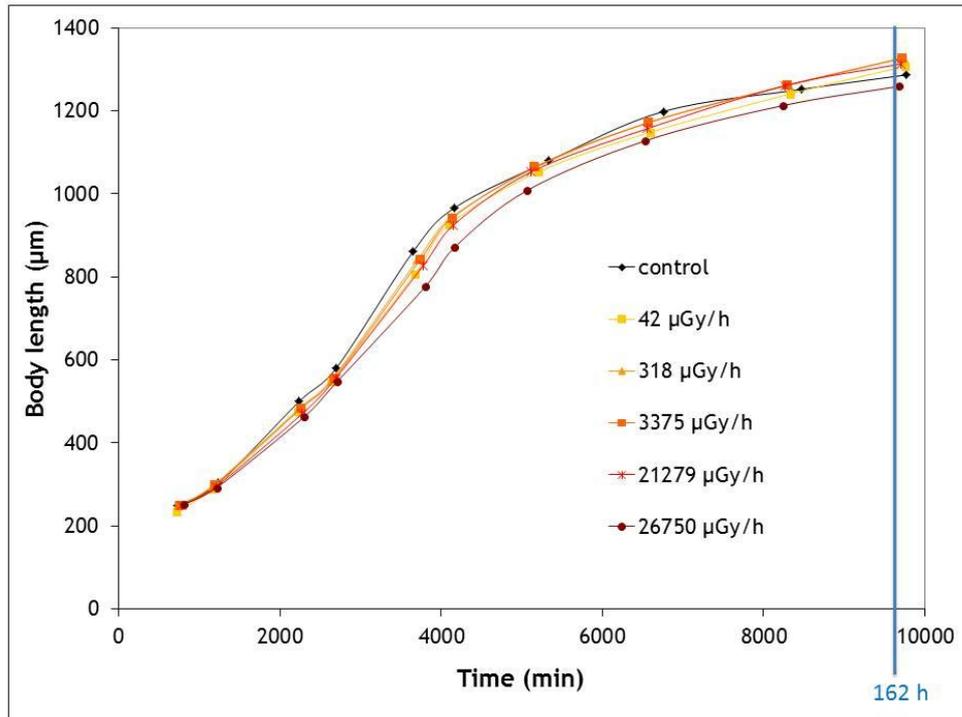
b)

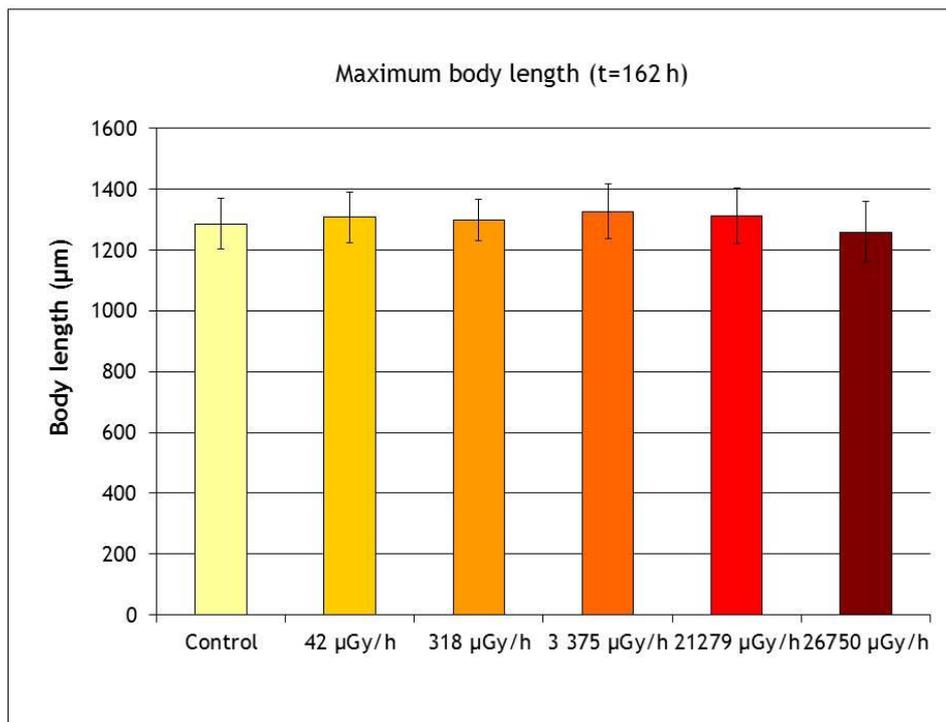*Figure 25: a) size of C. elegans from hatching to the end of experiment, b) maximum body size in function of gamma dose rates.*

4.3.3.2. Reproduction

No impact on hatchability and larvae survival was observed in our experimental conditions (data not shown). However, we observed a reduced cumulated number of larvae for organisms exposed to dose rates up to 21,279 µGy/h (Figure 26). The difference to the control was statistically significant (p-val <0.0001) for the highest tested dose rate (26,750 µGy/h) and corresponded to 18% reduced number of larvae. Our results were consistent with previous published studies reporting the sensitivity of reproduction to chronic radiation exposure. Gilbin et al. (2008) showed a reduced brood size for *daphnia magna* exposed to 31 mGy/h. Similarly, a significant decrease of eggs and larvae number was observed for *O. diadema* exposed to 7.3 and 13.7 mGy/h (Knowles and Greenwood, 1994; 1997). Hertel-Aas et al. (2007) also reported a significant impact of chronic gamma exposure on the hatchability of soil invertebrate *Eisenia fetida* at 43 mGy/h. In our study, as no impact on hatchability was observed we can consider i) that all the embryos were produced from healthy gametes and ii) that no additional damage was induced during embryos development. The reduced number of eggs laid may be linked to a reduced number of gametes. Germ cell apoptosis and cell cycle arrest resulting from radiation induced DNA damage may support this hypothesis.
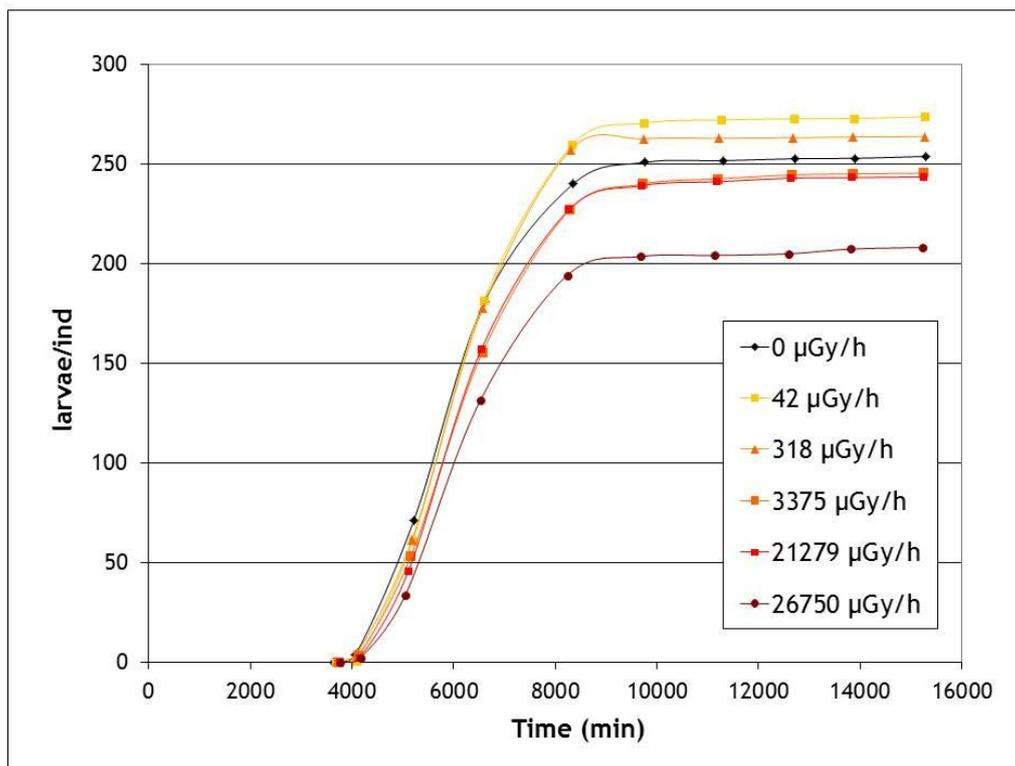

Figure 26: Number of larvae produced by C. elegans during the period of gamma radiation exposure.
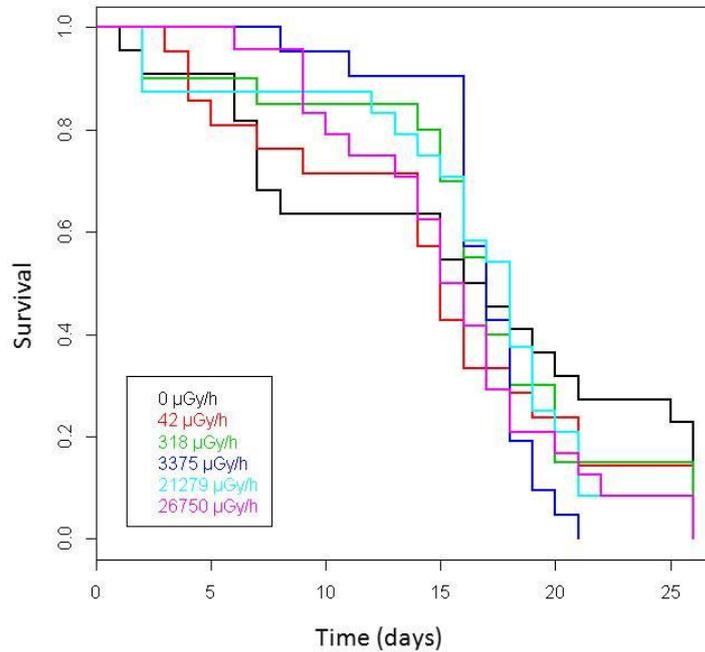
Figure 27: Survival rate in function of gamma dose rates.

4.3.3.3. Longevity

Results presented in Figure 27 show a better survival rate for organisms exposed to chronic gamma radiation during the first 15 days of exposure. Beyond this date, we observed a reversed trend and a reduced longevity for the exposed organisms. However, no significant difference was observed between control and exposed organisms. This may be partly due to the small number of replicates.

The data was used to evaluate the effects of gamma irradiation through a DEBtox method. This method aims to link external concentration of toxicants to effects on endpoints (such as growth, reproduction, survival) and was used to estimate the No Effect Concentration (NEC) and insights on the physiological/metabolic mode of action as described in the deliverable D-N°5.1.

4.3.4 Future experiment: comparison between gamma and alpha chronic exposure

A new experiment is planned in order to compare the effect of gamma and alpha radiation in chronic exposure condition. *C. elegans* will be exposed to increasing concentration of ^{241}Am in

order to test similar range of dose-rates as that studied with gamma radiation. The same experimental design as chronic gamma exposure (one individual per plate, exposure from eggs to the end of reproduction) will be used. The effects of alpha radiation will be measured on growth and reproduction.

4.3.4.1. Selection of the range of ^{241}Am concentrations to be tested

The dose rates for nematodes were calculated following a classical three steps approach.

First, external and internal Dose Conversion Coefficients (DCCs, Table 16) were calculated for ^{241}Am with the EDEN software version 2.3 (Beaugelin-Seiller et al., 2006), the nematode mean dimensions being described as an ellipsoid of 1 mm long and 0.05 mm diameter. These DCCs were weighted using the weighting factor of each radiation type. Secondly, a concentration ratio (CR) was used to estimate the organism ^{241}Am internal concentrations. In the absence of *C. elegans* specific information, we used ^{241}Am- CR values corresponding to 10% and 20% of internalisation. Third, internal and external dose rates were calculated using different ^{241}Am concentrations and the *ad hoc* DCCs. The sum of internal and external dose rates gave then the total estimated dose rate absorbed by *C. elegans*. Table 17 showed that dose rates are impacted by the CR and highlights the need of an accurate estimate of internal concentration of ^{241}Am. A pilot study will be done to select the concentration of ^{241}Am likely to give significant effects on growth and reproduction for further DEBtox analysis.

4.3.4.2. Pilot study for *C. elegans* specific ^{241}Am CR characterisation

C. elegans eggs will be individually exposed for four days (until young adult life stage) to NGM medium (seeded with *E. coli* layer) contaminated with concentrations of ^{241}Am ranging from 0.4 to 4000 Bq/mL. Table 18 gives the dose rates estimated from the range of ^{241}Am that will be tested during the pilot experiment and a theoretical CR = 1 x 10^{-1}. This range of predicted dose rates frames those previously tested during the chronic gamma radiation assay. After exposure, *C. elegans* will be collected, washed to remove *E. coli* contamination and ^{241}Am bioaccumulation will be estimated.

Experimental condition to test the effect of chronic alpha radiation on growth and reproduction of *C. elegans* will be determined according to the results of this pilot study.

Table 16: DCCs (µGy/h per Bq/g) calculated for adult C. elegans exposed to ^{241}Am with EDEN v2.3. $*\alpha=10,\ \beta=3,\ \gamma=1$

	Unweighted
Internal	1.37
External	1.35
	Weighted*
Internal	13.96
External	13.46

Table 17: Predicted dose rates using a) unweighted and b) weighted DCCs and two different concentration ratios (CR)

	Dose rate (µGy/h)			
	CR = 1.10^{-1}		CR = 2.10^{-1}	
Bq/mL	0.3	3000	0.3	3000
a) Unweighted				
External	0.41	4050	0.41	4050
Internal	0.041	411	0.08	822
Total	0.451	4461	0.49	4872
b) Weighted				
External	4.04	40380	4.04	40380
Internal	0.42	4188	0.84	40380
Total	4.46	44568	4.88	48756

Table 18: Predicted dose rates on a range of ^{241}Am concentration (using DCCs from Table 16 and CR = 1 x 10^{-1}) (to be tested during the pilot experiment)

		^{241}Am (Bq/mL)						
		0.4	1.5	5.6	77.4	288.7	1076.0	4011.1
Dose rate (µGy/h)	External	5.4	20.1	75.0	1042.2	3885.0	14481.8	53982.4
	Internal	0.6	2.1	7.8	108.1	402.9	1502.0	5598.8
	Total	6.0	22.2	82.8	1150.3	4288.0	15983.8	59581.2

4.4 Daphnids (preliminary results)

4.4.1 Background

With a small size and short life cycle, the cladoceran microcrustacean *Daphnia magna* is particularly suitable biological model for studying effects of toxic contaminants over several generations. Many studies in the literature show that *D. magna* response to various metals or chemical contaminants might differ across generations (appearance of a tolerance, increase in sensitivity…) depending on the tested toxicant (LeBlanc, 1982; Bodar et al., 1990; Sánchez et al., 2000; Muyssen and Janssen, 2004; Pane et al., 2004; Guan and Wang, 2006; Alonzo et al., 2008; Dietrich et al., 2010; Massarin et al., 2010; Kim et al., 2012). These observations demonstrate that measured effects in one generation might not be representative of toxicity in the following offspring generations, and ultimately of the population response. Multigenerational exposures are a much more representative of the exposure context of field populations for which contaminations can last for durations which largely exceed individual longevity and involve exposure of many successive generations.

The daphnid *D. magna* is one of the few animal species for which *in vivo* effects data of chronic internal alpha radiation are available in the literature (Alonzo et al., 2006, 2008). These studies were achieved in the framework of the EC program ERICA. A multigeneration exposure over three successive generations (to Am-241 concentrations of 0.4, 4.0 and 40 Bq / mL yielding average dose rates from 0.3 to 15 mGy / h) showed that a strong increase in effects on survival, fecundity and mass investment per egg occurred from one generation to the next. Chronic effects of external Cs-137 gamma irradiation were also investigated in *D. magna* during the ERICA program. However, gamma exposure was limited to one unique generation, yielding slight effects only at tested dose rates (from 0.4 to 31 mGy / h) (Gilbin et al., 2008), whereas a chronic multigenerational exposure was never tested for a potential increase in effect severity of gamma radiation over successive generations.

4.4.2 The case of depleted uranium in *Daphnia magna*: linking DNA damage and perturbation(s) of energy budget

At IRSN, a multigenerational investigation of toxic effects was conducted recent years in *D. magna* exposed to waterborne depleted uranium (DU) over three generations (F0, F1 and F2) (Massarin et al., 2010). Uranium is a radionuclide from the actinide series, naturally present in the environment and freshwaters at concentrations from 0.01 to 11.1 µg/ L. Local increases in concentrations due to anthropogenic activities associated with the nuclear fuel cycle or military purposes raise concerns for natural ecosystems (due to chemical toxicity which dominates over radiological toxicity in the case of DU). In *D. magna* exposed to concentrations from 10 to 75 µg / L, results showed that uranium effects increased in severity across generations. A mechanistic analysis of reductions in somatic growth and reproduction using the DEBtox approach (Dynamic Energy Budget theory

applied to toxicology) suggested that uranium primarily affects assimilation, a metabolic mode of action confirmed through measured reduction in carbon assimilation and observed alterations of the digestive epithelium (Massarin et al., 2010; Massarin et al., 2011). However, the mechanism involved in the transgenerational increase in toxicity was not clearly understood. One may hypothesize that this observation was a mere result of a difference in exposure conditions between F0 and subsequent generations (uranium exposures were started with freshly hatched neonates in F0 whereas the embryo stage was exposed in F1 and F2) pointing the embryo stage as a potentially sensitive life stage. Besides a possible influence of embryo exposure, DU-induced aberrations in DNA might be transmitted from exposed daphnids to their eggs and involved in the increase in effect severity over generations.

These hypotheses were investigated by Plaire et al. (2013) who aimed to examine the mechanisms involved in the transgenerational increase in sensitivity to depleted uranium (DU) using daphnids exposed to concentrations from 2 to 50 µg L / L over two successive generations. Genotoxic effects were assessed using random amplified polymorphic DNA and real time PCR (RAPD-PCR). Effects on life history (survival, fecundity and somatic growth) were monitored from hatching to release of brood 5. Different exposure regimes were tested to investigate the specific sensitivity of various life stages to DU. Results reflected some degree of correlation between the accumulation of DNA damage and the increase in effects severity across generations and suggested that DNA damage might be an early indicator of future effects on life history:

1) When daphnids were exposed continuously or from hatching to deposition of brood 5, results demonstrated that DNA damage accumulated in females and were transmitted to offspring in parallel with an increase in severity of effects on life history across generations.

2) When daphnids were exposed during the embryo stage only, DU exposure induced transient DNA damage which was repaired after neonates were returned to a clean medium. Effects on life history remained visible after hatching and did not significantly increase in severity across generations.

4.4.3 Objectives and experimental set up

a) Objectives

In the present study, daphnids were exposed to Cs-137 gamma radiation over three successive generations (F0, F1 and F2). Survival, growth and reproduction were monitored until release of brood 5 and DNA samples were prepared in order:

- to investigate the possible mode of action of gamma radiation in *D. magna* using DEBtox;

- to test whether effects increased in severity across generations;

- to apply the RAPD technique to gamma-radiated daphnids to examine whether DNA alterations were accumulated and transmitted from one generation to the next, with a special emphasis on linking toxicity between the molecular and organism levels.

b) Exposure conditions

Experimental conditions are similar to those maintained during the Am-241 contamination experiment (Alonzo et al., 2008).Daphnids were kept in individual 50 mL-vials filled with culture medium (M4 pH8) at 20°C under a 16:8h light:dark photoperiod and a light intensity of 30 µE m^{-2} s^{-1} following the guideline 211 of OECD (2008).Daphnids were fed an individual daily ration of 100 µgC with fresh exponentially growing cultures of the green algae *Chlamydomonas reinhardtii* in axenic conditions. Each generations was initiated with freshly deposited eggs (<24h) from brood 5, exposed at the same dose rate as their parents.
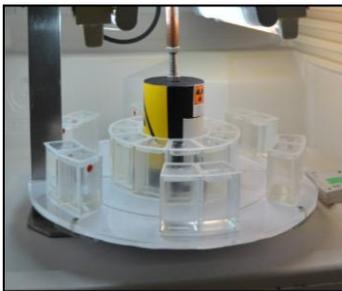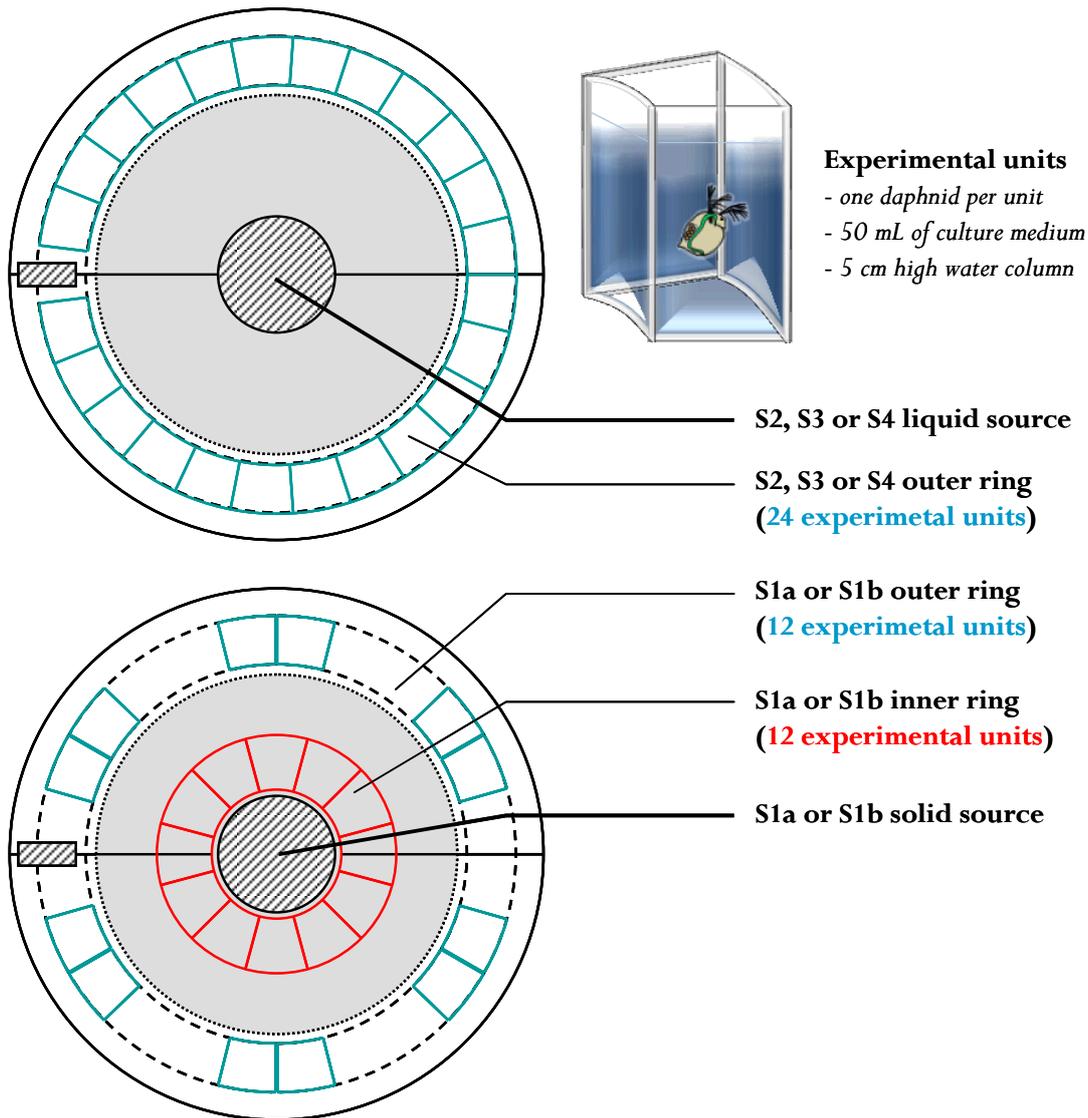
Gamma radiation exposure was achieved at IRSN (Cadarache) using the MIRE irradiation facility. Experimental units were placed along two rings around gamma sources depending on whether we aimed to minimize variability in the dose rates (outer ring) or to maximize dose rate (inner ring for the highest dose rate) (Figure 28). Five different dose rates were tested ranging from 0.008 to 32 mGy/h (Table 19). Twenty-four daphnids were exposed at each dose rate (10 daphnids for monitoring of survival and fecundity and 14 daphnids for size measurements and DNA analysis).

Table 19. Average dose rates (with variability depending on the location of daphnids inside their vials) during the external Cs-137 gamma radiation exposure of Daphnia magna

Gamma source	Position	Dose rate ± variability	Replicates
S1 (a and b)	inner ring	32.0 ± 18.9 mGy/h	n = 10 survival / fecundity n = 14 biometry / DNA analyses
S1 (a and b)	outer ring	4.40 ± 1.4 mGy/h	
S2	outer ring	0.76 ± 0.24 mGy/h	
S3	outer ring	0.075 ± 0.024 mGy/h	
S4	outer ring	0.008 ± 0.002 mGy/h	

c) DNA analyses

As described in Plaire et al. (2013), DNA extracts were sampled at the start of each generation (within 24h of hatching) and upon release of brood 1 (~day 10) and brood 5 (~day 23), based on 8 replicates of 10 neonates and 5 replicates of one adult daphnid. As part of an ongoing study (Florian Parisot's PhD project), DNA alterations will be quantified by RAPD-PCR at the end of 2013 or the beginning of 2014.

Experimental units
- *one daphnid per unit*
- *50 mL of culture medium*
- *5 cm high water column*

S2, S3 or S4 liquid source

S2, S3 or S4 outer ring
(24 experimetal units)

S1a or S1b outer ring
(12 experimetal units)

S1a or S1b inner ring
(12 experimental units)

S1a or S1b solid source

S1a or S1b experimental setup   *S2, S3 or S4 experimental setup*   *Daily medium renewal in an experimental unit containing one daphnid*
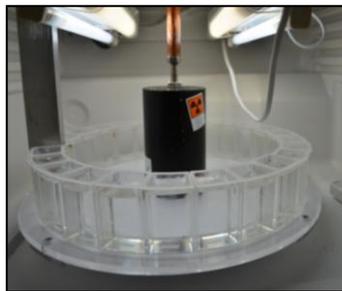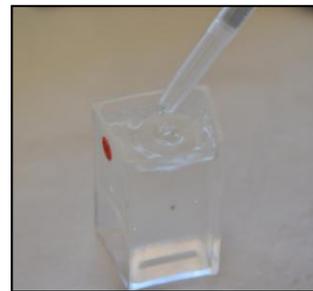
Figure 28. Experimental setup employed during the external gamma irradiation experiment of Daphnia magna (photos by J-M Bonzom).

The random amplified polymorphic DNA (RAPD) method was successfully used to investigate genetic alterations in *D. magna* exposed to benzo[a]pyrene (Atienzar et al., 1999; Atienzar et al., 2000) and depleted uranium (Plaire et al., 2013). This technique has the potential to detect a large variety of DNA damage and mutations at the whole genome level. The RAPD technique was recently improved using relative quantitative PCR instead of agarose gel electrophoresis (Cambier et al., 2010) and allowing the quantification of hybridization sites of a RAPD probe (Geffroy et al., 2012; Lerebours et al., 2013).

4.4.4 First results

Figure 29 depicts chronic effects of internal alpha radiation and reports effects of external gamma radiation on survival, body size and fecundity over 3 generations of daphnids. Results show that gamma radiation induced a significant reduction in fecundity and a possible increase in mortality (at 4.4 mGy/h). A gradually increasing delay in somatic growth and brood releases suggests that gamma radiation might affect energy budget through an increase in costs for growth and maturation. However, this effect is slight and requires to be confirmed by DEBtox analysis.

4.4.5 Future directions: a mechanistic insight in RBEs based on DEBtox analyses and molecular damage of gamma and alpha radiation exposures

a) Considering kinetics of radiological stress to compare stress functions

Ratios of biological effectiveness (RBE) can be calculated for individual-level endpoints such as survival, somatic growth and reproduction, based on the chronic 21-day exposure commonly used in standard ecotoxicity tests(OECD, 2008). However, such comparisons are made difficult for several reasons.

1) A calculation of RBE should be based on dose rate response curves which are not possible to derive considering the limited extent in effect levels recorded (maximum of 32% and 46% for gamma and alpha radiation respectively). If one considers reductions in 21-day fecundity of ~23% or ~33% measured with gamma radiation (at 4.4 or 32.0 mGy/h respectively) and alpha radiation (at 1.5 or 0.3 mGy/h respectively), the value of RBE might vary from 3 to 10 in *Daphnia magna*.

2) Calculations of RBE are based on average dose rate and effect values whereas the way how radiological stress is induced and biological processes respond strongly differs between gamma and alpha radiation. Whereas external gamma radiation and radiological stress remain relatively constant over the duration of exposures, alpha radiation requires first that the alpha emitter Am-241 internally accumulates in daphnids tissues to produce a dose. As a consequence, the alpha dose rate which organisms are exposed to progressively increases as a function of age (Table 20) together with the intensity of the biological effects. In this context, dose rates, radiological stress and biological perturbations need to be analysed as dynamic processes, necessarily using

a biological-based toxico-kinetic and toxico-dynamic approach, such as a DEBtox model. This approach provides a conceptual framework to compare mechanistically-derived values of biological effectiveness between alpha and gamma radiation based on stress functions which describe how perturbations of energy budget are correlated to a "stress metrics" such as alpha or gamma dose rate, total cumulated dose or a pool of damage (Jager et al., 2011; Jager and Zimmer, 2012).
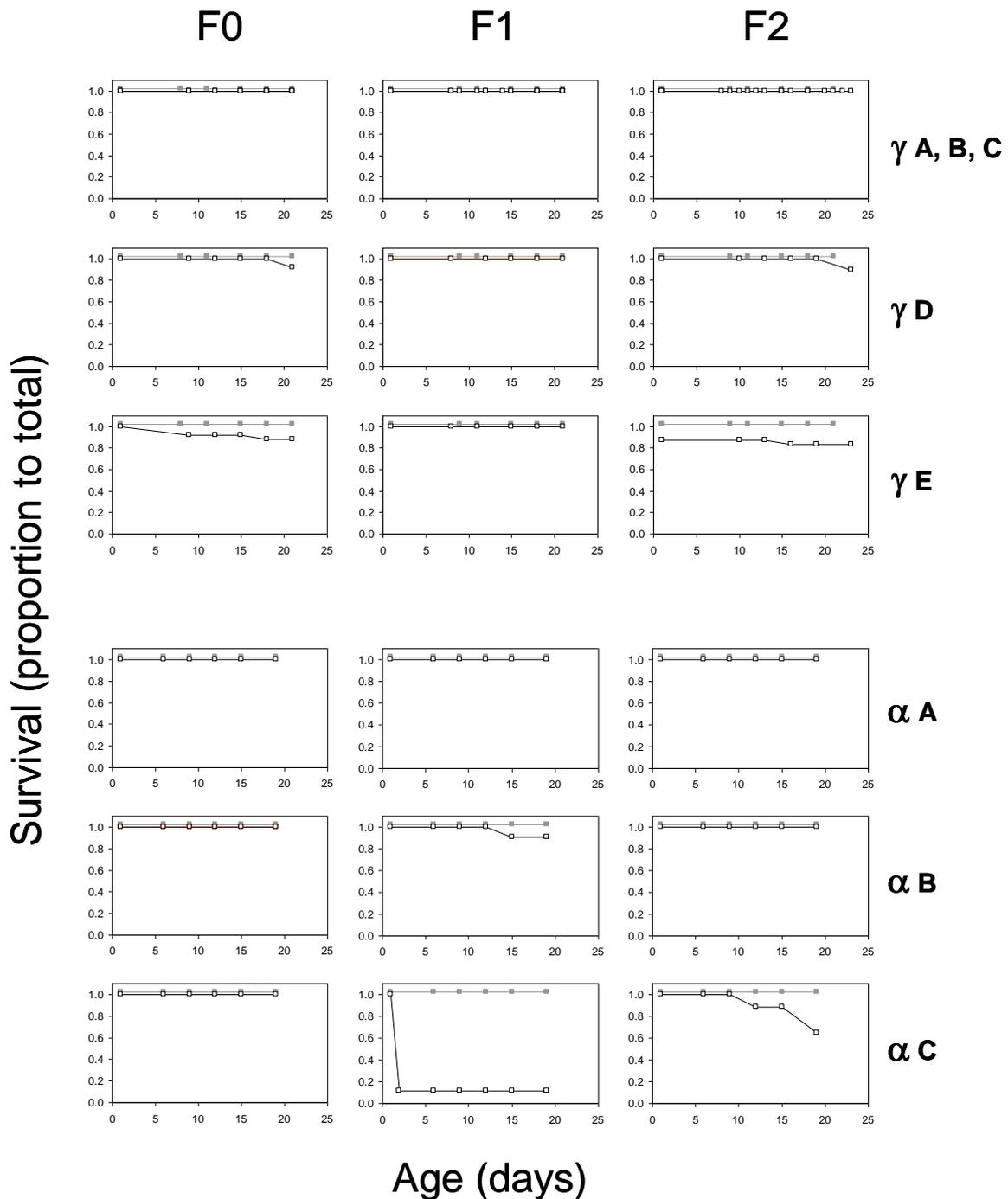
Figure 29. Chronic effects of external gamma radiation and internal alpha radiation on survival, body size and fecundity in relation to age over 3 generations of daphnids (F0, F1 and F2) at average gamma dose rates of (A) 0.008 mGy/h, (B) 0.075 mGy/h, (C) 0.76 mGy/h, (D) 4.40 mGy/h, (D) 32.0 mGy/h, and average alpha dose rates of (A) 0.3 mGy/h, (B) 1.5 mGy/h and, (C) 15.0 mGy/h. Error bars indicate standard deviations (n = 10) with associated statistical significance (* p < 0.05; ** p < 0.01; *** p < 0.001) of differences with the control (grey curves), vertically in body size and number of eggs and horizontally in age of brood deposition.

Figure 29. Continued

F0   F1   F2

Fecundity (eggs per daphnid)

γ A

γ B

γ C

γ D

γ E

α A

α B

α C

Age (days)
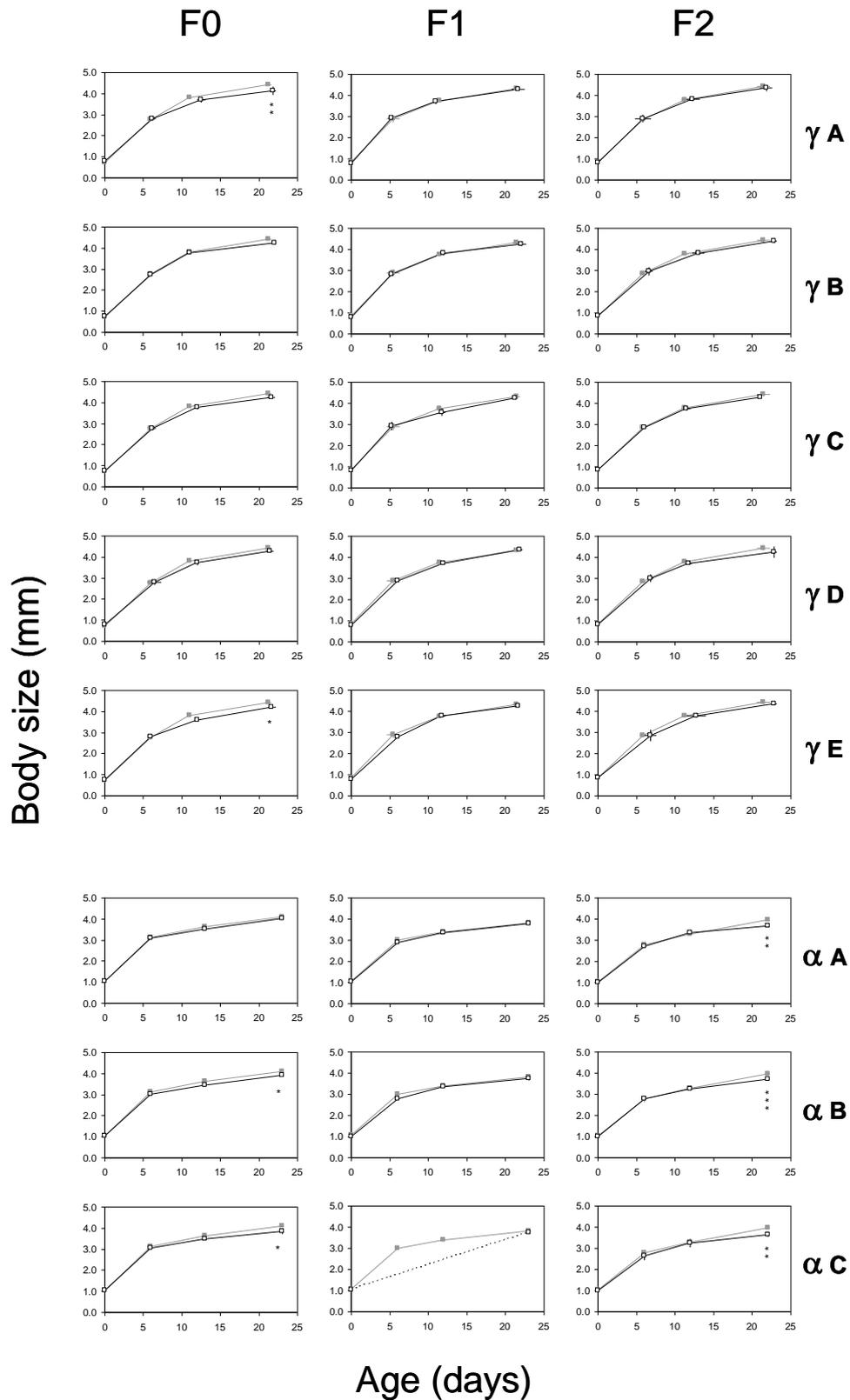
Figure 29. Continued

Table 20. Alpha dose rates as a function of age during the waterborne Am-241 contamination of Daphnia magna (Alonzo et al., 2008)

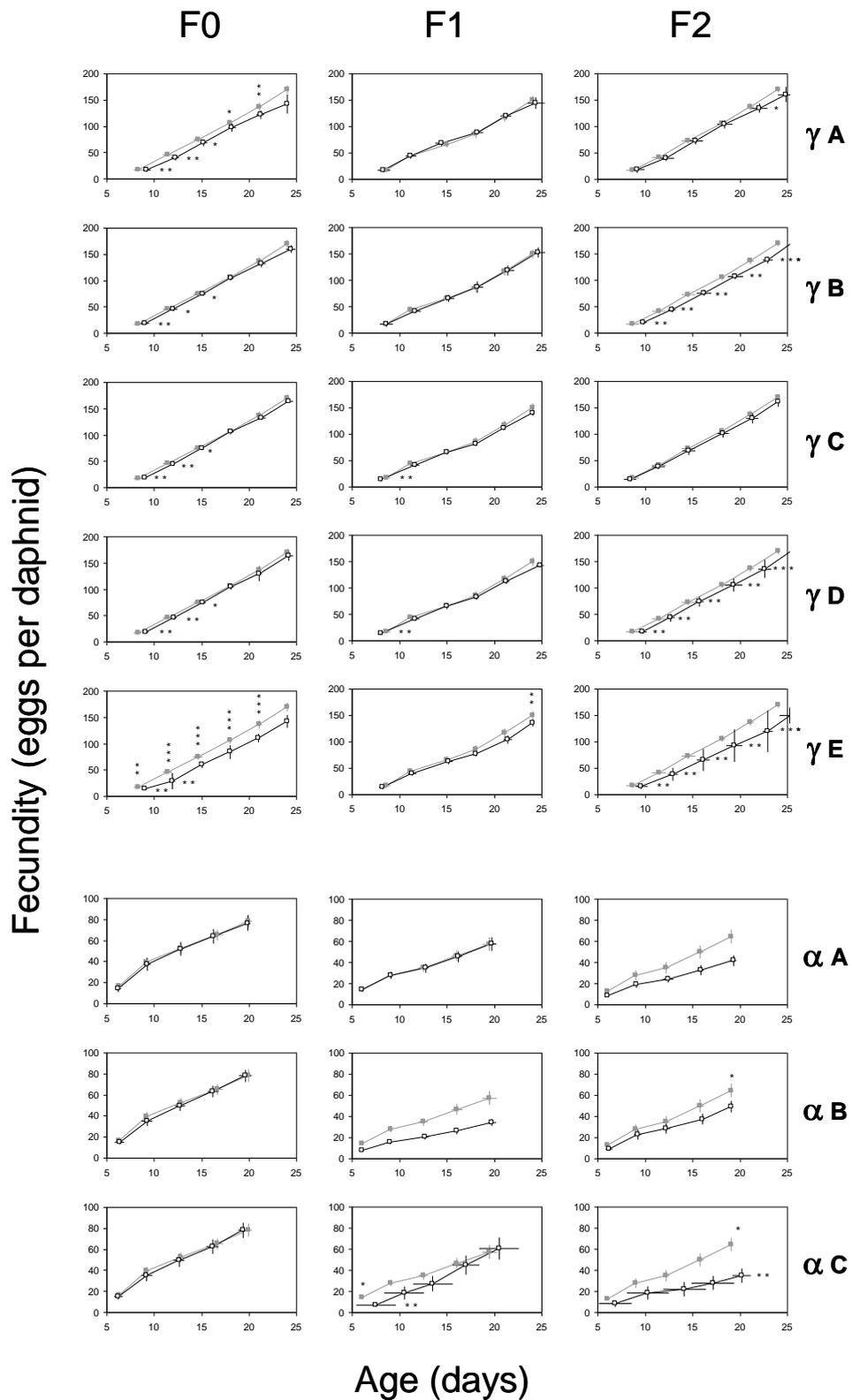| Am-241 concentration	Age	Dose rate ± S.D.	Replicates
40 Bq/mL	0	5.9 ± 1.1 mGy/h	
	6	16.3 ± 10.4 mGy/h	
	13	23.2 ± 5.3 mGy/h	
	23	20.5 ± 10.3 mGy/h	n = 10
4.0 Bq/mL	0	0.52 ± 0.10 mGy/h	
	6	1.03 ± 0.10 mGy/h	survival / fecundity
	13	1.83 ± 1.03 mGy/h	n = 14
	23	2.19 ± 0.72 mGy/h	biometry / DNA analyses
0.4 Bq/mL	0	0.28 ± 0.03 mGy/h	
	6	0.35 ± 0.05 mGy/h	
	13	0.32 ± 0.05 mGy/h	
	23	0.38 ± 0.18 mGy/h	

b) Comparing metabolic modes of action

The standard DEBtox model considers that a toxic stress affects energy budget through five possible modes of action including (i) a reduction in assimilation, (ii) an increase in costs for somatic growth and maturation, (iii) an increase in costs for somatic and maturity maintenance, (iv) an increase in costs for an egg and (v) an increase in mortality during oogenesis. Because the different modes of action have different consequences for growth and reproduction, fitting DEBtox models to alpha and gamma radiation effects data will make it possible to identify the most likely mode of action for each type of radiation, on the basis of goodness of fits. Two situations can occur (Figure 30):

- Identifying a same mode of action for alpha and gamma radiation will strongly suggest that radiological stress affects organisms through a same metabolic mechanism independent of the radiation type, making the comparison of the biological effectiveness between alpha and gamma radiation simple and straightforward (by a direct comparison of stress functions).

- Identifying different modes of action for alpha and gamma radiation will suggest that radiological stress may affect organisms through different metabolic mechanisms depending on the radiation type and biological effectiveness of alpha and gamma radiation will be less comparable. In this second case, one can nonetheless hypothesize that gamma and alpha radiation act through a unique mode of action. Under this assumption, identifying the most likely mode of action can be attempted, by fitting a common DEBtox model to both alpha and gamma radiation effects data with the value of RBE concomitantly fitted as an extra parameter of the stress function.
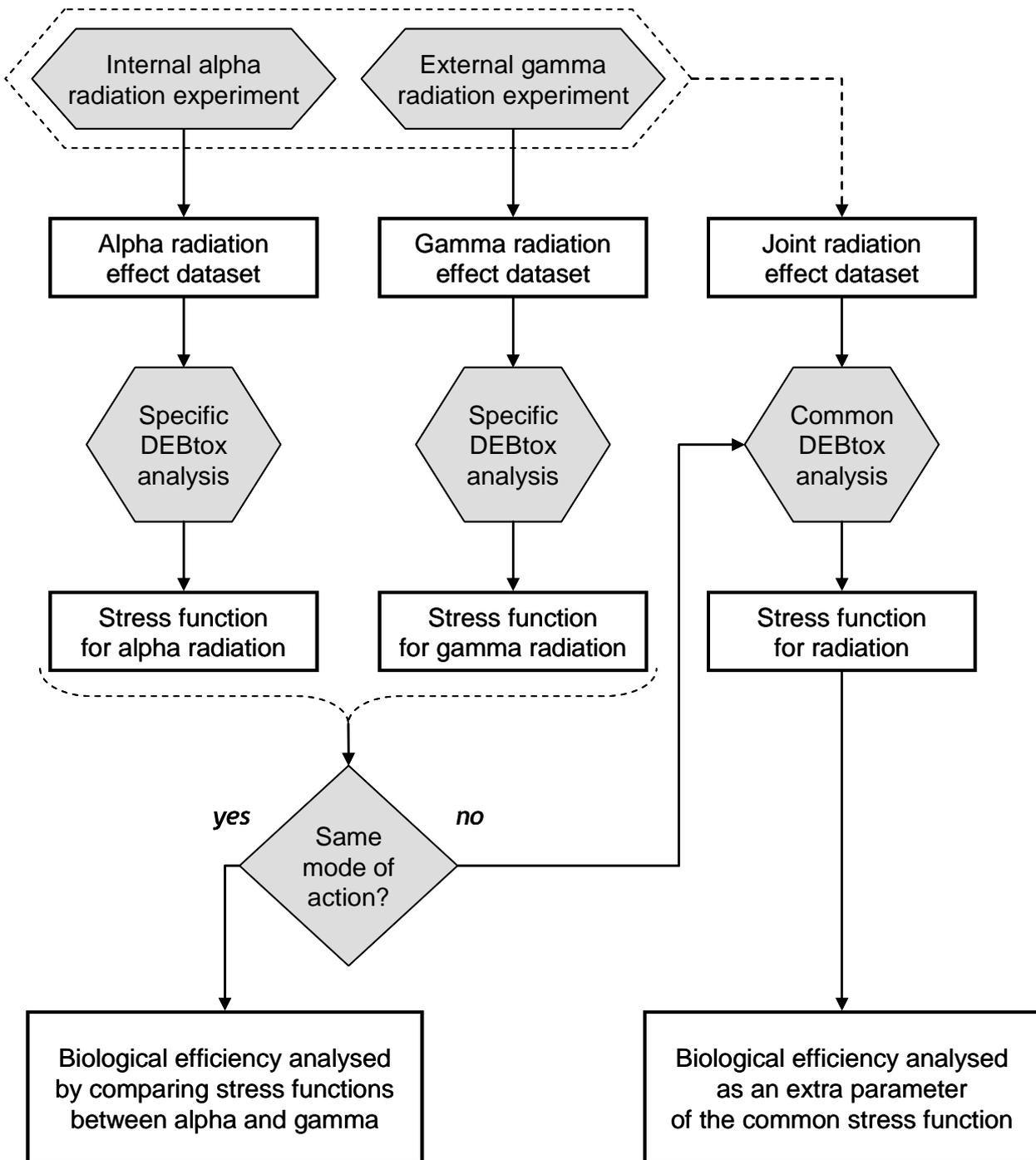
Figure 30. Suggested scheme for a mechanistic analysis of the biological efficiency of alpha and gamma radiation using DEBtox.

c) Comparing DNA damage by RAPD-PCR

During exposure to depleted uranium, increasing DNA damage across daphnids generations was interpreted as evidence that a pool of damage is accumulated in females and transmitted to

offspring. This damage is considered as a source of toxic stress which explains the observed increase in uranium toxicity across generations. DNA damage as quantified by RAPD-PCR may be a molecular marker of this pool of damage (simple correlation) or the source of the stress itself (cause consequence relationship).

Multigenerational exposures to alpha and gamma radiation offer two additional case studies to validate or invalidate the hypotheses (Figure 30). DNA samples collected over three generations of daphnids exposed to gamma radiation will be analysed in the coming months while a contamination of daphnids by Am-241 remains to be conducted to collect DNA samples for RAPD-PCR analyses.

Comparing DNA damage between alpha and gamma radiation will allow:

- to test whether DNA damage is accumulated across generations when effects severity increases.

- to test whether a direct correlation exists between the level of DNA damage measured by RAPD-PCR and the intensity of radiological stress predicted by DEBtox analyses.

- to test the validity of DNA damage as a fitness-related molecular marker of radiological stress.

5. General discussion, lessons learnt, limitations and perspectives for improvements

Effects of low doses of ionising radiation are still poorly understood. Studies deriving Species Sensitivity Distributions (SSD) suggest that only minor effects could be observed on aquatic ecosystems for dose rates below 10 µGy/h (Garnier-Laplace et al., 2006). However the lack of knowledge on the effects of low doses of ionising radiation does not meant that there will be no effects below this value. Exposure to alpha emitters is one scenario where the doses may exceed 10 µGy/hr, due to the weighting factor applied for alpha emitters. However what the weighting factor might be for different endpoints and organisms is more unclear. This means that a broad mechanistic approach focused on studying MoA through a variety of biomarkers will aid in understanding the extrapolation between different types of exposure experiments.

From the few studies allowing a direct comparison between gamma and alpha exposure, it would appear that, in line with established data, the effects of alpha irradiation are greater than gamma (same doses). However there are exceptions, such as the occurrence of DNA double strand breaks in fish cell cultures. Furthermore the variety of experiments and endpoints demonstrates quite clearly that the relative differences in biological effectiveness between alpha and gamma emitters will depend very much on the endpoint or biomarker analysed, the time after irradiation, and the tissue or organ in which the measurement is taken. Differences in distribution of alpha and gamma exposure within the organism need to be addressed, and more work will be needed to link molecular level changes with those at tissue and organism levels. This will require focused and hypothesis driven comparisons, and the preliminary data on biomarker and future omics analysis.

Table 21 Comparison of alpha v gamma effects

Organism	Endpoint	Relative effectiveness
Arabidopsis	Root growth	Alpha > gamma
	Photosynthesis	Only gamma
	PARP2	Alpha > gamma
		difficulty to calculate RBE due to differential distribution of alpha among organs
Nematodes	Survival, body size and fecundity	Only gamma
Fish cell cultures	DNA double strand breaks	Gamma > alpha (ca. 2)*
	Apoptosis	Alpha > Gamma (ca. 5)*
Daphnia	Survival, body size and fecundity	Alpha > Gamma (ca. 3-10)

** Temporary effect difference, lasting up to 4 hours

6. References

Alper EL. 1998. Radiation Biophysics. Second edition. Academic Press. ISBN 0-12-053085-6, Chapter 5

Alonzo F, Gilbin R, Bourrachot S, Floriani M, Morello M, Garnier-Laplace J (2006) Effects of chronic internal alpha irradiation on physiology, growth and reproductive success of Daphnia magna. Aquat Toxicol 80, 228-236

Alonzo F, Gilbin R, Zeman FA, Garnier-Laplace J (2008) Increased effects of internal alpha irradiation in Daphnia magna after chronic exposure over three successive generations. Aquat Toxicol 87, 146-156

Ankley, GT, Bencic, DC, et al. (2009). Endocrine disrupting chemicals in fish: developing exposure indicators and predictive models of effects based on mechanism of action. Aquat. Toxicol 92, 168-178.

Atienzar FA, Conradi M, Evenden AJ, Jha AN, Depledge MH (1999) Qualitative assessment of genotoxicity using random amplified polymorphic DNA: Comparison of genomic template stability with key fitness parameters in Daphnia magna exposed to benzo[a]pyrene. Environ Toxicol Chem 18, 2275-2282

Atienzar FA, Cordi B, Donkin ME, Evenden AJ, Jha AN, Depledge MH (2000) Comparison of ultraviolet-induced genotoxicity detected by random amplified polymorphic DNA with chlorophyll fluorescence and growth in a marine macroalgae, Palmaria palmata. Aquat Toxicol 50, 1-12

Azzam EI, de Toledo SM, Gooding T, Little JB (1998) Intercellular communication is involved in the bystander regulation of gene expression in human cells exposed to very low fluences of alpha particles. Radiat Res 150(5),497-504.

Barcellos-Hoff MH, Brooks AL (2001) Extracellular signaling through the microenvironment: a hypothesis relating carcinogenesis, bystander effects, and genomic instability. Radiat Res. 156, 618-27.

Beresford, 2007

Beaugelin-Seiller K, Jasserand F, Garnier-Laplace J, Gariel JC, (2006) Modelling radiological dose in non-human species : principles, computerization and application. Health Phys, 90(5): 484-493

Biermans G, Horemans N, Vanhoudt N, *et al.*, 2013. An organ-based approach to dose calculation in the assessment of dose-dependent biological effects of ionising radiation in Arabidopsis thaliana. *Journal of Environmental Radioactivity*.

Bodar CWM, Van der Sluis I, Van Montfort JCP, Voogt PA, Zandee DI (1990) Cadmium resistance in Daphnia magna. Aquat Toxicol 16, 33-40

Boverhof and Gollapudi, 2011

Brenner S, 1974. The genetics of *Caenorhabditis elegans*. *Genetics* **77**, 71-94.

Bustamante P, Teyssié J-L, Fowler SW, Warnau M (2006) Assessment of the exposure pathway in the uptake and distribution of americium and cesium in the cuttlefish (Sepia officinalisà at different stages of its life cycle. J Exp Marine Ecol Biol. 331, 198-207.

Cambier S, Gonzalez P, Durrieu G, Bourdineaud J.-P (2010) Cadmium-induced genotoxicity in zebrafish at environmentally relevant doses. Ecotoxicol Environ Saf 73, 312-319

Chambers DB, Osborne RV, Garva AL. (2006) Choosing an alpha radiation weighting factor for doses to non-human biota. J Environ Radioact. 87(1):1-14. Epub 2005 Dec 27.

Copplestone D, Hingston J, Real A. (2008) The development and purpose of the FREDERICA radiation effects database. J Environ Radioact. 99(9):1456-63. doi: 10.1016/j.jenvrad.2008.01.006. Epub 2008 Mar 17.

Cucinotta FA, Kim MH, Chappell LJ, Huff JL. (2013). How safe is safe enough? Radiation risk for a human mission to Mars. PLoS One. 8(10):e74988. doi: 10.1371/journal.pone.0074988.

Dietrich S, Ploessl F, Bracher F, Laforsch C (2010) Single and combined toxicity of pharmaceuticals at environmentally relevant concentrations in Daphnia magna – A multigenerational study. Chemosphere 79, 60-66

ERICA Deliverable 5

FASSET (2003) Deliverable 2,

Faucher K, Floriani M, Gilbin R, Adam-Guillermin C (2012). Uranium-induced sensory alterations in the zebrafish Danio rerio. Aquatic Tox, 124-125, 94-105.

Friedrich T, Grün R, Scholz U, Elsässer T, Durante M, Scholz M (2013) Sensitivity analysis of the relative biological effectiveness predicted by the local effect model. Phys Med Biol. 2013, 58(19):6827-49. doi: 10.1088/0031-9155/58/19/6827. Epub 2013 Sep 11.

Garnier-Laplace J, Della-Vedova C, Gilbin R, Copplestone D, Hingston J, Ciffroy P, (2006) First derivation of predicted-No-Effect values for freshwater and terrestrial ecosystems exposed to radioactive substances. Environ Sci Technol 40, 6498-6505

Geffroy B, Ladhar C, Cambier S, Treguer-Delapierre M, Brèthes D, Bourdineaud JP (2012) Impact of dietary gold nanoparticles in zebrafish at very low contamination pressure: The role of size, concentration and exposure time. Nanotoxicology 6, 144-160

Gilbin R, Alonzo F, Garnier-Laplace J (2008) Effects of chronic external gamma irradiation on growth and reproductive success of Daphnia magna. J of Environ Radioact 99(1):134-145

Gilbin R, Alonzo F, Garnier-Laplace J (2008) Effects of chronic external gamma irradiation on growth and reproductive success of Daphnia magna. J Environ Rad 99, 134-145

Gonzalez P, Dominique Y, Massabuau J-C, Bourdineaud J-P (2005). Comparative effect of dietary methymercury on gene expression in liver, skeletal muscle, and brain of the zebrafish (Danio rerio). Environ. Sc. Technol., 39, 3972-3980.

Goodhead DT (2006) Energy deposition stochastics and track structure: what about the target? Radiat Prot Dosimetry. 122(1-4):3-15. Epub 2007 Feb 2

Guan R, Wang WX (2006) Multigenerational cadmium acclimation and biokinetics in Daphnia magna. Environ Pollut 141, 343-352

[STAR]   89/94
(D-N°: 5.3) – Radiation Quality: studying sub-cellular modes of action using biomarkers and "omics" tools
Dissemination level: PU
Date of issue of this report: 29/11/2013

Hertel-Aas et al. (2007) Effects of Chronic Gamma Irradiation on Reproduction in the Earthworm Eisenia fetida (Oligochaeta). Radiat Res 168(5):515-526.

Higley KA, Kocher DC, Real AG, Chambers DB. (2012) Relative biological effectiveness and radiation weighting factors in the context of animals and plants. Ann ICRP. 2012 Oct-Dec;41(3-4):233-45. doi: 10.1016/j.icrp.2012.06.014. Epub 2012 Aug 22.

Howell, R.W., M.T. Azure, V.R. Narra and D.V. Rao (1994). Relative Biological Effectiveness of Alpha-Particle Emitters In Vivo at Low Doses. Radiation Research, 137, 352-360.

ICRP 58, 1990. RBE for Deterministic Effects. Ann. ICRP 20 (4), 1990

ICRP 92, 2003. Relative biological effectiveness (RBE), quality factor (Q), and radiation weighting factor (wR) Ann. ICRP, 33 (4) (2003)

ICRP108, 2008. Environmental Protection - the Concept and Use of Reference Animals and Plants. ICRP. Ann. ICRP 38 (4-6)

ICRU Report 33 - Radiation Quantities and Units Pub: International Commission on Radiation Units and Measurements, Washington D.C. USA issued 15 April 1980, pp.25

Jager T, Alda Alvarez O, Kammenga JE, Kooijman SALM (2005) Modelling nematode life cycles using dynamic energy budgets. Funct Ecol, 19(1), 136-144

Jager T, Zimmer E (2012) Simplified dynamic energy budget model for analysing ecotoxicity data. Ecol Model 225, 74-81

Jager, T, Albert, C, Preuss, T.G, Ashauer, R (2011) General unified threshold model of survival - A toxicokinetic-toxicodynamic framework for écotoxicologie. Environ Sci Technol 45, 2529-2540

Jarvis RB, Knowles JF (2003) DNA damage in zebrafish larvae induced by exposure to low dose rate [gamma]-radiation: Detection by the alkaline comet assay. Mutat Res-Gen Tox En 541,63–69.

Kellerer AM (2002) Electron spectra and the RBE of X-rays. Radiat. Res. 158, 13-22.

Kim H, Lee M, Yu S, Kim S (2012) The individual and population effects of tetracycline on Daphnia magna in multigenerational exposure. Ecotoxicology 21, 993-1002

Knowles J, Greenwood L (1994) The effects of chronic irradiation on the reproductive performance of Ophryotrocha diadema (polychaeta, dorvilleidae). Mar Environ Res 38(3):207-224.

Knowles J, Greenwood L (1997) A comparison of the effects of long-term β-and γ-irradiation on the reproductive performance of a marine invertebrate Ophryotrocha diadema (Polychaeta, Dorvilleidae). J Environ Radioact 34(1):1-7.

Kocher DC, Trabalka JR. (2000) On the application of a radiation weighting factor for alpha particles in protection of non-human biota. Health Phys. 79(4):407– 411.

Kooijman SALM (2000) Dynamic Energy and Mass Budgets in Biology Systems. Cambridge University Press, Cambridge

LeBlanc GA (1982) Laboratory investigation into the development of resistance of Daphnia magna (Straus) to environmental pollutants. Environment Pollut Ser A 27, 309-322

Lerebours A, Bourdineaud J-P, Van der Ven K, Vandenbrouk T, Gonzalez P, Camilleri V, Floriani M, Garnier-Laplace J, Adam-Guillermin C (2010) Sublethal effects of waterborne uranium

[STAR]   90/94
(D-N°: 5.3) – Radiation Quality: studying sub-cellular modes of action using biomarkers and "omics" tools
Dissemination level: PU
Date of issue of this report: 29/11/2013

exposures on the zebrafish brain : transcriptional responses and alterations of the olfactory bulb ultrastructure. Environ Sc Technol, 44, 1438-1443.

Lerebours A, Cambier S, Hislop L, Adam-Guillermin C, Bourdineaud JP (2013) Genotoxic effects of exposure to waterborne uranium, dietary methylmercury and hyperoxia in zebrafish assessed by the quantitative RAPD-PCR method. Genet Toxicol Environ Mutagen 755, 55-60

Malard V, Chardan L, Roussi S, Darolles C, Sage N, Gaillard JC, Armengaud J (2012) Analytical constraints for the analysis of human cell line secretomes by shotgun proteomics. J Proteomics 75,1043-1054.

Massarin S, Alonzo F, Garcia-Sanchez L, Gilbin R, Garnier-Laplace J, Poggiale JC (2010) Effects of chronic uranium exposure on life history and physiology of Daphnia magna over three successive generations. Aquat Toxicol 99, 309-319

Massarin S, Beaudouin R, Zeman F, Floriani M, Gilbin R, Alonzo F, Pery ARR (2011) Biology-based modeling to analyze uranium toxicity data on Daphnia magna in a multigeneration study. Environ Sci Technol 45, 4151-4158

Mothersill C, Seymour C (1997) Survival of human epithelial cells irradiated with cobalt 60 as microcolonies or single cells. Int J Radiat Biol, 72(5), 597-606.

Mothersill C, Seymour C B (2004) Radiation-induced bystander effects – implications for cancer. Nat. Rev. Cancer 4, 158–164.

Muyssen BTA, Janssen CR (2004) Multi-generation cadmium acclimation and tolerance in Daphnia magna Straus. Environ Pollut 130, 309-316

NCRP, 1990. The Relative Biological Effectiveness of Radiations of Different Quality. National Council on Radiation Protection and Measurements Report No. 104. Bethesda, MD.

NRC, 2007 National Research Council (NRC), Toxicity Testing in the 21st century: A Vision and a Strategy, National Academies Press, Washington, DC (2007).

OECD (2008) OECD 211: Daphnia magna Reproduction Test

Pane EF, McGeer JC, Wood CM (2004) Effects of chronic waterborne nickel exposure on two successive generations of Daphnia magna. Environ Toxicol Chem 23, 1051-1056

Pereira S, Bourrachot S, Cavalie I, Plaire D, Dutilleul M, Gilbin R, Adam-Guillermin C (2011) Genotoxicity of acute and chronic gamma-irradiation on zebrafish cells and consequences for embryo development. Environ Toxicol Chem, 30, 2831-2837.

Pereira S, Malard V, Ravanat J-L, Armengaud J, Foray N, Adam-Guillermin C (2013). Low doses of gamma-irradiation induces an early bystander effect in zebrafish cells which is sufficient to radioprotect cells. Submitted to PlosOne.

Plaire D, Bourdineaud JP, Alonzo A, Camilleri V, Garcia-Sanchez L, Adam-Guillermin C, Alonzo F (sous presse) Linking DNA damage and effects on life history in a multigenerational exposure of Daphnia magna to uranium. J Compar Biochem Physiol C 158, 231-243

Postiglione, I., A. Chiaviello, Palumbo G (2010). Twilight effects of low doses of ionizing radiation on cellular systems: a bird's eye view on current concepts and research. Med Oncol 27(2): 495-509.

Queval G, Noctor G, 2007. A plate reader method for the measurement of NAD, NADP, glutathione, and ascorbate in tissue extracts: Application to redox profiling during Arabidopsis rosette development. *Analytical Biochemistry* **363**, 58-69.

R Core Team, 2013. R: A language and environment for statistical computing. R Foundation for Statistical Computing, Vienna, Austria. URL http://www.R-project.org/.

Reinardy H, Teyssié J-L, Jeffree RA, Copplestone D, Henry TB, Jha AN (2011) Uptake, depuration and radiation dose estimation in zebrafish exposed to radionuclides via aqueous or dietary uptake. Sc Tot Env, 409, 3771-3779.

Saenen E, Horemans N, Vanhoudt N, *et al.*, 2013. Effects of pH on uranium uptake and oxidative stress responses induced in Arabidopsis thaliana. *Environmental Toxicology and Chemistry* **32**, 2125-33.

Salomaa S, Prise KM, Atkinson MJ, Wojcik A, Auvinen A, Grosche B, Sabatier L, Jourdain JR, Salminen E, Baatout S, Kulka U, Rabus H, Blanchardon E, Averbeck D, Weiss W. (2013) State of the art in research into the risk of low dose radiation exposure--findings of the fourth MELODI workshop. J Radiol Prot. 2013 Sep;33(3):589-603. doi: 10.1088/0952-4746/33/3/589. Epub 2013 Jun 27

Sánchez M, Ferrando MD, Sancho E, Andreu E (2000) Physiological perturbations in several generations of Daphnia magna straus exposed to diazinon. Ecotoxicol Environ Saf 46, 87-94

SENES Consultants Limited (SENES), 2005. Review and evaluation of published literature on alpha radiation weighting factors for non-human biota. Prepared for Cogema Resources Inc., www.senes.ca/services/radioactivity/index.html.

Sinclair W.K. Expermental RBE values of high LET radiations at low doses and the implications for quality factor assignment. Radiat. Prot.Dosimetry 1985;13(1-4):319-326.

Stiernagle T, 2006. Maintenance of C. elegans. *WormBook: the online review of C. elegans biology*, 1-11.

Swain SC, Keusekotten K, Baumeister R, Stürzenbaum SR, 2004. *C. elegans* Metallothioneins: New Insights into the Phenotypic Effects of Cadmium Toxicosis. *Journal of molecular biology* **341**, 951-9.

Tran D, Bourdineaud J-P, Massabuau J-C, Garnier-Laplace J (2005) Modulation of uranium bioaccumulation by hypoxia in the freshwater clam Corbicula fluminea: induction of multixenobiotic resistance protein and heat shock protein 60 in gill tissues. Environ Toxicol Chem 24, 2278-2284.

van Aggelen, et al., 2010. Integrating omic technologies into aquatic ecological risk assessment and environmental monitoring: hurdles, achievements, and future outlook. Environ Health Perspect. 118, 1-5.
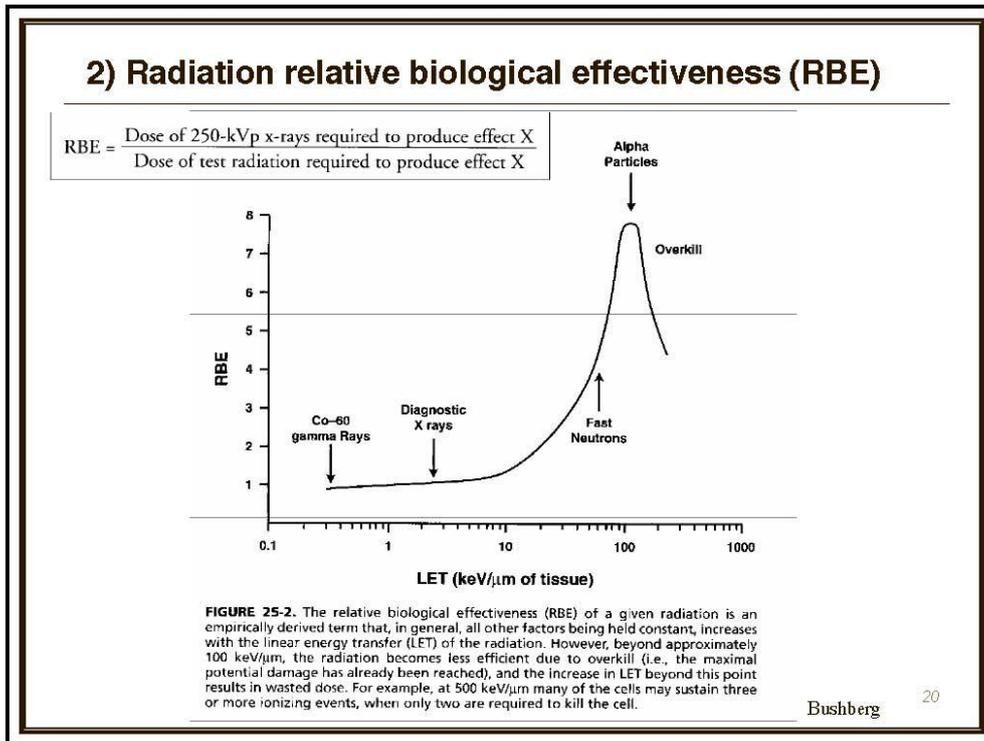
Vanhoudt N, Vandenhove H, Smeets K, *et al.*, 2008. Effects of uranium and phosphate concentrations on oxidative stress related responses induced in Arabidopsis thaliana. *Plant Physiology and Biochemistry* **46**, 987-96.

Véran M-P (1998). Etude des transferts de l'Am-241 en eau douce. Application à l'écosystème Rhodanien. Thèse de doctorat de l'université Aix Marseille 1

[STAR] 92/94
(D-N°: 5.3) – Radiation Quality: studying sub-cellular modes of action using biomarkers and "omics" tools
Dissemination level: PU
Date of issue of this report: **29/11/2013**

Yasuda T, Aoki K, Matsumoto A, Maruyama K, Hyodo-Taguchi Y, Fushiki S, Ishikawa Y (2006) Radiation-induced brain cell death can be observed in living medaka embryos. J Radiat Res (Tokyo) 47, 295–303.

Zotina T, Trofimova E, Demendtyev D, Bolsunovski A (2011) Transfer of Am-241 from food and water to organs and t issues of the Crucian carp. Radioprotection 46, S69-S73.

[STAR] 93/94
(D-N°: 5.3) – Radiation Quality: studying sub-cellular modes of action using biomarkers and "omics" tools
Dissemination level: PU
Date of issue of this report: **29/11/2013**

7. Annexes

Example of Change of RBE with LET: Cell survival curves